https://doi.org/10.59761/RCR5222

Nonviral nucleic acid delivery systems: specific features of polymeric carriers

Evgeny D. Shaputkin,[a,b] **Ilya E. Nifant'ev,**[a,b*] **Pavel V. Ivchenko**[a,b]

[a] *Faculty of Chemistry, Lomonosov Moscow State University, 119991 Moscow, Russian Federation*
[b] *A.V.Topchiev Institute of Petrochemical Synthesis, Russian Academy of Sciences, 119991 Moscow, Russian Federation*

Gene therapy has found broad application in the prevention and treatment of cancer, infectious diseases, and neurodegenerative and metabolic disorders. At the same time, the development of formulations capable of efficient and targeted delivery of nucleic acids has been and remains a challenging interdisciplinary task. Polymeric delivery systems for such biomolecules have considerable potential for enhancing transfection efficiency owing to their ability to efficiently bind nucleic acids and facilitate the endosomal escape of genetic material, as well as to the high tunability of their structure and properties. This review discusses the principles of nonviral delivery of mRNA, plasmid DNA, and siRNA that are common to low- and high-molecular-weight carriers. The distinctive features of cationic polymers are considered, and promising directions for the further development of polymeric transfection reagents are identified.
The bibliography includes 333 references.
Keywords: transfection, lipid nanoparticles, nucleic acids, polymeric carriers, biodegradable polymers.

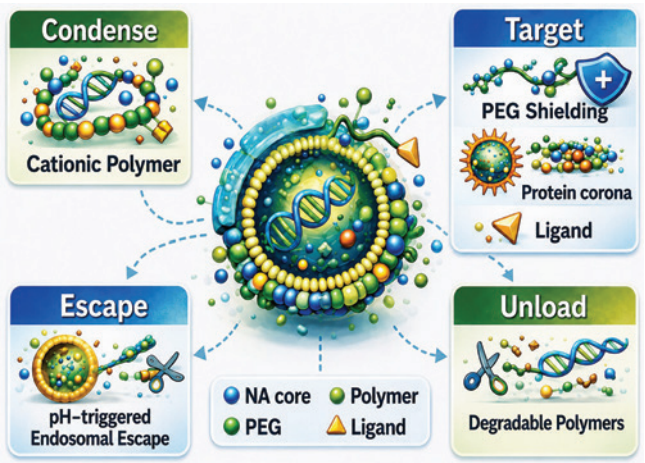

Contents

E.D.Shaputkin. Post-graduate student of the Faculty of Chemistry, MSU, Junior Researcher of TIPS RAS.
E-mail: evgeny.shaputkin@yandex.ru
Current research interests: transfection, biodegradable polymers.
I.E.Nifant'ev. Doctor of Chemical Sciences, Professor at the MSU Faculty of Chemistry, Head of a laboratory of TIPS RAS.
E-mail: ilnif@yahoo.com
Current research interests: coordination catalysis in the polymerization and oligomerization of olefins and dienes, biodegradable polymers, catalytic processes in small-scale chemistry, polymer and composite materials for bone surgery and orthopaedics, polymeric drug and gene delivery systems.
P.V.Ivchenko. Doctor of Chemical Sciences, Leading Researcher at the MSU Faculty of Chemistry, Leading Researcher at TIPS RAS.
E-mail: phpasha1@yandex.ru
Current research interests: coordination catalysis in the polymerization and oligomerization of olefins, biodegradable polymers, Catalytic processes in small-scale chemistry, DFT simulation of organic reactions and catalytic processes.
Translation: Z.P.Svitanko

Received 4 March 2026

1. Introduction

Recent years have witnessed rapid development of therapeutic methods based on the use of various types of nucleic acids (NAs) in diagnosis, therapy, and vaccination.[1] The real application of NAs in medicine began in 1998, when the drug fomivirsen (Vitravene®) was approved by the U.S. Food and Drug Administration (FDA) for the treatment of human cytomegalovirus retinitis.[2] This drug was a synthetic antisense oligonucleotide (ASO) and was administered without additional delivery agents. In the subsequent years, large-scale research was undertaken with the aim of expanding the range of therapeutic NAs.

A key problem of NA application in medicine is to provide their targeted and effective delivery to the cells of a living organism. The biological methods for NA delivery (Fig. 1) are based on the use of viral agents (transduction).[3] The nonviral approaches to the delivery of NAs,[4,5] which are called transfection, make use of physical and chemical methods that are also shown in Fig. 1. Most physical methods are aimed at increasing the permeability of the cell membrane and involve the direct introduction of NAs into the cell; chemical methods are based on the use of various chemical compounds that act as NA carriers.[6]

The delivery of NAs into a cell or the cell nucleus may serve various purposes; the mechanisms of gene therapy are discussed in detail in a number of biomedical reviews.[7–9] Irrespective of the target effect, the delivery of NAs into a cell is a challenging interdisciplinary problem. The development of viral delivery systems is a laborious task,[10] which typically takes a lot of time. Furthermore, these agents raise concerns related to immunogenicity (insertional mutagenesis) and limited therapeutic cargo.[11,12] An example of effective and fast solution of the pressing challenge of protecting the population during the SARS-CoV-2 coronavirus pandemic was the development of the Sputnik V vaccine based on the Ad26 and Ad5 adenoviruses[13,14] and its analogues.[15,16] The use of adeno-associated viruses and lentiviruses reduces the risk of mutagenesis (a vivid example is the Zolgensma® drug developed by Novartis[17]); however, the wide use of such drugs is considerably held up by their cost (~$3.2 million for a treatment course with Elevidys® manufactured by Sarepta Therapeutics and ~$2 million for Zolgensma®).

Obvious drawbacks of physical transfection methods (see Fig. 1) are the need for specialized equipment and low throughput; the practical application of such methods *in vivo* is limited.[18] At the current stage of research, chemical methods and approaches are usually utilized for effective NA delivery into a living organism. In scientific periodicals and extensive review literature dealing with the development of chemical NA delivery systems,[19–22] these vectors are traditionally subdivided into three main types: nanoparticles (NPs), liposomes (including lipid nanoparticles, LNPs), and polymers.

The role of a chemical carrier is to bind NAs and counterbalance their negative charge, protect NAs from degradation during the delivery, and ensure NA penetration into the cell. The first examples of compounds capable of forming cell-penetrating NA complexes are diethylaminoethyl dextran (DEAE-dextran, 1965)[23–25] and nano-sized hydroxyapatite (HAp, 1973) co-precipitated with NAs.[26] Note that the application of HAp is still relevant,[27–29] and other inorganic[30–33] and hybrid organic-inorganic[34] carriers based on NPs are also intensively studied.

DEAE-dextran (Fig. 2) is a cationic polymer that successfully binds and compacts NAs; however, the transfection efficiency of these complexes turned out to be low. Chitosan is a readily available natural analogue of DEAE-dextran, which has attracted attention of researchers since 1998[35] and up to now.[36] The synthesis of cationic lipids, which are still widely used today, was a milestone in the development of transfection agents. *N*-[1-(2,3-Dioleyloxy)propyl]-*N*,*N*,*N*-trimethylammonium (DOTMA) reported in 1987[37] was the first example of such a carrier. The further development of the concept of cationic lipids led to the design of ionizable lipids, that is, amphiphilic molecules that contain aliphatic amino groups that can be protonated.[38–42] The amphiphilic nature of cationic and ionizable lipids accounts for the liposomal features of morphology of their complexes with NAs in physiological media.

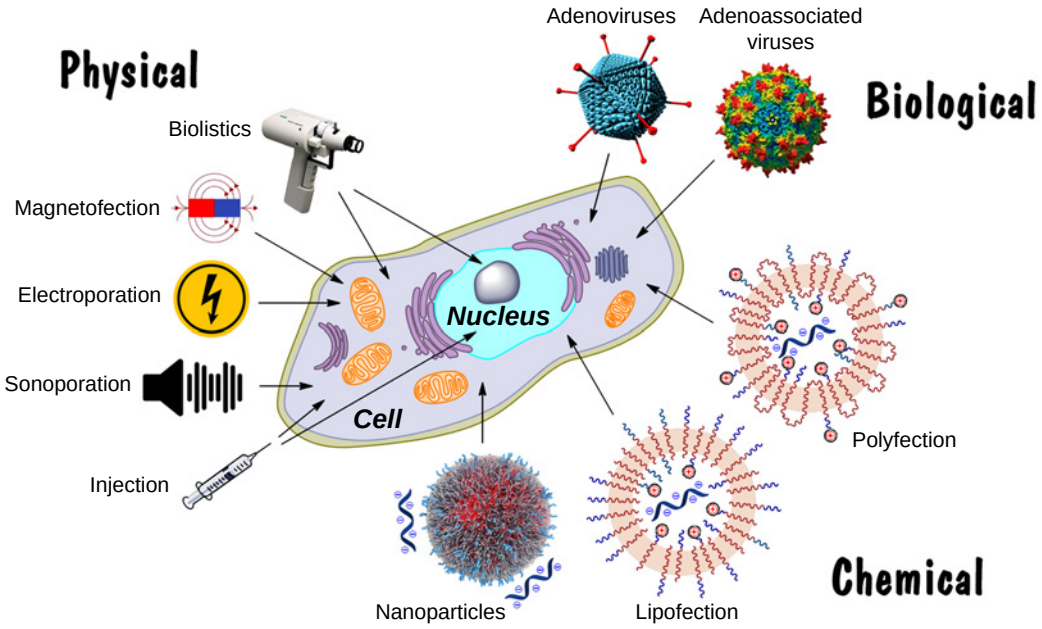

Figure 1. Key approaches to delivery of nucleic acids into cells.

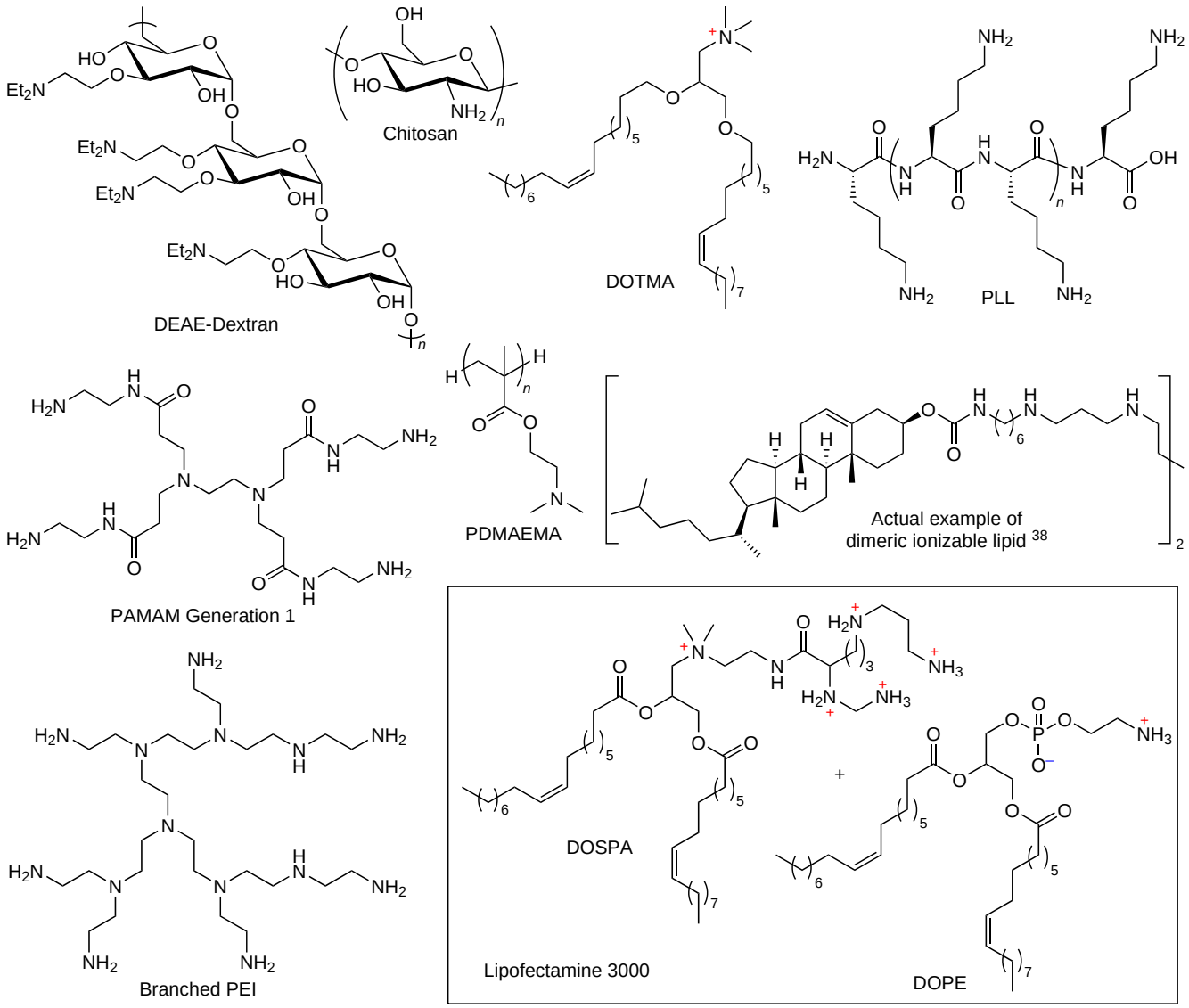

Figure 2. Structures of DEAE-dextran, chitosan, DOTMA, PLL and PDMAEMA polymers, branched PAMAM and bPEI, dimeric ionizable lipid, and the Lipofectamine 3000 formulation.

In the late 1980s and early 1990s, various amino-containing oligomers and polymers were investigated as carriers for NAs. Among these, mention should be made of poly(*L*-lysine) (PLL, 1988),[43] dendrimer polyamidoamine (PAMAM, 1993),[44] polyethylenimine (PEI, 1995),[45] and poly[2-(dimethylamino)-ethyl methacrylate] (PDMAEMA, 1996),[46] which have formed the toolbox of polymeric transfection agents for many years to come (see Fig. 2).

In the subsequent years, large-scale research was undertaken to expand the range of therapeutic NAs and develop methods for their delivery; during this time, effective two- and multi-component transfection agents were obtained.[19,39,47–53] An example of widely used two-component transfectant is Lipofectamine 3000, which is based on ionizable lipids, DOSPA {2,3-dioleyloxy-*N*-[2-(sperminecarboxamido)ethyl]-*N*,*N*-dimethyl-1-propylammonium hydrochloride} and DOPE (1,2-dioleoyl-*sn*-glycero-3-phosphoethanolamine) taken in ~3 : 1 ratio (see Fig. 2).[54]

The advances in NA delivery techniques using LNPs led to the development of patisiran (Onpattro) drug based on small interfering RNA (siRNA), which was approved by FDA in 2018.[55] This led to the exceptionally rapid development of SARS-CoV-2 vaccines based on messenger RNA (mRNA) by Moderna and Pfizer/BioNTech.[56] According to a report by the American Society for Gene & Cell Therapy, approximately 1250 NA-based drugs were undergoing clinical trials in 2025.[57] The issues of practical use of NA therapy are addressed in a number of reviews (see, *e.g.*, Refs 8, 58–60). The total number of FDA-approved gene therapy protocols and drugs is currently approaching 40 (Table 1); however, the proportion of nonviral agents among them is low.

A large number of reviews published in the last decade address general issues related to transfection[61–63] and the prospects for its use in specific applications.[64,65] There are publications devoted to nonviral[66–69] delivery of NAs by means of NPs,[20] including cationic LNPs[19,47–51] and LNPs based on ionizable lipids.[39] Particular attention has been given to mRNA delivery systems.[41,70–74] Some reviews consider the general issues of NA delivery using polymeric carriers[75–83] and specific types of these carriers based on poly(amino esters),[84,85] including poly(β-amino esters) (PβAE),[86–90] PEI,[91,92] PAMAM,[93] and chitosan.[36,94–96] In the context of the present review, mention should be made of earlier publications in *Russian Chemical Reviews*,[97–100] which address issues

Table 1. List of gene therapy drugs approved by FDA and/or other organizations (according to Refs 8, 58–60).

Drug name	Manufacturer	Indications	Year	Control organization
		Using lentiviruses (*including CAR-T*)		
Kymriah	Novartis	Acute lymphocytic leukemia; diffuse large B-cell lymphoma; follicular lymphoma	2017	FDA
Zynteglo	Bluebird bio	Beta-thalassemia	2019–2022	EMA, FDA
Breyanzi	Bristol Myers Squibb	Large B-cell lymphoma; relapsed or refractory chronic lymphocytic leukemia and small-cell lymphocytic lymphoma; follicular lymphoma, mantle cell lymphoma and marginal zone lymphoma	2021, 2024, 2025	FDA
Abecma	Bluebird bio	Multiple myeloma	2021	FDA
Carteyva (Relma-cel)	JW Therapeutics (Shanghai)	Diffuse large B-cell lymphoma; follicular lymphoma; mantle cell lymphoma	2021	NMPA
Skysona	Bluebird bio	Childhood cerebral adrenoleukodystrophy	2021	FDA
Carvykti	Legend Biotech	Multiple myeloma	2022	FDA
Lyfgenia	Bluebird bio	Sickle cell anemia	2023	FDA
Libmeldy/ Lenmeldy	Orchard Therapeutics	Metachromatic leukodystrophy	2020/2024	EMA, FDA
Tecelra (Afami-cel)	Adaptimmune	Synovial sarcoma	2024	FDA
		Using adenoviruses		
Gendicine	Shenzhen SiBiono GeneTech	Head and neck cancer	2003	CFDA
Oncorine	Shanghai Sunway Biotech	Head and neck cancer; nasopharyngeal cancer	2005	CFDA
Adstiladrin	Merck and Co.	Bladder cancer	2022	FDA
		Using adeno-associated viruses		
Glybera	UniQure	Lipoprotein lipase deficiency	2012	EMA
Luxturna	Spark Therapeutics (Roche)	Leber congenital amaurosis; retinitis pigmentosa	2017	FDA/EMA
Zolgensma	Novartis	Spinal muscular atrophy	2019	FDA
Upstaza	PTC Therapeutics	Aromatic *L*-amino acid decarboxylase deficiency	2022	EMA
Hemgenix	UniQure	Haemophilia B	2022	FDA
Elevidys	Sarepta Therapeutics	Duchenne muscular dystrophy	2023	FDA
Roctavian	BioMarin	Haemophilia A	2022	FDA
Beqvez	Pfizer	Haemophilia B	2024	FDA
BBM-H901	Belief BioMed	Haemophilia B	2025	NMPA
		Using herpes simplex viruses		
Imlygic	Amgen	Melanoma	2015	FDA, EMA
Vyjuvek	Krystal Biotech	Epidermolysis bullosa dystrophica	2023	FDA
Delytact	Daiichi Sankyo	Malignant glioma	2021	MHLW
		Using retroviruses (including CAR-T) [a]		
Rexin-G	Epeius Biotechnologies	Solid tumours	2006	BFAD
Strimvelis	Orchard Therapeutics	Adenosine deaminase deficiency	2016	EMA
Yescarta (*ex vivo*)	Kite Pharma (Gilead)	Large B-cell lymphomas; follicular lymphoma	2017	FDA
Tecartus	Kite Pharma (Gilead)	Relapsed or refractory mantle cell lymphoma; relapsed or refractory precursor B-acute lymphoblastic leukemia	2020, 2021	FDA
		Targeted delivery using galactosamine (GalNAc)		
Givlaari	Alnylam	Acute hepatic porphyria	2019	FDA
Oxlumo	Alnylam	Primary hyperoxaluria type 1	2020	FDA
Leqvio	Novartis	Hypercholesterolemia	2020	FDA
Amvuttra	Alnylam	Hereditary transthyretin amyloidosis	2022	FDA
Rivfloza	Novo Nordisk A/S	Primary hyperoxaluria	2023	FDA
		Using CRISPR/Cas9 (see [b])		
Casgevy	Vertex Pharmaceuticals CRISPR Therapeutics	Sickle cell anemia; thalassemia	2025	FDA

Table 1 (continued).

Drug name	Manufacturer	Indications	Year	Control organization
		Using lipofection		
Onpattro	Alnylam and Sanofi	Hereditary transthyretin amyloidosis	2018	FDA
Comirnaty	Pfizer BioNTech	COVID-19 vaccine	2020	EMA, FDA (see[c])
Spikevax	Moderna	COVID-19 vaccine	2020	EMA, FDA (see[c])

Note. EMA is the European Medicines Agency, NMPA is the National Medical Products Administration, CFDA is the China Food and Drug Administration. [a] CAR-T are chimeric antigen receptor T-cells; [b] CRISPR are clustered regularly interspaced short palindromic repeats; [c] considered on an expedited basis.

directly related to the development of chemical delivery systems for nucleic acids.

This review consists of two logical parts. The first part is introductory (Section 2) and describes the key issues of transfection that are common to polymeric and low-molecular-weight carriers (nonviral vectors). The second part is devoted to high-molecular-weight carriers and NA delivery using them (so-called polyfection), including the design and synthesis of polymeric NA carriers (Section 3) and to the diversity of their characteristics, which make it possible to control the amphiphilicity, buffer capacity, polymer chain topology, and, ultimately, the efficiency of NA delivery (Section 4). The summarizing Section 5 compares lipofection and polyfection and highlights relevant trends in the development of polymeric NA carriers. A distinctive feature of the present review is the attempt to identify the key trends of polyfection, since most studies on transfection are devoted to lipid carriers, whereas important experimental studies on polymeric carriers are often overlooked in broader reviews. While preparing this review, we sought to pay particular attention to chemical aspects of polyfection at all stages of the research ranging from polymer design and synthesis to the identification of structure–property relationships as applied to specific NA delivery tasks.

2. Conceptual issues of transfection

2.1. Biological barriers

Along the path to their destination, exogenous NAs encounter a few barriers, including

(1) the negatively charged phospholipid membrane of the cell, which prevents the penetration of negatively charged hydrophilic NA molecules;

(2) endosomal (or lysosomal) vesicles in which the captured NAs are cleaved;

(3) the nuclear envelope, which prevents DNA from entering the nucleus.

These barriers can be overcome only through fine-tuning of interactions between NA molecules, the carrier, and cell compartments.

2.1.1. The phospholipid membrane of the cell

The initial stage of cellular internalization of a nonviral vector is binding to the cell membrane. This binding can be achieved in two ways: through specific interaction between the receptor and the ligand and through nonspecific interaction between the negatively charged outer surface of the plasma membrane and the positively charged NA–carrier complexes. In the former case, the complexes should be additionally modified with specific ligands, which enables the targeted delivery of NAs to particular cells and tissues. Thus, a well-known strategy is the mannosylation of lipid, peptide, and other carriers to achieve targeting of the cells that express the mannose receptors: macrophages, immature dendritic cells, and endothelial cells.[101] In the latter case, the cationic complexes are attached to the cell membrane *via* Coulombic attraction forces.[a] As the charge of the complex increases, the efficiency of binding to the cell increases due to interactions with negatively charged phosphatidylserine, sulfated glycosaminoglycans, and sialic acids.[103,104] Weiss *et al*.[105] showed that for a series of cationic carbon nanoparticles with similar ζ-potentials, the cellular uptake and toxicity are better correlated with the surface charge density rather than with the absolute ζ-potential value.

After adhesion of the nanoparticle carrier on the cell membrane, the next stage is internalization of either the whole particle or the NA being delivered. The simplest form of internalization, that is, direct fusion of the carrier with the cell membrane, occurs in rare cases, *e.g.*, under the action of cell-penetrating peptides (CPP).[106] They constitute a family of peptides not more than 30 amino acids long, enriched with positively charged groups; for example, the R9 peptide carries only guanidine groups as substituents.

The decoration of various polymers ranging from poly(trimethylene carbonate) to polynorbornene with guanidine-containing groups is a known strategy for the design of NA carriers possessing CPP-mimetic behaviour.[107–109] As an example, consider the class of NA carriers reported by Jeon *et al*.,[110,111] that is, poly(oxanorbornene)imides with guanidine groups in the side chain (PONI-Guan) (Fig. 3). For these systems, a model of direct internalization *via* fusion was proposed instead of the classical endocytic model of cellular uptake (see below). In 2023, it was shown[110] that ~170 nm[b] polyplexes (complexes of NA and polymers) produced a diffuse cytosolic signal from Cy3-labelled siRNA after incubation with RAW264.7 (macrophage-like cells). After 6 h, the complexes showed little colocalization with LysoTracker, while 92.4% of the cells were Cy3-positive, which was inconsistent with conventional endosomal accumulation. Functionally, the use of these polymers was accompanied by a more than 70% inhibition of eGFP expression (GFP is green fluorescent protein) in genetically modified RAW264.7:eGFP cells at a guanidinium : phosphate ratio of ~30. The developed system surpassed the Lipofectamine RNAiMAX commercial delivery system by ~25%. The key mechanistic argument of the authors[110] was based on the fact that depletion of membrane

[a] Vasir and Labhasetwar[102] directly measured the adhesion force between cells and PLL-modified nanoparticles by atomic force microscopy.

[b] Here and below, the presented particle diameter was determined using dynamic light scattering (DLS) unless otherwise specified.

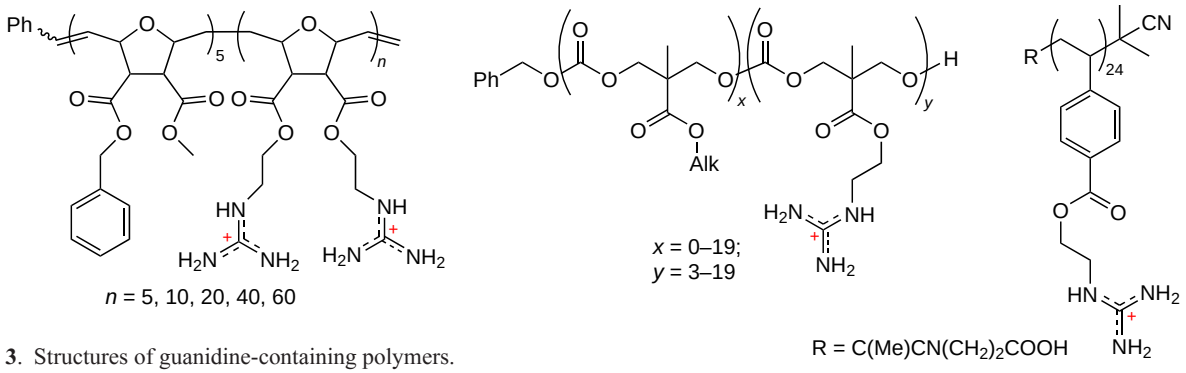

Figure 3. Structures of guanidine-containing polymers.

cholesterol under the action of nystatin and methyl-β-cyclodextrin[c] decreased the gene knockdown by more than 75%, whereas endocytosis inhibitors had only a minor effect (< 10%). This fact served as evidence supporting the hypothesis of direct internalization of polyplexes depending on membrane fluidity. For therapeutic siRNAs against the TNF-α gene, the carrier showed a >65% decrease in TNF-α secretion[d] and a ~ 80% decrease in the amount of mRNA for TNF-α *in vitro*, and also a >80% inhibition of TNF-α expression *in vivo* in lipopolysaccharide (LPS)-stimulated mouse cells at a low dose of siRNA (0.28 mg kg^{-1}).

Endocytosis is a more frequent mechanism for NA uptake than direct translocation of NA into the cytoplasm. The main endocytosis types include clathrin-mediated endocytosis (CME), caveolae-mediated endocytosis (CvME), and macropinocytosis; implementation of a particular mechanism depends on the type of cytoplasmic proteins involved and/or composition of lipid rafts (Fig. 4).[49,112] The initiation of a particular mechanism is also influenced by the physical characteristics (size, shape, and surface charge) and chemical properties of the complexes (composition of the carrier and ligands on the nanoparticle surface) as well as by the type of cells.[113,114]

The clathrin-mediated endocytosis consists in the assembly of clathrin proteins at the ligand–receptor binding site and the formation of a plasma membrane invagination, followed by the formation of vesicles with a diameter of 70–150 nm. This mechanism is implemented in the uptake of nutrients (such as transferrin) and is often used to capture small nanoparticles. In addition, CME is preferred for cationic NPs due to strong electrostatic interactions with the negatively charged cell surface. The vesicles formed during CME are acidified and transformed into late endosomes and lysosomes.

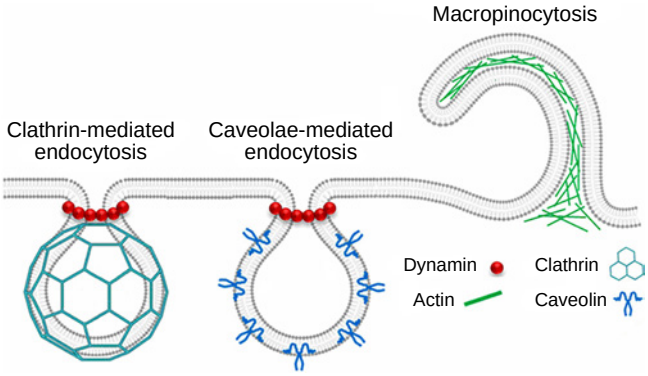

Figure 4. Illustration of the main types of endocytosis.

The caveolae-mediated endocytosis is characterized by the formation of flask-shaped invaginations (50–100 nm in size) rich in caveolins, cavins, cholesterol and sphingolipids. Caveosomes can fuse with early endosomes or be directed toward the endoplasmic reticulum or the Golgi apparatus, in some cases avoiding lysosomal degradation. CvME can be initiated by bacterial toxins, albumin, folic acid, and other compounds. This mechanism is preferred for neutral or negatively charged nanoparticles.

Finally, macropinocytosis is a non-selective process that forms large macropinosomes (0.2–5 μm), which capture both liquids and particles without a strict receptor dependence. Subsequently, the contents of the macropinosome may recirculate to the plasma membrane and develop into lysosomes. Macropinocytosis is stimulated by growth factors, phosphoinositides, diacylglycerol, and other compounds. This route is characteristic of large nanoparticles and aggregates (>500 nm); it is more probable for charged NPs an for NPs carrying so-called protein coronas,[115] structures that are formed on the NP surface in biological media (for details, see Section 4.6.3).

Both the physical factors (particle shape, size, and surface topography) that influence the initiation of a specific endocytosis pathway[113,115] and the chemical factors related to the particle composition and surface charge are adequately covered in the scientific literature. The effect of the carrier charge on the mechanism of NA internalization by lipid and polymeric vectors deserves separate consideration. Zhao *et al.*[116] investigated a series of LNPs based on 1,2-dioleoyl-*sn*-glycero-3-phosphocholine (DOPC) and 3-[*N*-(*N*′,*N*′-dimethylaminoethyl)-carbamoyl]cholesterol (DC-Chol). By varying the proportion of the cationic lipid, the researchers set different ζ-potentials for NPs (from +32 to +43 mV), while the NP size was invariable (~ 100 nm). It was shown that an increase in the positive charge is accompanied by increasing efficiency of LNP uptake by cells and decreasing nanoparticle stability and tendency to capture proteins from the medium to form their own corona. However, the mechanism of cellular uptake remains the same, even on switching to negatively charged LNPs based on DOPC, 1,2-dioleoyl-*sn*-glycero-3-phosphoglycerol (DOPG), and cholesterol. In both cases, CME virtually does not take place, and the uptake of NPs is largely determined by the interaction of the corona with heparan sulfate proteoglycans. Thus, the addition of dextran sulfate to the system caused an approximately twofold decrease in the cellular uptake of both positively and negatively charged LNPs.

[c] Nystatin is a polyene macrolide that binds to membrane sterols; methyl-β-cyclodextrin is a cyclic oligosaccharide with a hydrophobic cavity capable of extracting cholesterol from the plasma membrane.
[d] TNF-α is the tumour necrosis factor alpha, a key pro-inflammatory cytokine produced by macrophages.

The relationship between the endocytosis mechanism and the charge as applied to polyplexes the characteristics of which differ from those of LNPs was addressed by Mott *et al*.[117] The authors studied the efficiency of the delivery of plasmid DNA as a PGA–PEI–plasmid ternary polyplex [PGA is poly(α-glutamic acid)] to the HEK293, U-87MG, and HeLa cells,[e] the effect of the component ratio in the mixture on the choice of the endocytosis pathway, and particle aggregation with bovine serum albumin (BSA). The best results for all three tested cell lines were obtained for a polyplex with a component ratio of 1.5 : 3 : 1 (by mass), a ζ-potential of +11 mV, a hydrodynamic diameter of approximately 200 nm, and moderate aggregation with BSA. Thus, the introduction of PGA partially suppressed the particle aggregation with BSA (isoelectric point of 4.9, negative charge at physiological pH), which simulated the anionic protein environment in the cellular medium. According to experiments, transfection proved to be less effective for negatively charged polyplexes, despite their internalization in amounts similar to those of positively charged polyplexes. Hence, the efficiency of transfection is limited not by the internalization, but rather by differences in the intracellular transport of the polyplexes. The positively charged polyplexes were mainly detected in endosomal compartments containing caveolin, whereas nearly half of the negatively charged polyplexes were transported to acidic late endosomes or lysosomes, which was a result of clathrin-dependent endocytosis.

Thus, at the level of interaction between cells and nanocarriers, similar selection mechanisms operate for LNPs and polyplexes, ensuring the NA transport *via* a particular endocytosis mechanism. This mechanism, in turn, determines the rate and degree of acidification of the arising vesicle and the probability of successful NA delivery.

2.1.2. Endosome and lysosome

Despite the differences in the internalization mechanisms discussed above, it is necessary to bear in mind that both macropinosomes and caveosomes can fuse with early endosomes, which predetermines their evolution into lysosomes. Therefore, endosomal escape is a common bottleneck for virtually any transfection system. This challenge is addressed in a number of recent reviews.[118–122]

During maturation, the endosome pH gradually decreases from a physiological value of 7.4 down to ~6.5 in the early endosome, 6.0–4.8 in the late endosome, and 4.5 in the lysosome.[123] The carrier inability to bring NAs out of the endo(lyso)somal compartments results in the elimination of loaded NAs *via* exocytosis or in their enzymatic degradation. Thus, to achieve a productive release from these compartments is a key condition for effective transfection. According to some studies, the fraction of nanoparticles that escape from endosomes is exceptionally low (1–2% for siRNA[124] and < 10% for mRNA in experiment using easy-to-transfect HEK293 cells)[125] even in systems such as lipid nanoparticles that are already used in clinical practice.

Different nanocarriers tend to use different mechanisms of endosomal escape. In lipoplexes, the major component, ionizable lipid, is responsible for this process. At physiological pH values, the ionizable lipid is neutral and insoluble, but it becomes charged and water-soluble as pH decreases. Electrostatic interactions arising between cationic lipids and anionic lipids of the endosome give rise to cone-shaped ion pairs and trigger a phase transition of the endosomal membrane lipids from a bilayer structure (lamellar phase in Fig. 5) to an inverted micelle structure (hexagonal phase).

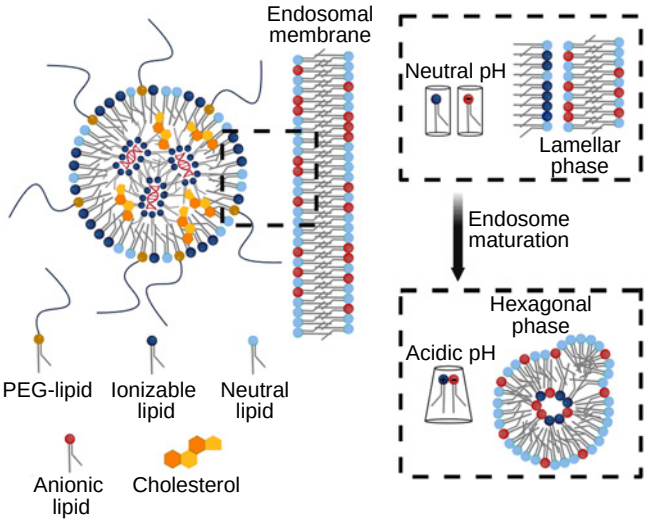

Figure 5. Mechanism of endosomal escape of lipids.

The descriptions of the endosomal escape of NAs transported by polymeric carriers take into account specific effects of the carrier macromolecules: polymer swelling, polycation intercalation into the endosome membrane, and the proton sponge effect (Fig. 6), which is widely discussed in scientific literature.[126]

The proton sponge concept is based on the buffering action of polymers the pK_a values of which fall within a physiologically relevant range. This model is often mentioned in studies dealing with PEI, PLL, PAMAM, and other polyamines.[127] This effect is due to the formation of a buffer system as the polymer amino groups are being protonated during endosomal acidification: the ongoing activity of the vacuolar H^+-ATPase results in the accumulation of protons, the entry of counter-ions (primarily Cl^-), and the osmotic influx of water. The arising swelling of the endosomal compartment and increasing tension of its membrane, together with the destabilizing effect of the protonated polymer on the membrane lead to the loss of integrity of the endosomal membrane and escape of NAs into the cytosol.[128] The buffering function of polyamines (particularly PEI) in the endosome was confirmed by *in situ* experiment.[129] The transfection efficiency was shown to markedly decrease on going from PEI to its quaternized derivatives.[130] However, the proton sponge concept remains controversial. For example in the above-mentioned study by Mott *et al*.,[117] transfection was also accomplished by a PEI-based carrier, but the addition of bafilomycin A1, an endosome acidification inhibitor, had no effect on this process. Quite a few arguments *pro et contra* were summarized by Vermeulen *et al*.[131] under the title *The Proton Sponge Hypothesis: Fable or Fact*? Currently, the proton sponge concept has not been abandoned, but has appreciably changed. It is believed that the buffer capacity of a polymer is indeed important and can serve as a criterion for selecting an effective polymeric carrier,[132] but it does not by itself guarantee effective transfection:[133] Nucleic acids are released not as a result of complete lysosome breakdown, but due to local leaks of its contents.[134,135] The polymer itself may possess endosomolytic properties and directly participate in membrane destabilization.[136]

[e] HEK293 are human embryonic kidney cells, U-87MG are glioblastoma (brain tumour) cells.

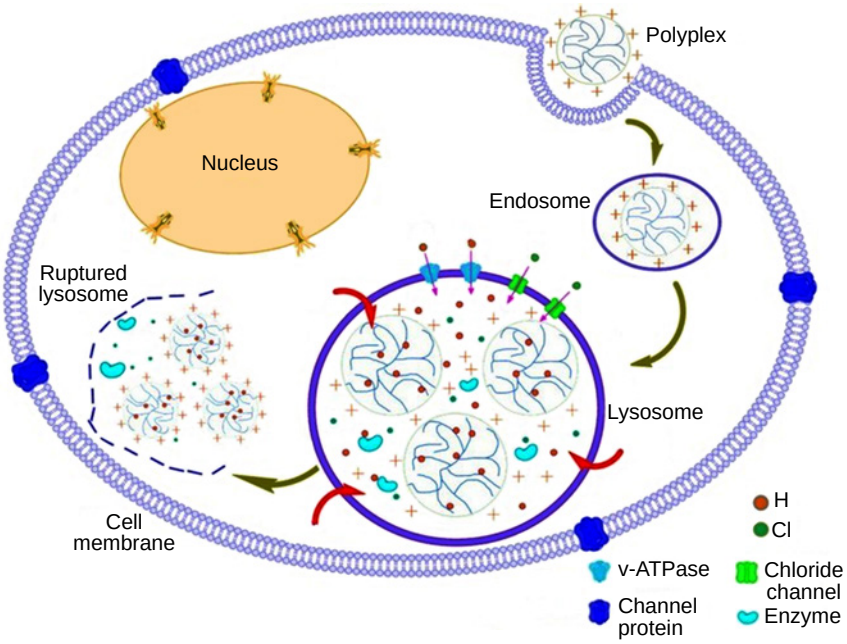

Figure 6. Schematic picture of the proton sponge effect.[126] Published under the CC-BY 4.0 license.

2.1.3. Nuclear membrane

Another difficulty in the targeted delivery of NAs is overcoming the nuclear membrane. The passive transport of NAs into the nucleus is possible during mitosis due to the temporary disassembly of the nuclear envelope; this mechanism makes a higher contribution to the transfection of proliferating cells and a lower contribution for slowly dividing cells such as neurons.[137] The active transport is driven by importin proteins, which recognize specific peptide sequences structurally similar to CPPs, known as nuclear localization signals (NLS). Modification of the carrier with NLS allows nuclear delivery of molecules with a molecular weight (M) of up to 40 kDa; meanwhile, usually, particles larger than 9 nm, which corresponds to $M \approx 1$ kDa, cannot pass through nuclear pore complexes.[138]

Although the nuclear membrane is a double bilayer, the mechanism of crossing the membrane is similar to that involved in crossing the cytoplasmic membrane. The positive charge of the carrier ensures adhesion of the complex on the membrane, which may be followed by penetration of either free DNA molecule[139] or the whole NA–carrier complex[140] into the cell nucleus. This enables transfection of post-mitotic, non-dividing cells.[141,142]

2.2. Types of nucleic acids

Synthetic carriers optimized for one type of nucleic acids are often ineffective for transporting NAs of other types. This may be due to differences in physical properties, such as the size of the biomolecule, or to the need to deliver particular NAs to different intracellular compartments. Kauffman *et al.*[143] showed that a lipid system optimized toward siRNA is not optimal for the therapy using mRNA. A similar fact was established by Kulkarni *et al.*[144] for RNA and plasmid DNA (pDNA). Thus, each major type of NA requires a distinct delivery approach. Specific features of the delivery of mRNA, pDNA, short two-stranded RNA (siRNA, microRNA), and ASO are considered below.

2.2.1. Plasmid DNA

Plasmids are circular DNA molecules ranging in length from 2–3 to 20–100 thousand base pairs, carrying one or more genes. The delivery of DNA vectors opens up the possibilities for three different therapeutic applications:

(1) inhibition of protein expression *via* RNA interference,

(2) temporary protein production by means of expression vectors,

(3) stable expression or knockout of proteins through gene editing.

For functioning of plasmid DNA, it is necessary that it should enter the nucleus where the transcription apparatus is located. However, the first significant problem along this line is cytoplasm. First, the diffusion of DNA molecules, possessing relatively large size and charge, in viscous cytoplasm is severely limited. Second, DNA is subject to the action of nucleases: it was shown that out of the 2–100 thousand copies of the plasmid delivered to the cytoplasm by polyplexes and lipoplexes, only 1–10% enter the nucleus.[145]

The efficiency of nonviral DNA delivery largely depends on characteristics of the DNA vector. As a rule, small size of the vector leads to higher transfection: indeed, the efficiency of lipofection of AoSMC cells proved to be 77 times lower for a plasmid consisting of 52 500 base pairs (bp) than for minicircle DNA (2900 bp).[146] Thus, the absence of a bacterial scaffold (such as a bacterial origin of replication and antibiotic resistance genes) makes the use of minicircle DNA a promising strategy for improving the therapeutic efficacy of DNA vectors.[147] The possible causes for this effect include the increased diffusion coefficient and improved nuclear internalization, as well as more effective transcription of gene expression cassettes with minicircle DNA.[47]

Recent publications report successful *in vivo* delivery of large plasmids (10–15 kbp) using polyplexes (*e.g.*, those based on PAMAM-modified polymethacrylate),[148] lipoplexes (based on DOPE and polycationic OH4 lipid),[149] and hybrid systems.[150] All of the above approaches are combined in a common strategy: increasing the positive charge density of the carrier for more

efficient compaction of large DNA molecules, which includes the use of dendrimer cationic moieties within a polymer, ethyleneimine trimer as a part of OH4 lipid, and polyethylenimine as the condensing core of the hybrid carrier nanoparticle. This assumption is consistent with the published data [151,152] on the importance of DNA compaction for penetration through the nuclear pore complex of postmitotic cells. A relatively less frequent strategy for improving the efficiency of large-size plasmid delivery is the destabilization of the nuclear membrane, achieved either by enlarging the nuclear pores under the action of dexamethasone or by transfecting cells synchronized in the S-phase.[153]

2.2.2. Messenger RNA

The delivery object studied most intensively in recent years [41,70–74] is mRNA, a single-stranded molecule with a length of 1000–5000 nucleotides. The mRNA configuration includes a cap at the 5′-end, 5′-untranslated region, which is followed by open reading frame, 3′-untranslated region, and 3′-poly(A)-tail (Fig. 7*a*). Untranslated regions play a key role in regulating mRNA degradation and translation efficiency, with the 3′- and 5′-untranslated regions influencing the mRNA half-life and efficiency of translation initiation, respectively. The issue of mRNA stability is highly acute even in comparison with other typical therapeutic NAs: due to the action of cellular and serum nucleases, the half-life of RNA administered *in vivo* is approximately 70 s;[154] for pDNA and siRNA, this value is in the range of 5–10 min,[155,156] while that for ASO is >1 h.[157] The efforts to enhance mRNA stability include nucleoside modifications [replacement of uridine by pseudouridine (Ψ), especially by N^1-methylpseudouridine ($m^1\Psi$) (see Fig. 7*c*) [158]],[f] codon optimization, and the use of methyl-guanosine cap analogues for protection against enzymatic decapping.[159] The clinical applications of mRNA include, first of all, mRNA vaccines and mRNA replacement therapy. Meanwhile, mRNA does not need to enter the nucleus; hence, it can be expressed in non-dividing cells, such as liver cells, muscles, and immune cells. This fact accounts for the high value of mRNA for therapy and vaccine development. Irrespective of the particular application, the agent that performs the medicinal function is the encoded protein.

Like the use of DNA, the use of mRNA is faced with the problem of inverse relationship between transfection efficiency and the length of the genetic construct. Teko-Agbo *et al.*[160] demonstrated that upon switching from mRNA with a length of approximately 1 kb to mRNA ~4.8 kb in length, expression of the target protein decreases by two orders of magnitude for the same CPP carrier. The issue of delivery of large RNA molecules is especially relevant in view of the growing interest in self-amplifying RNA (saRNA), in which the target gene is encoded together with alphavirus components. This modification results in higher protein expression per delivered RNA molecule compared to conventional mRNA, which provides a higher efficacy of saRNA vaccines. However, since the size of saRNA is as long as 10 kb, their delivery requires special transfection agents: macromolecular linear PEI [161] or its copolymers with poly(propyleneimine) (PPI),[162] poly(β-amino ester) with

[f] The use of $m^1\Psi$ in mRNA-1273 and BNT162b2 is considered to be a key factor for the high expression and low innate immunogenicity of vaccines.

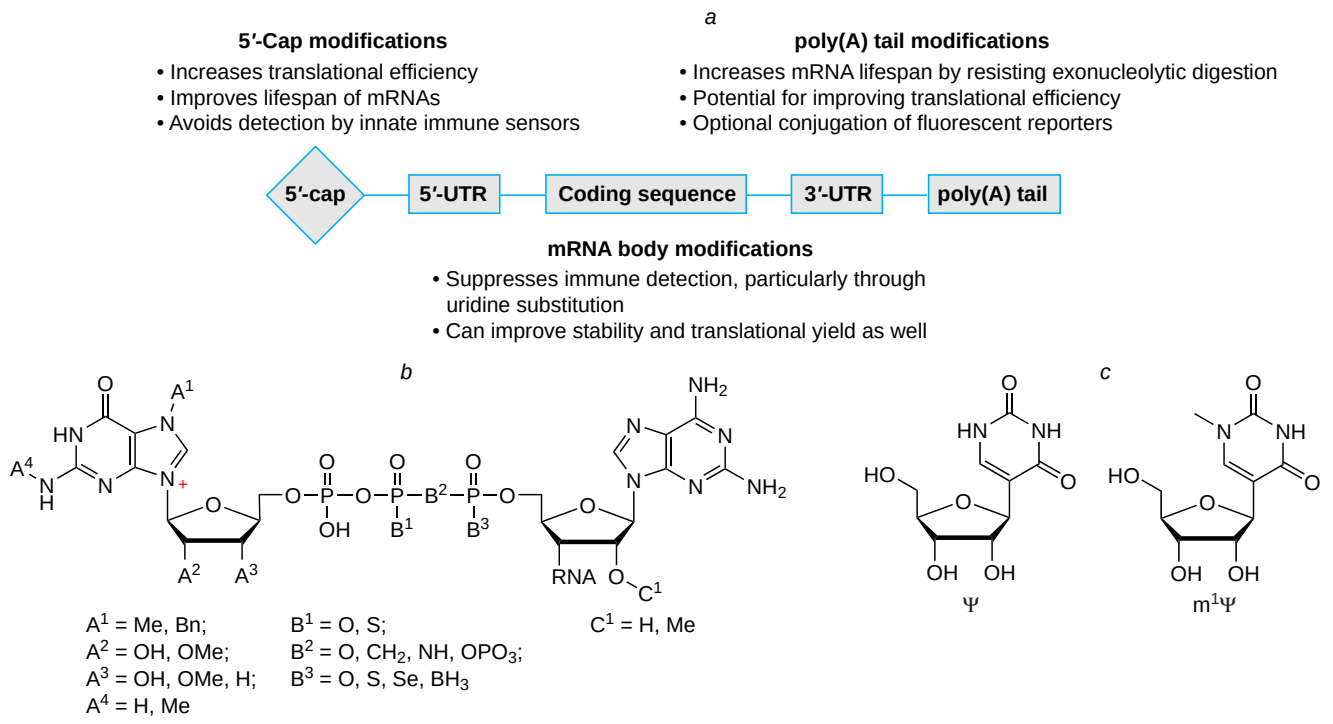

Figure 7. Structure of therapeutic mRNA: cap modification and replacement of mRNA nucleotides by modified nucleotides important for evading the innate immunity and reducing the rate of hydrolysis (*a*), chemical formula of 5′-cap: eukaryotic methylated caps[g] are usually modified at the first base (designated by A), triphosphate (B), or the second base (C) (*b*), and pseudouridine structures (*c*).

[g] mRNA cap is a modified 5′-end of the molecule usually represented by 7-methylguanosine connected to the first mRNA nucleotide by an unusual 5′–5′ triphosphate bond. The cap protects mRNA from exonucleases, participates in the ribosomal recognition, and enhances translation efficiency.

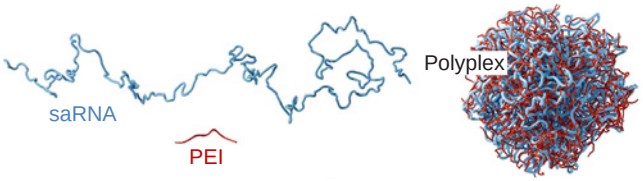

Figure 8. Schematic picture of mRNA and PEI chains and polyplexes they form.[169] Copyright Nature 2025.

increased molecular weight,[163–165] or LNPs with optimized composition.[166–168]

In 2025, branched PEI with $M = 22.5$ kDa was used to develop saRNA vaccines.[169] According to this study, the key to effective for PEI formulations for saRNA is to switch to a specific format of compact monomolecular polyplexes. In the presence of excess polyethylenimine, some saRNA chains (~3 MDa) rearrange from an extended conformation to a dense globule (Fig. 8), thus forming ultrasmall particles (~30 nm) with a high packing density and relatively low proportion of the polymer in the complex. An increase in the ratio of nitrogen-containing (N) groups of the reagent to the phosphate groups (P) of NA (especially if N : P ⩾100) leads to increasing fraction of 'dissolved' (not precipitating) saRNA molecules in polyplexes and monomolecular species, as determined by AF4-MALS and AUC analytical methods[h] and a combination of small-angle neutron scattering (SANS) and small-angle X-ray scattering (SAXS); this finding is correlated with the biological activity. Functionally, this is manifested as a gradual increase in luciferase expression in *in vitro* and *in vivo* experiments with increasing N:P ratio; in vaccination models, this means that comparable humoral and T-cell responses can be elicited at markedly lower doses of saRNA (in terms of the administered RNA, the activity is enhanced as this ratio increases).[169] Under optimized conditions, an approximately tenfold increase in the activity compared to that of conventional saRNA–PEI polyplexes was demonstrated, along with the absence of noticeable toxicity.

Another important aspect of the cited study is detailed physicochemical verification of the compactness and composition of the complexes: the gyration radius (R_g) of the particles was ~12–13 nm and the particles had signs of core–shell structure with PEI-enriched shell, and changes in the RNA secondary structure were observed upon complex formation. In addition, the authors demonstrated the practical 'pharmaceutical' applicability of these polyplexes, particularly their high colloidal stability, retention of integrity (or activity) upon dilution and after freezing or drying, protection of RNA from degradation, and the absence of release into serum. In combination, these factors define the PEI-induced saRNA compaction as a versatile tool for the preparation of ultrasmall, stable, and highly active polymeric RNA vaccines or carriers.

Among numerous studies focused on optimization of the composition of the carrier, few studies that propose new strategies can be distinguished. One such strategy is the design of macromolecules directed toward decreasing immune or allergic reactions, *e.g.*, those containing polysarcosine,[170] instead of widely used hydrophilic poly(ethylene glycol) (PEG), or carriers with variable positive charge[171,172] (these issues are described in more detail in Section 4.1).

[h] AF4-MALS is asymmetrical flow field-flow fractionation coupled with multi-angle light scattering, AUC is analytical ultracentrifugation.

2.2.3. Short double-stranded RNA (siRNA and microRNA)

Small interfering RNA (siRNA, microRNA) are short (~21–23 bases) double-stranded RNA able to induce silencing of particular genes. To achieve the desired effect, siRNA must penetrate into the cytoplasm of the target cells; this is followed by cleavage of the duplex with Dicer endonuclease to form the nucleoprotein RNA-induced silencing complex (RISC) suppressing mRNA targets, which subsequently cuts the complementary mRNA target. Small interfering RNA and related microRNA and short CRISPR sequences (crRNA) are specific delivery objects. On the one hand, their small size facilitates penetration into tissues (some cells can take up such oligonucleotides by themselves), and, on the other hand, small-sized NAs are extremely vulnerable to nucleases and are faster eliminated from the body. Effective intracellular delivery of siRNA requires either chemical modification of the molecules or the use of nanoparticles as carriers. Currently, six siRNA drugs have been approved, and only one of them, patisiran (siRNA targeting the transthyretin gene), is delivered using LNPs. Other drugs are amphiphilic conjugates carrying a trivalent *N*-acetylgalactosamine ligand (Fig. 9). This modification of the siRNA molecule made it possible to develop a series of carrier-free drugs designed for regulating gene expression in the liver (for example, the cholesterol-lowering drug inclisiran).[173] Other conjugates comprise lipids, peptides, sugars, and various functional groups.[174,175] This modification makes it possible to tailor the tissue specificity of the siRNA agent and facilitate cellular uptake by using amphiphilic conjugates. For example, siRNA decorated with a lipid based on distearoylglycerol is not only far superior to nonmodified siRNA in the circulation time and bioavailability, but also surpasses LNPs with the commercial jetPEI carrier regarding the siRNA accumulation rate in a tumour.[176]

Despite the great clinical success of conjugates, the delivery of siRNA using synthetic carriers is also being actively studied.[110,132,177–181] The double-stranded nature is a key distinction of siRNA from mRNA, which must be taken into account in the development of transfection agents. Hayashi *et al.*[182] showed that the rigidity of nucleic acid alone can hinder the secondary self-assembly of polyplexes even for the same nature and charge stoichiometry. A comparison of single-stranded RNA (ssRNA, flexible chain) and siRNA (rigid short duplex) with the same sequence of 21 bases showed that at low concentrations, both systems form 1 : 1 adducts with the PEG-PLL block copolymer (*i.e.*, one polymer molecule per NA molecule) and with single polyion complexes (uPIC). However, above the critical association concentration, the behaviour of uPIC is appreciably different: ssRNA–uPIC are aggregated to micelles of ~30–70 nm size, while siRNA–uPIC retain stability as small complexes (~10 nm). This difference is crucially important for systemic administration:[i] small and well-determined size of uPIC should ensure more predictable pharmacokinetics, decrease the tendency toward concentration-dependent aggregation, and reduce the probability of non-specific capture of particles by the mononuclear phagocytic system compared to that for larger and more polydisperse associates.

Apart from conjugation, an integral feature of siRNA is the possibility of chemical modification of the proper oligonucleotide

[i] Administration methods of therapeutic agents fall into two main categories: systemic (affecting the whole body) and topical (targeting a particular site).

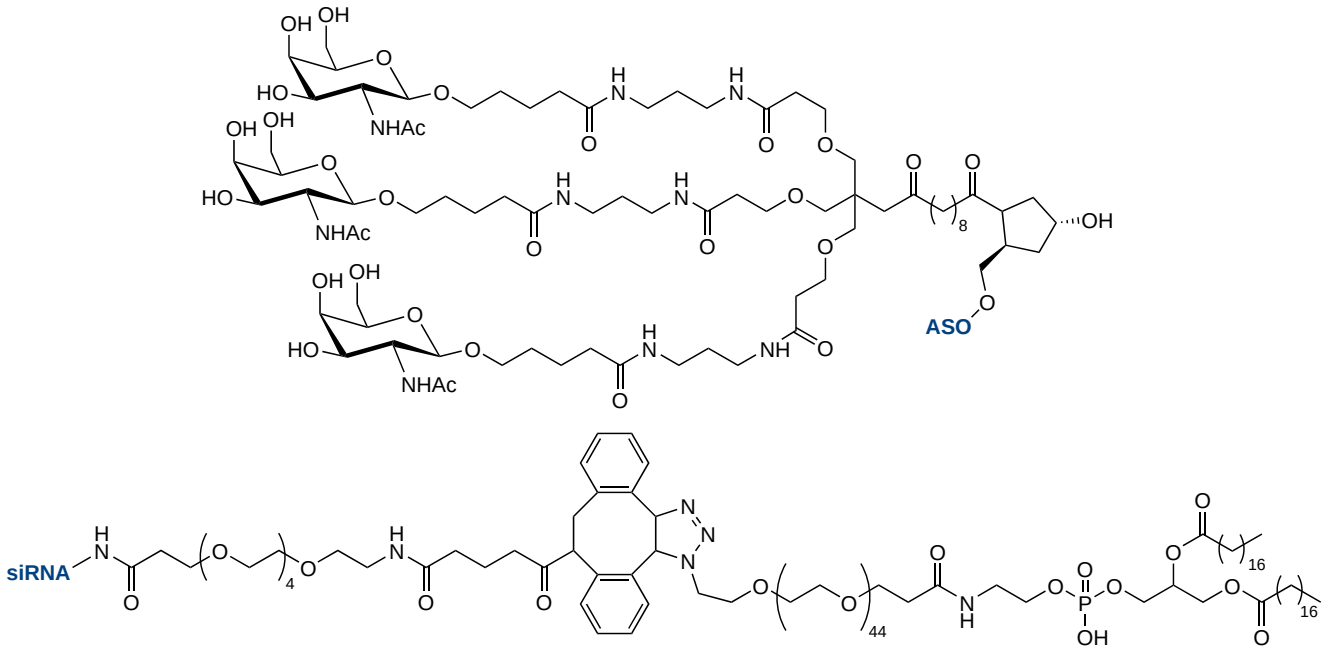

Figure 9. Structures of TriGalNAc (*above*) and siRNA lipoconjugate (*below*).

chain, with the goal to enhance binding to target sequences, increase the stability against nucleases, optimize the pharmacokinetic properties, and minimize side effects. Modifications may affect the phosphate backbone, sugar residues, and nitrogenous bases (Fig. 10). The following changes are most popular in the siRNA chemistry: replacement of the ribose 2′-OH group by 2′-OMe and 2′-F groups; replacement of phosphate groups by phosphorothioate groups, typically two at the 5′-end of the sense strand and at both ends of the antisense strand (Fig. 11).[183]

In addition, various oligomerization strategies based on covalent or ionic binding are used to increase the stability of therapeutic siRNA in the body. At the laboratory level, good results were achieved for disulfide cross-linked linear poly-siRNA, thiol–maleimide cross-linked branched poly-siRNA, and siRNA oligomerized owing to short complementary A(5–8)/T(5–8) 3′-overhanging ends.[184] Oligomeric RNAs are the subject of a review by Kim *et al.*[185] published in 2022. Oligomerization can be achieved by introducing a thiol group at the 5′-end of the sense and antisense sequences (Fig. 12 *a*),[186] which gives rise to siRNA as a mixture of oligomers sensitive to redox processes. 'Polymerized' siRNA forms smaller and more stable NPs with PEI and ensures more effective decrease in the target gene expression than 'monomeric' siRNA. Polyacrylamide gel electrophoresis reveals a broad molecular weight distribution of 'polymerized' siRNA and the regeneration of the monomeric form on treatment with dithiothreitol (see Fig. 12 *b*).

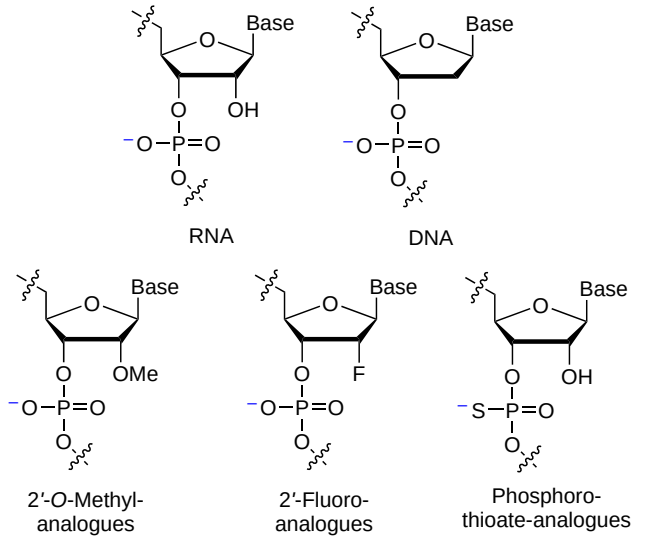

Figure 10. Structures of nucleotides and their modified analogues.

Hong *et al.*[187] demonstrated the effect of branching reagents (Fig. 13). As the number of branches increased, the size of the polyplexes of microhydrogels with linear PEI decreased: ~100 nm for YY-siRNA, ~215 nm for M-siRNA, and micrometre-scale aggregates for 'monomeric' siRNA. Simultaneously, the efficiency of knockdown increased. For example, upon transfection of the MDA-MB-435 cells with the YY-siRNA–PEI system, the expression of the GFP gene decreased to 27.9% compared to the control, whereas the use of M-siRNA and 'monomeric' siRNA resulted in expression values of 70.5 and 87.7%, respectively.[187]

2.2.4. Antisense oligonucleotides

Antisense oligonucleotides (ASO) are short (usually, 15–25 nucleotides long) single-stranded molecules complementary to definite mRNA targets (Fig. 14). These compounds do not trigger the RNA interference mechanism; the mechanism of their action involves blocking of translation or change in splicing.[188] Currently, they are considered to be the most numerous class among approved NA-based pharmaceuticals; and many of them are gapmers, that is, compounds in which two series of modified ribonucleotides are separated by a sequence of deoxyribonucleotides (Fig. 15). The chemical structure of ASOs generally undergoes more extensive chemical modification than siRNAs. As a rule, phosphorothioate linkers completely replace the phosphate groups, and if the nucleoside

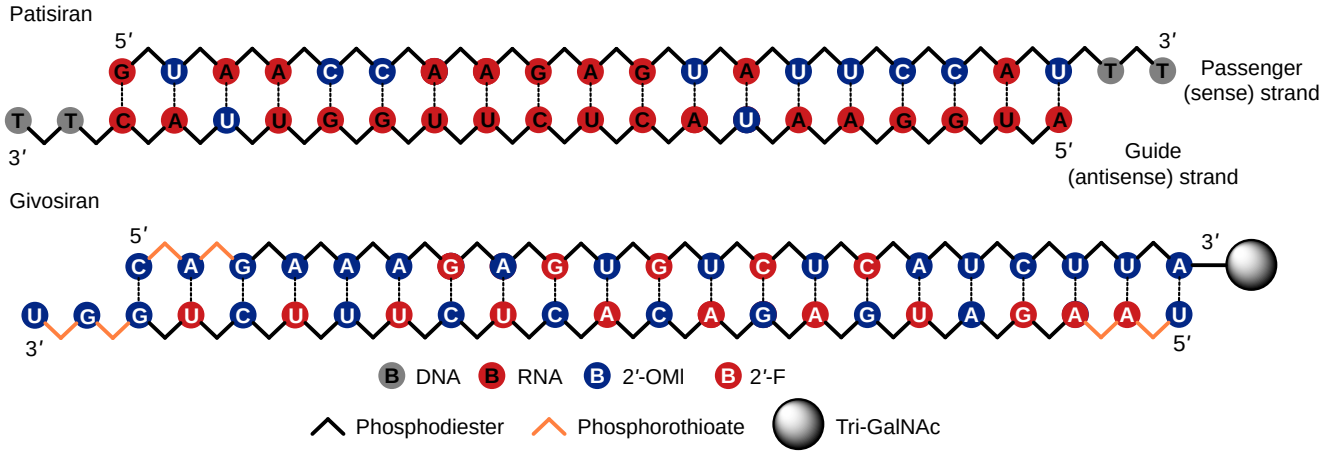

Figure 11. Structures of siRNA-based drugs.

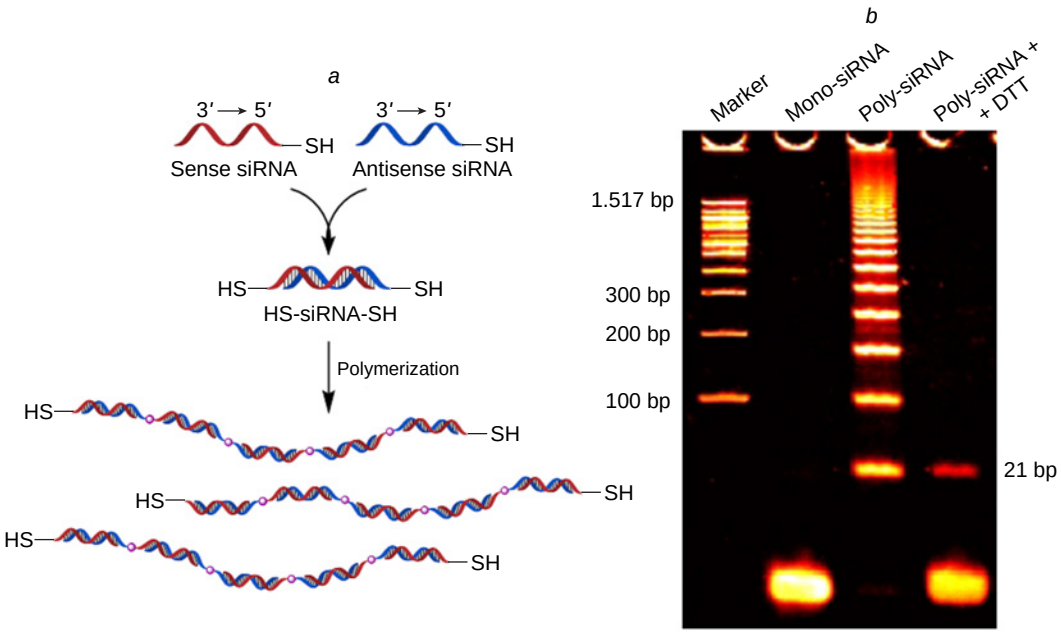

Figure 12. siRNA oligomerization strategies: introduction of a thiol group at the 5′-end of the sense and antisense sequences (*a*) and results of polyacrylamide gel electrophoresis of 'polymerized' siRNA (*b*).[186] Copyright Elsevier 2010.

is not a deoxyribose derivative, the 2′-hydroxyl group is always protected (most often, by the methoxyethyl protection). In addition, the 5-position of the pyrimidine base is often modified in ASO.

Nucleoside analogues other than carbohydrates have also been used in the ASO design, *e.g.*, morpholine derivatives (already FDA-approved), propylene glycol derivatives (glycol-nucleic acid, GNA), *N*-(2-aminoethyl)glycine derivatives (peptide-nucleic acid, PNA), *etc.*, and the resulting compounds are being evaluated in clinical trials.[174,189,190] Chemical modifications endow ASO molecules with the ability to bind to blood plasma proteins and penetrate into cells without the need for special carriers (for example, nusinersen is administered into the cerebrospinal fluid as an aqueous solution). However, some approved ASO-based drugs are GalNAc conjugates, which gives them considerable advantages. For example, eplontersen modified at the 5′-end is administered to patients in a five times lower dose and four times less frequently than the analogous inotersen drug without a ligand.[188] Synthetic carriers, both lipid- and polymer-based ones, are still rarely used for ASO. They serve for addressing special issues such as

— targeted delivery of ASO to tumour tissues (an example is four-component LNP with PEG-lipid modified with iRGD peptide, which contains the arginine–glycine–aspartic acid, the integrin receptor recognition site of cell membranes),[191]

— delivery of ASO to sentinel lymph nodes to suppress metastasis (*e.g.*, glycine–lysine oligopeptide with a PEG block optimized in length),[192] or

— crossing the blood–brain barrier in the central nervous system by ASO [*e.g.*, copolymer of thiol- and nicotinamide-modified poly(*L*-lysine) with PEG].[193]

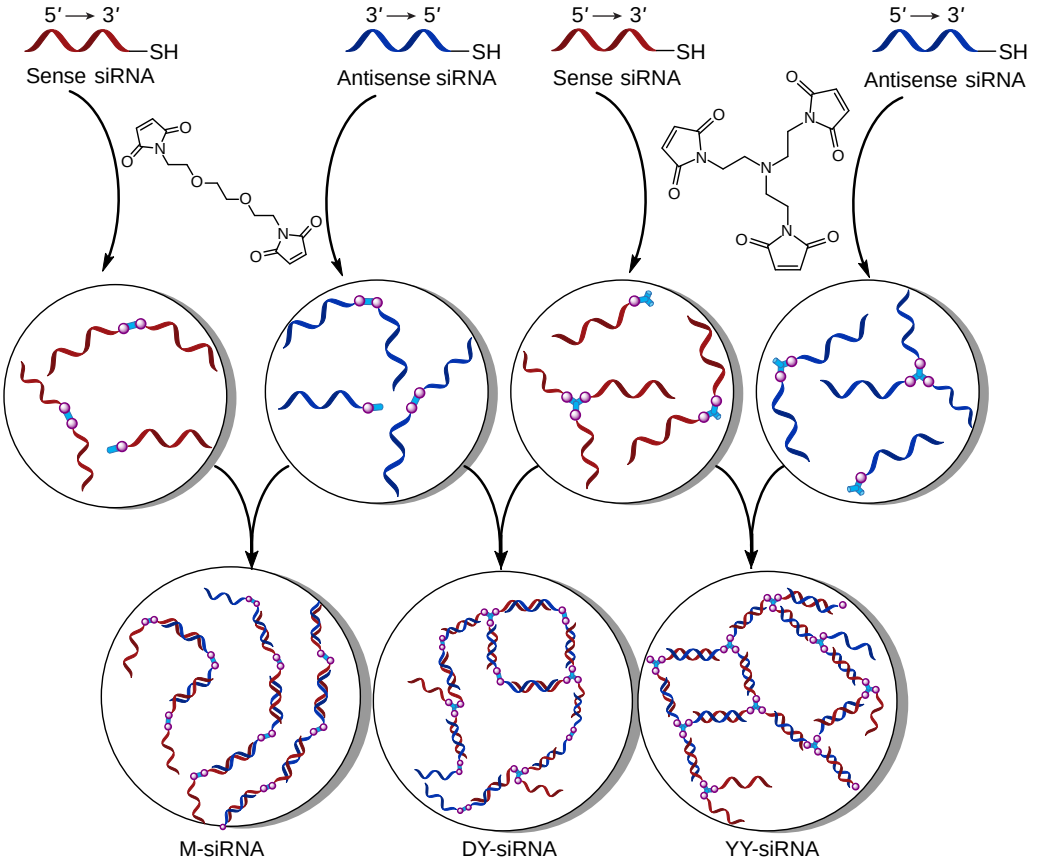

Figure 13. Schematic diagram of the preparation of microhydrogels based on 3 ′-mercapto siRNA derivative involving dimeric and trimeric maleimide linkers.[187]

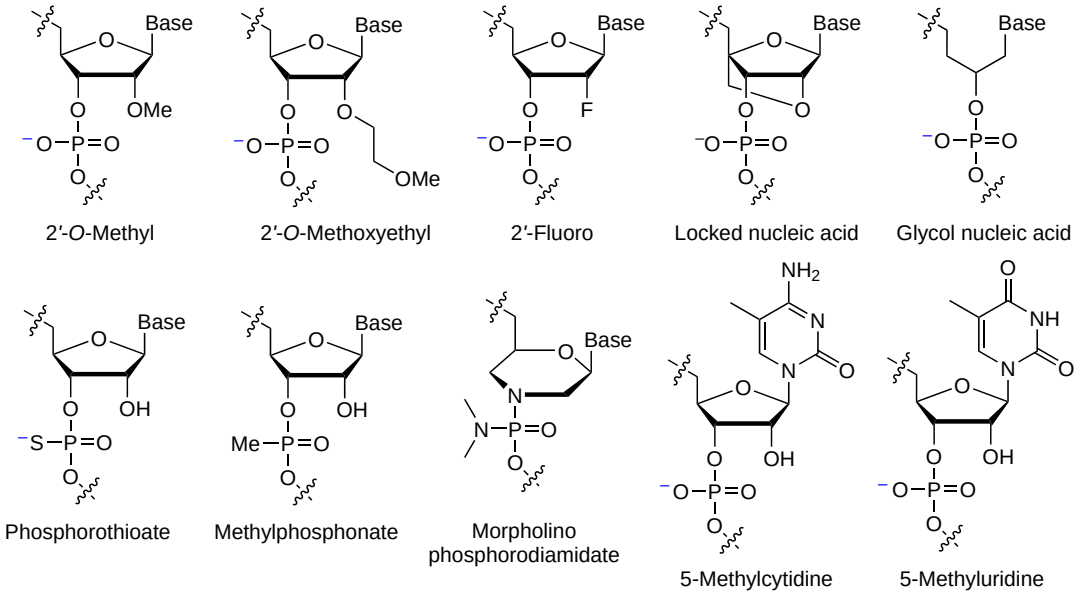

Figure 14. Structures of modified nucleotides.

3. Polymeric carriers for NAs: main types and synthetic approaches

3.1. Main types of polymeric carriers for NAs

Macromolecules with positively charged groups are traditionally considered as polymeric carriers for NAs. The vast majority of these polymers contain amino groups or ammonium cations (R_3N^+), although there are also examples of macromolecules with phosphonium (R_3P^+) or sulfonium (R_2S^+) cations. The main structural types of polymers that are of interest for NA delivery can be divided into two fundamentally different groups. The first group comprises polycations, which may optionally include a reactive group intended for subsequent

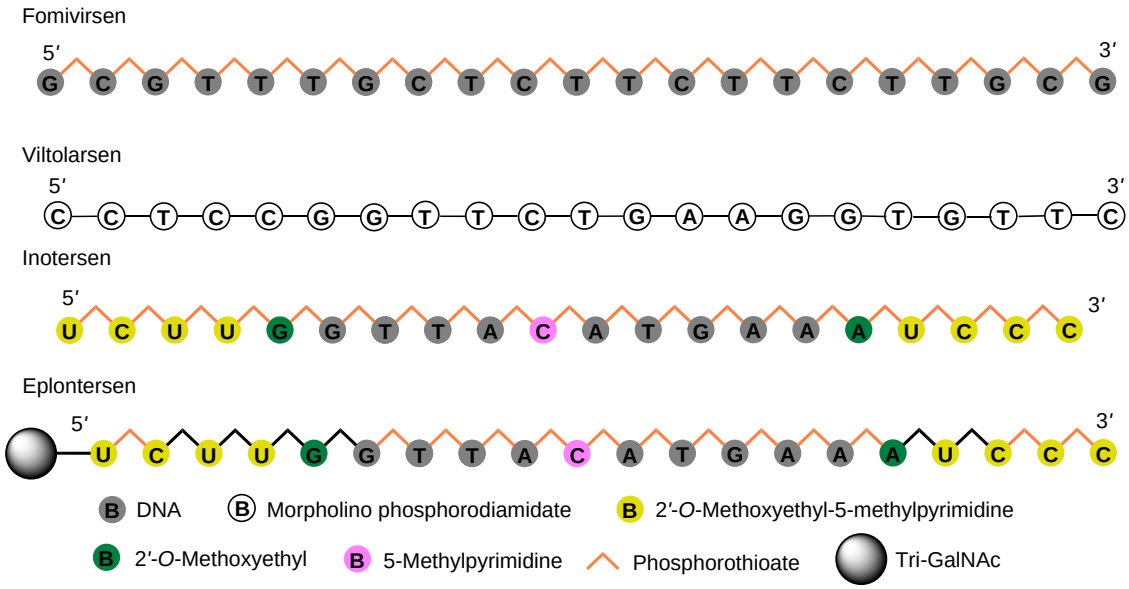

Figure 15. Structures of pharmaceutical agents based on antisense oligonucleotides.

functionalization, or a structural moiety that serves as a receptor for targeted delivery. The second group consists of amphiphilic macromolecules designed according to the all-in-one principle. These polymeric carriers for NAs combine all (or almost all) required functions in one macromolecule. A classic example of these systems are charge-altering releasable transporters (CART), polymeric delivery systems developed by Waymouth's research team (see Section 4.1). The structural types of polymers of the former group can obviously be used for the design of more complex systems.

Both natural and synthetic polymers are used for NA delivery. Among natural polymers, a lot of attention has been devoted to proteins (in particular, histones enriched with ionizable *L*-lysine and *L*-arginine moieties, Fig. 16).[76] In a study published in 2020, Kuzmich *et al.*,[194] demonstrated high efficiency of the histone H2A adduct with the platelet-derived growth factor receptor (PDGFR) for the delivery of DNA to the PDGFR-positive gastric cancer cells. Histones are nontoxic; however, their clinical use raises reasonable concerns due to the risks of interfering with the natural processes of chromatin formation.

Gelatin is much safer and more readily available than histones and is attractive because of the presence of RGD sequence, which promotes cell adhesion.[76] However, there are no recent publications on the NA delivery using gelatin, presumably due to the greater efficiency of synthetic polymers and chitosan (see below). The application of *L*-arginine-enriched protamine (see Fig. 16) for the NA delivery is the subject of a review by Pascolo and co-workers.[195] Furthermore, promising results in the cancer therapy were demonstrated by protamine-containing agents based on mRNA[196,197] and siRNA.[198,199] Protamine forms stable complexes with NAs and, therefore, it can be used as a part of transfecting agents that are effective even upon intranasal administration.[200]

DEAE-dextran (the structure is presented above), one of the first polymeric NA delivery agents, can also be classified as a polymer of natural origin.[23–25] The relatively low efficiency, inability to form stable polyplexes, and proven immunogenicity and cytotoxicity[201] resulted in the loss of interest in this carrier. However, in 2019, Siewert *et al.*[202] reported the use of DEAE-dextran as a model compound for the preparation of mRNA polyplexes. Cyclodextrin is not a polycation; however, when combined with the block copolymer composed of methyl-polyethylene glycol (mPEG), ε-caprolactone (εCL), and PEI, it forms a hydrogel for the delivery and controlled release of pDNA, which lasts for up to 7 days.[203]

Chitosan remains an intensively studied polycationic polymer of natural origin; it is the subject of a number of recent reviews.[36,94–96] The safety of chitosan-containing formulations is still an open issue, with potential complications associated with the use of chitosan being related to the nature of the source and the isolation and purification methods. This is a common problem in the biomedical application of naturally occurring polymers (a classic example is the contamination of silk fibroin with sericin),[204] which is an argument in favour of developing synthetic polymers with strictly defined composition, microstructure, and topology.

Structurally related PAMAM, PEI, PPI[91–93] should rather be classified as oligomers with a dendrimer topology; they represent relatively simple organic molecules containing a large number of ionizable moieties of primary, secondary, and tertiary aliphatic amines. These polycations have been widely studied and continue to be studied as NA delivery agents, as they have high complex-forming capacity. However, use of these compounds into clinical practice is reasonably complicated by the high toxicity characteristic of polyamines. Meanwhile, the application of these polymers in genetic techniques *ex vivo* is fairly efficient. In 2025, a manufacturer reported the registration of a linear PEI-based reagent for use in the production of adeno-associated viral vectors.[205] The benefits of PEI are synthetic availability and high buffer capacity. Numerous studies addressing the decrease in the toxicity of this polymer by introducing biodegradable moieties into the molecule are covered in a recent review.[206]

In terms of its structure, PDMAEMA (see Section 1) is a synthetic vinyl polymer. The polymerization products of vinyl monomers, although commercially available, have an insurmountable drawback: high chemical stability of the backbone; therefore, they are currently being displaced by biodegradable polymers.

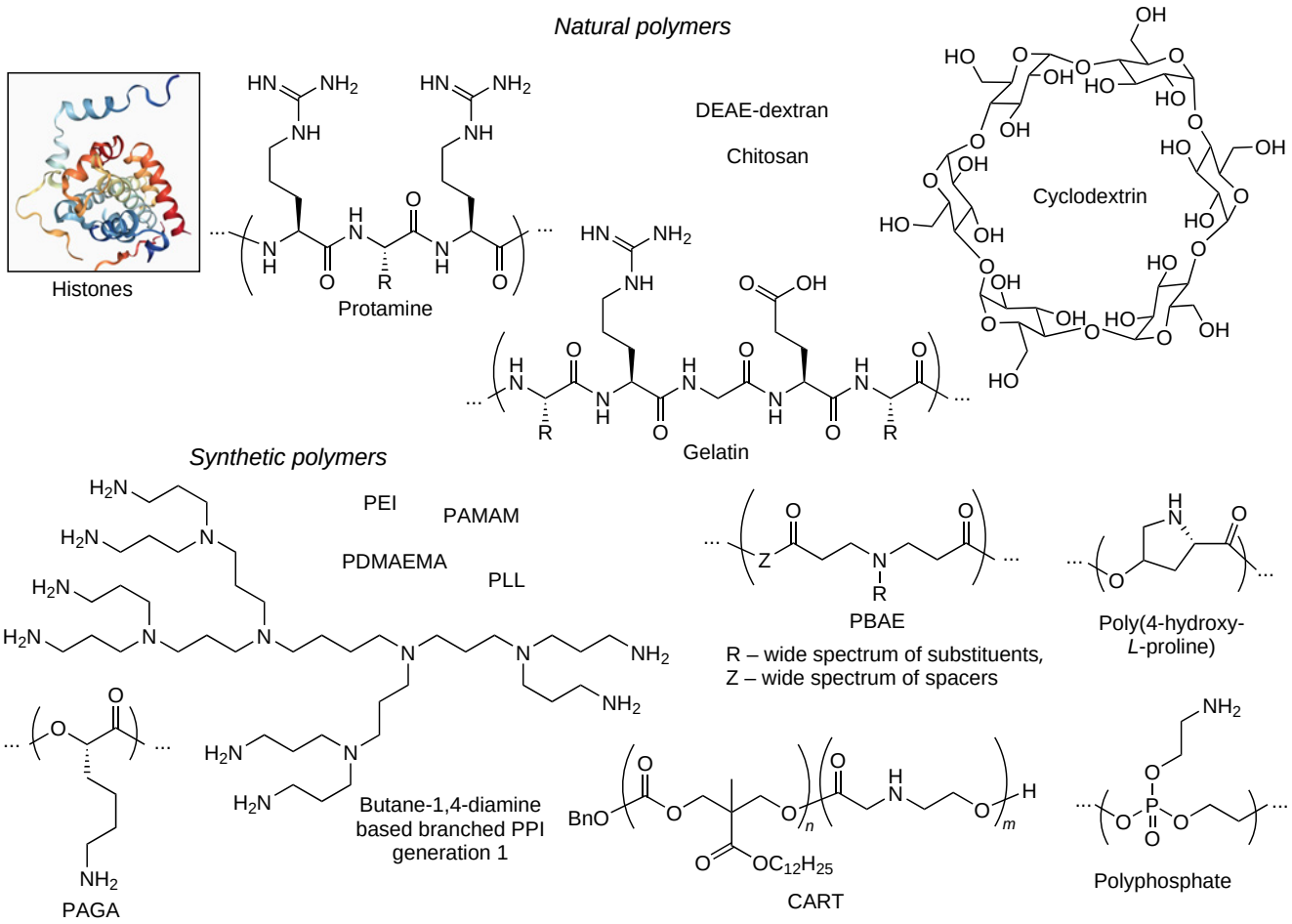

Figure 16. Main structural types of polymeric NA carriers.

Synthetic polyamides, *e.g.* PLL, refer to biodegradable polymers. PLL was intensively studied up to the mid-2010s;[207] However, only two papers describing the use of PLL as a carrier for NAs appeared over the past five years. Alazzo *et al*.[208] used hyperbranched PLL containing histidine moieties for the delivery of siRNA. Korzhikova-Vlakh and co-workers[209] utilized PLL moieties for the preparation of hyaluronic acid-based graft copolymers that formed particles of 173–262 and 160–185 nm sizes with model siRNA and salmon testes DNA, respectively.

Unlike study of PLL, investigation of poly(β-amino esters) obtained by reactions of amines with diacrylates are still relevant.[86] The interest in these systems stems from the ease of synthesis (see Section 3.2) and the possibility of varying the structure of polymers of this type over wide limits at minimal cost. Owing to the considerably lower toxicity compared to those of PEI, PPI, and PAMAM and extensive design opportunities involving variation of hydrophilicity, hydrophobicity, and macromolecular topology, PβAE still attract keen attention of researchers.[86–90] The biodegradability of these polymers is achieved by introduction of labile groups into the Z moiety (see Fig. 16).

Meanwhile, the biodegradability of polymeric NA delivery systems can also be achieved by introducing reactive groups into the backbone such as regularly repeating ester moieties. The products of polycondensation of 4-hydroxy-*L*-proline (see Section 3.2) known since the late 1990s were the first examples of polymers of this type.[210] Currently, there is increase in the interest in these systems caused by the ease of their hydrolytic degradation to release NAs (see Section 4.1). A promising trend in the design of polymeric NA carriers is the preparation of macromolecules that degrade to give low-molecular-weight neutral (or at least zwitter-ionic) products, which is accompanied by the release of NAs. An early example of such polymers is poly[α-(4-aminobutyl)-*L*-glycolic acid] (PAGA).[211] The PAGA structural moiety was successfully used by Korzhikova-Vlakh and co-workers[212] to develop an amphiphilic block copolymer for the delivery of siRNA.

The idea of NA release upon the polyester chain degradation to low-molecular-weight products incapable of binding NAs was further developed in the design of CART (see Fig. 16; for more detailed consideration, see Section 4.1). These block copolymers, which contain lipophilic and polycationic segments, serve as a complete polymeric delivery system for NA.

Apart from carboxylic acid polyesters, polyesters derived from phosphoric acid were also studied as NA carriers. Among the advantages of polyphosphoesters (see Fig. 16), mention should be made of the possibility of varying substituents at the phosphorus atom and relative ease of the synthesis from five-membered cyclic monomers (see Section 3.2).[213]

A specific group of polymeric NA delivery systems are so-called dynamic covalent polymers that contain functional groups that can degrade in the cell.[75,214] Examples of the synthesis of systems of this type are depicted in Schemes 1–3.

Upon backbone degradation, polymers containing only reactive C(O)NH**NH=CH** groups (see Scheme 1) form low-molecular-weight cationic fragments that bind NAs less effectively. Polymers that are depicted in Scheme 2 act in a

Scheme 1

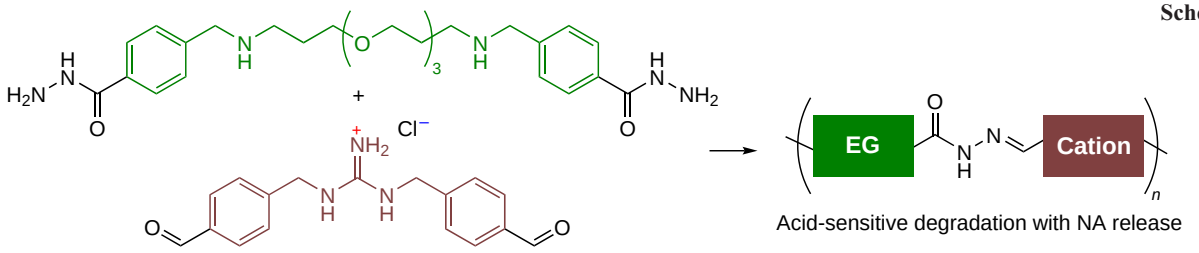

Scheme 2

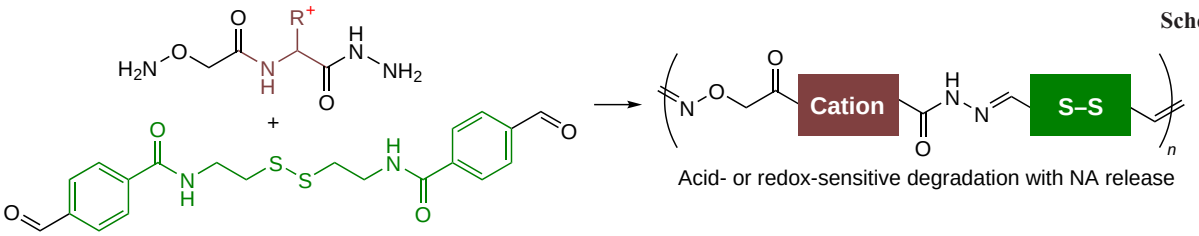

Scheme 3

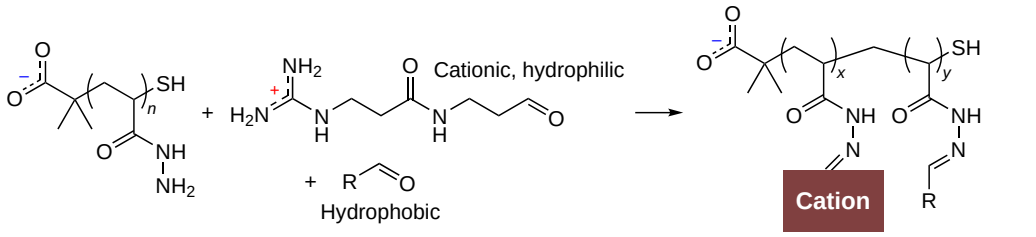

similar way, that is, they undergo degradation of the backbone. The degradation of these systems may occur by a hydrolytic mechanism owing to the presence of labile C(O)NH**NH=CH** and ONH**NH=CH** moieties or by a redox mechanism through cleavage of the disulfide bridge.

The hydrolytic mechanism also underlies the action of polymers that are depicted in Fig. 3; however, these polymers degrade with retention of their backbone, which loses the ability to bind to NAs.

Amines are not the only functional group capable of forming cations that are stable in physiological media. Dozens of studies have been devoted to the synthesis and investigation of polymers containing phosphonium or sulfonium cationic groups (see, for example, Refs 215 and 216, respectively). However, the studies did not achieve any breakthrough results that would have counterbalanced the complexity of synthesis and the potential risks associated with the toxicity and immunogenicity of such systems. The amino group still remains the major functional group for NA binding.

3.2. Synthesis of polymeric carriers for NAs

The synthesis of polymeric carriers for nucleic acids is inseparable from the design of the macromolecule, which, in turn, is determined by the particular task (the type of NA to be delivered, the characteristics of the target cells or organs) and the requirements for the carrier (see Section 4). The biodegradability is determined by the type of polymer backbone, which either contains or does not contain labile structural moieties. Depending on the type of the polymer backbone and microstructure, the carriers are prepared using free radical (co)-polymerization, polycondensation, polyaddition, and ring-opening polymerization.

The design and the synthesis of a macromolecule are determined, in particular, by the general type of the polymer carrier, first of all, the number of functional components. Quite a few polymeric carriers are relatively simple polycations that are used in formulations for the delivery of NAs. Qualitatively different and substantially more complex and research-intensive approaches are aimed at developing polymeric carriers that combine the key functions of multicomponent systems used for lipofection. The main chemical approaches to the synthesis of structurally diverse polymeric NA carriers are considered below. In this Section, we aimed to draw attention to the key chemical aspects of particular processes in the light of the goal to design effective agents for polyfection. The main challenge in the synthesis of such polymers is correspondence of the model developed during the macromolecule design to the actual result. A criterion of correspondence is analysis of reaction products, which is often a non-trivial task.

3.2.1. Free radical polymerization

Despite the obvious problems with biodegradability of the products of polymerization of vinyl monomers, studies of these compounds still remain relevant. Only advanced methods of free radical polymerization that can ensure a high degree of control over the polymer chain are applicable for the synthesis of polymeric NA delivery systems. A special review[217] devoted to the use of radical polymerization for the synthesis of NA carriers attribute these methods to living polymerization processes; Russian authors use the term 'pseudo-living polymerization'.[218] This attribution is due to the specific nature of free radical polymerization, which does not allow for the prolonged existence of a 'bare' end of the growing polymer chain, usually represented by a tertiary alkyl radical. Particularly the preservation of the chain reactivity through reversible

binding of the active site is implied when free-radical polymerization mechanisms are attributed to living polymerization. This camouflage is achieved using the following main approaches:

— polymerization mediated by stable radicals (most often, nitroxide radicals) (Scheme 4),

Scheme 4

Stable free radical polymerization

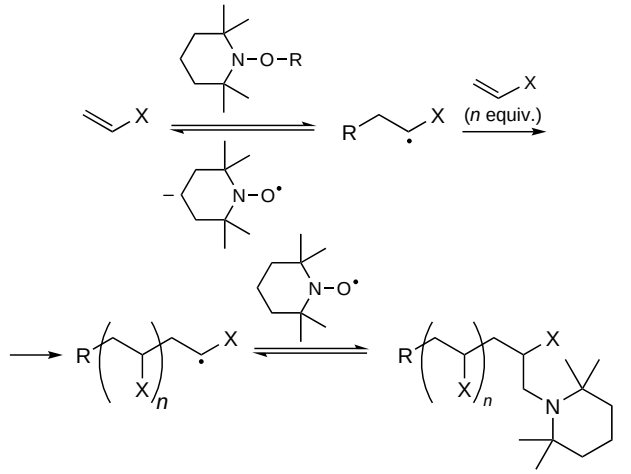

— atom transfer radical polymerization (ATRP) (Scheme 5),

Scheme 5

Atom transfer radical polymerization (ATRP)

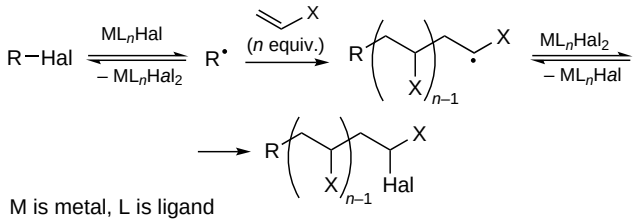

M is metal, L is ligand

— Reversible addition fragmentation chain transfer (RAFT) polymerization (Scheme 6).

Scheme 6

Reversible addition-fragmentation chain transfer (RAFT)

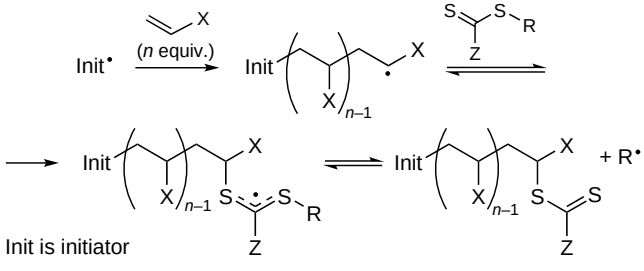

Init is initiator

Most often, RAFT and ATRP processes are used to synthesize polymers for NA delivery, with amino-containing esters and amides of methacrylic acid being typically used as monomers. Using ATRP, the PDMAEMA polymer with a number-average molecular weight (M_n) > 300 kDa was successfully synthesized.[219] In 2026, copolymers of (2-aminoethyl)methacrylamide and 2-hydroxyethyl methacrylate were synthesized using RAFT polymerization (It is worth noting that the authors[220] did not provide data on the molecular weight distribution of the copolymers). Living polymerization processes have been claimed to achieve a dispersity ($Đ_M$) of approximately 1,[217] which seems doubtful on general grounds. The review by Li *et al*.[80] devoted to relevant polymeric delivery agents for NAs virtually does not consider acrylates, probably due to their chemical stability. From this perspective, biodegradable polymers are more appropriate.

3.2.2. Polycondensation

The control of the polymer chain in the polycondensation is even more difficult than in the case of simple polymerization. It is possible to prepare polyesters and polyamides in this way; however, alternative approaches for the synthesis of these polymers have been developed, making it possible to achieve $Đ_M \approx 1$ (see Section 3.2.4).

3.2.3. Polyaddition

Polyaddition is a key step in the synthesis of PPI dendrimers, which includes the reaction of diamine with acrylonitrile and the subsequent hydrogenation, while repeating this reaction makes it possible to synthesize higher-generation dendrimers (Scheme 7).[221] The reaction with acrylates underlies also the synthesis of PAMAM dendrimers using NH_3, ethylenediamine, or $N(CH_2CH_2OH)_3$ as the starting compounds (an example with ethylenediamine is shown in Scheme 8); the reaction sequences include the step of condensation of ester with ethylenediamine.[222] The Michael polyaddition is an effective method for controlling the chain; however, for obvious reasons, in the case of PPI, this control applies only to dendrimers, since the hydrogenation of the nitrile group affords a primary amino group. During the synthesis of PPI and PAMAM, additional functional groups can be introduced into the dendrimer structure, and the size of the macromolecules is specified by the synthesis generation, that is, the number of reaction sequences.[223]

Currently, the Michael addition is widely used to prepare PβAE. Zhang *et al*.[224] reported the synthesis of an effective mRNA carrier from butane-1,4-diol diacrylate and 4-aminobutan-1-ol and the use of this carrier, in combination with dimannosylated poly(glutamic acid), for the targeted

Scheme 7

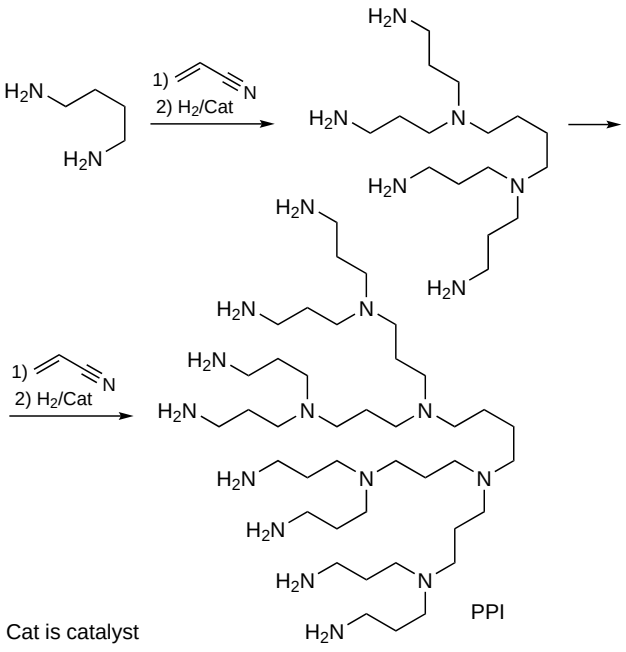

Cat is catalyst

Scheme 8

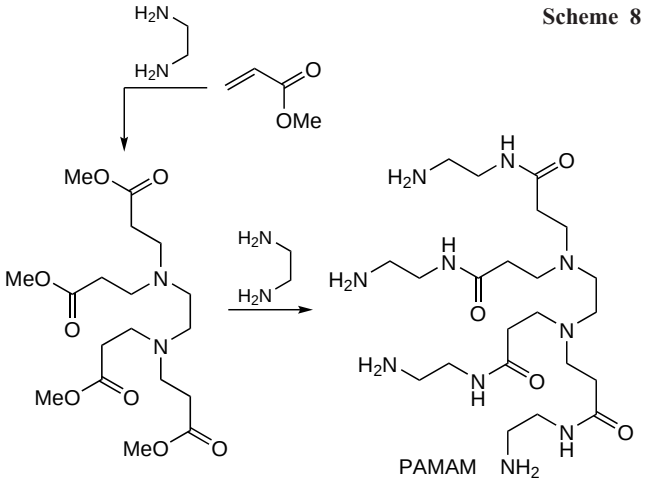

delivery of mRNA into macrophages (anti-tumour programming).

3.2.4. Ring-opening polymerization

Ring-opening polymerization (ROP) following transesterification mechanism (ROTEP) is an effective synthetic tool providing a high degree of control over the polymer chain (unlike ring-opening metathesis polymerization, ROMP). Among the known methods of additive polymerization, only ROTEP gives linear homopolymers and block copolymers characterized by $Đ_M \approx 1$. Despite the seeming simplicity of the method and the reaction mechanism (shown in Scheme 9 for coordination ROTEP), the successful design of a macromolecule and practical design implementation require a high level of experimental expertise (conducting reactions in an inert atmosphere and high purity of reactants) and judicious selection of cyclic substrates and catalysts. An additional benefit of ROTEP is inertness of the protected amino group [*e.g.*, using the *tert*-butoxycarbonyl (Boc) protection] when ROTEP is initiated by metal alkoxy complexes with alcohols (ROH) in the presence of basic organocatalysts.

Scheme 9

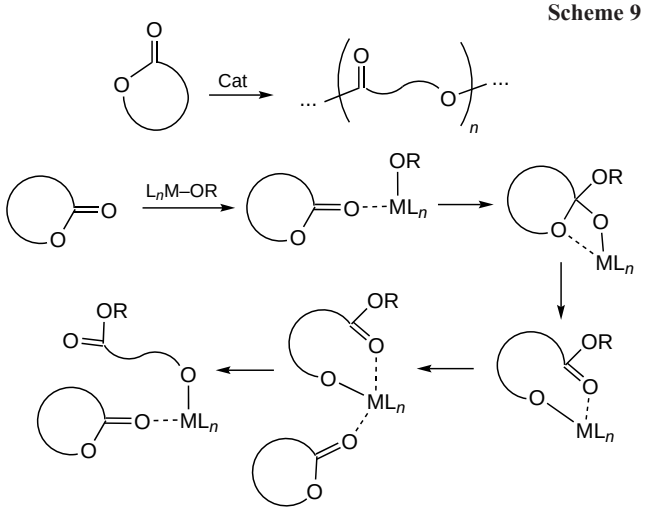

The ROP reaction can be driven by not only strain in the cyclic monomer, but also by the entropy factor. A classic example of additive polymerization to give a low-molecular-weight product, CO_2, which is responsible for the exergonic nature of the reaction is the synthesis of poly[α-(4-aminobutyl)-*L*-glycolic acid] (PAGA). Scheme 10 presents a relevant example of the synthesis of amphiphilic block copolymer using this approach.[212]

Scheme 10

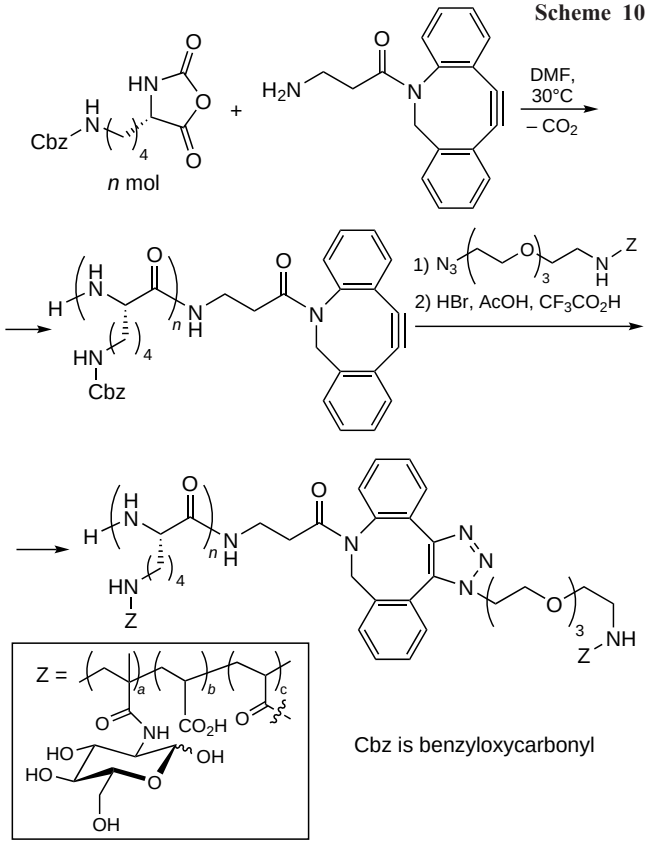

It is noteworthy that ROP is also used in the synthesis of PEI; the reaction gives either dendrimers or linear polymers depending on the type of starting monomer (Scheme 11).[225]

The reasonable choice of the monomer and selection of the catalyst are the key criteria of success in the synthesis of polymers by ROTEP. Examples of implementation of this design are studies on the synthesis of CART (see Section 4.1). The main classes of the polymeric carriers for NAs are summarized in Table 2.

Scheme 11

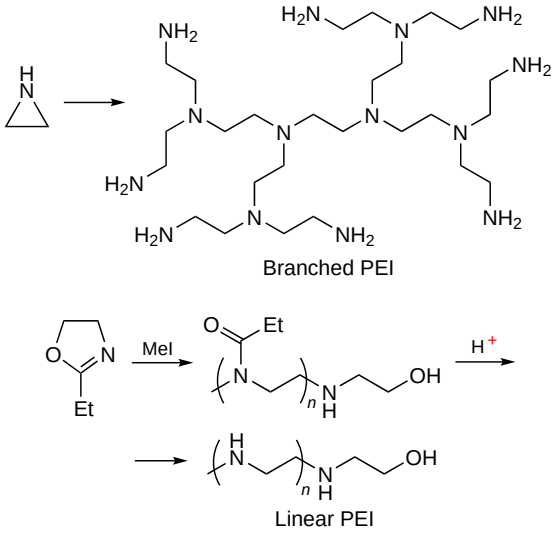

Table 2. Main classes of polymeric carriers for nucleic acids.

Class of polymeric carriers	Mechanism for the release of NAs or deactivation of the carrier	Key benefits	Key limitations
Poly(β-amino esters) (PβAE)	Hydrolysis of the β-amino ester chain, decrease in the molecular weight and cation density; partial dissociation of the polyplex	High synthetic variability, biodegradation, good compatibility with pDNA, mRNA, and siRNA, the possibility of fast screening of polymer libraries	Polydispersity, the necessity of complete modification of the terminal acrylate units, as well as sensitivity to pH and mixing conditions; potential cytotoxicity in the presence of excess polymer
Polymeric charge-altering releasable transporters (CART)	Degradation with charge altering: cationic carrier is converted into neutral small molecules, thus weakening the NA binding	Simple chemical design: strong binding to NA during the assembly of polyplex and fast loss of charge after delivery; low residual cationic toxicity	Sophisticated synthesis compared to that of simple polymers (*e.g.*, PβAE or PEI); the structure must be adjusted to ensure the desired degradation kinetics.
Poly(α-amino acids) from *N*-carboxyanhydrides (NCA)	Proteolytic or hydrolytic degradation of the polypeptide chain; release of NA also *via* the competition with intracellular polyanions	Bio-inspired polypeptide backbone, controlled NCA polymerization, and the possibility of precise tuning of *M* and architecture	PLL often binds NAs too strongly and poorly provides the endosomal escape; poly(*L*-arginine) (PLR) may be more membrane-active and toxic
Polyaspartamides (PAsp) and their derivatives	Hydrolytic or biodegradable polyaspartamide base; change in the proportion of protonated side-chain amino groups; dissociation upon competition with biomolecules	A very convenient platform for studying the structure–activity relationship: it is possible to change the polyamine and adjust the hydrophobicity of the carrier	High dependence on the degree of substitution and residual groups; cytotoxicity is possible at high cation density
Polyethyleneimine (PEI) and degradable PEI derivatives	For pristine PEI, dissociation is mainly due to competition with polyanions and intracellular dilution; for modified PEI, the degradation is redox-stimulated or caused by hydrolysis	Historical benchmark, high buffer capacity, simple formulation, extensive experience of application	Non-degradability, charge-mediated toxicity, aggregation with proteins, weak regulatory outlook for non-modified PEI
Polyamidoamine (PAMAM) dendrimers and dendron systems	Classic PAMAM virtually does not undergo chemical degradation; NA release as a result of protonation, competition of polyanions and dilution; in the case of modified analogues, NA release owing to labile linkers	Monodispersity, definite architecture, high density of functional groups	High cation toxicity, complexity of the synthesis of high-generation dendrimers, risk of two strong NA binding
Polymethacrylates and polyacrylaates with cationic and pH-sensitive groups	Reversible protonation or deprotonation; in the presence of hydrolyzable pH-sensitive or disulfide linkers, there are additional degradation pathways	Good control over the architecture *via* RAFT or ATRP processes; the possibility of creating any macromolecular architecture; the possibility of incorporating oligoethylene glycol units	The carbon–carbon backbone is chemically inert; cumulative toxicity is possible

4. Polymeric carriers for NAs: variable parameters

Initially, we planned to arrange this Section according to the classes of polymer molecules: PEI and its derivatives, polypeptides [first of all, PLL and poly(*L*-ornithine) (PLO)], poly(amino esters), and so forth. However, while preparing this review, we found out that considering the general characteristics common to all polymeric NA carriers, regardless of their class, is better suited to our goal to identify new degrees of freedom in the design of transfection agents, which are potential growth points for the further development of polyfection agents. Some of the parameters we discuss, such as positive charge density and the hydrophilic–lipophilic balance, are (with some reservations) common to both high-molecular-weight transfection agents and low-molecular-weight lipids. However, other parameters such as polymer topology or chain flexibility are structural characteristics specific to polymers. The key parameters of macromolecules that can be varied are listed in accordance with Kumar *et al*.[226] and Porello *et al*.,[78] although with minor changes: for example, thermosensitive polymers are discussed in a separate subsection.

Before passing to discussion of the effect of these parameters on the properties of polymers as transfecting agents, we should make a note. Despite the fact that narrowly focused conceptual studies attempt to elucidate the effect of a gradual change in a single parameter, *e.g.*, hydrophobicity, it is impossible to completely rule out the mutual influence of several parameters on one another. This is vividly demonstrated by a study by Berger *et al*.[132] The authors synthesized four similar PβAE (M_n = 2–4 kDa, $Đ_M$ = 1.2–3.8) by varying the length and the composition of the diol and diamine moieties (Fig. 17). It was shown that the properties of the resulting polymers were markedly different even at the level of basic parameters. The calculated hydrophobicity of the repeating unit (*C* log *P*) varied over a wide range from 0.99 for Poly0 (the most hydrophilic polymer) to 7.86 for Poly3 (the most hydrophobic polymer). Despite the presence of one-type tertiary amino groups, the p*K*a values of all polymers were considerably different, amounting to 6.91 for Poly0, 7.08 for Poly2, 8.29 for Poly2O, and 6.21 for

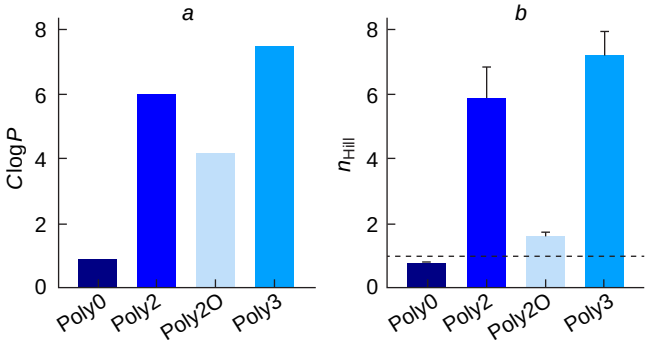

Figure 17. Evaluation of the hydrophobicity (*a*) and cooperativity of deprotonation (*b*) of copolymers obtained by Berger *et al*.[132] Copyright American Chemical Society 2024.

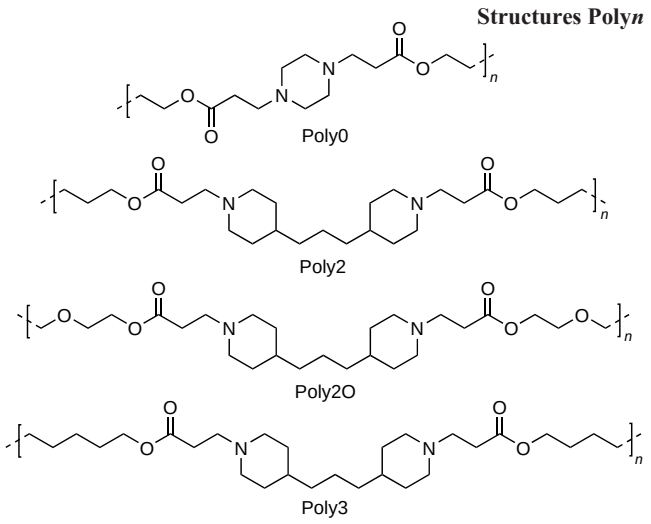

Poly3. These results provided a conclusion that was important for NA delivery: at physiological pH value of 7.4, the polymers Poly0, Poly2, and Poly3 are mainly deprotonated. Meanwhile, the oxygen-containing Poly2O remains largely protonated, which shifts its internal buffered pH beyond the pH range of endosomes. It turns out that by varying the chain structure between the diamine and diol moieties, it is possible to tune the chain rigidity, the lipophilicity of the macromolecule, and p*K*a of the amino groups.

Berger *et al*.[132] discussed separately the cooperativity of deprotonation, which was reflected by the Hill coefficient (n_{Hill}).[j] The cooperativity was high for Poly3 (n_{Hill} = 7.2) and Poly2 (n_{Hill} = 5.9) and moderate for Poly2O (n_{Hill} = 1.6), while in the case of Poly0 a low negative (< 1) cooperativity was found (n_{Hill} = 0.79). The authors attributed the increase in the n_{Hill} value to increasing flexibility of the chain upon elongation of the alkyl moiety between the ammonium cations. Hence, transition from a cooperative to an anti-cooperative deprotonation regime can be induced even by minor changes in the monomer structure within a series of polymers of the same type.

In a study of siRNA binding to polymers, a negative correlation between the binding constant and hydrophobicity was found:[132] the most hydrophilic polymer Poly0 had an eight times lower binding constant than the lead compound Poly3. This trend also held in transfection experiments. The Poly3 polyplexes formed in 5:1 mass ratio showed a 48% decrease in the target gene expression 3 days after the transfection, whereas the efficiency of other polymers did not exceed 16%. Thus, even using a small selection of polymers, it was clearly demonstrated how seemingly minor variation of the carrier structure influences the carrier properties and applicability for real biomedical problems.

[j] This is a dimensionless quantity that characterizes the cooperativity of polyfunctional ligand binding; as applied to polycations, it represents the cooperativity of deprotonation.

4.1. Positive charge

The positive charge of a polymeric carrier provides protection against nucleases and neutralizes the intramolecular repulsion of anionic phosphate groups in the NA chain, leading to compaction, similar to the compaction of histones in chromatin. The degree of ionization, determined by the polymer pK_a and positive charge density, is critical for the effective delivery of NAs, since it simultaneously influences NA binding and release from the polyplex, cellular uptake, and the ease of endosomal escape. Meanwhile, excess charge is a known cause of cytotoxicity.[226] For example, screening a library of 168 PβAE-based carriers showed that polymers with pK_a in the range of 6.2–6.5 exhibit greater efficiency in siRNA delivery and lower cytotoxicity compared to their analogues.[227] As has already been noted, pH of the environment varies during the intracellular transport of polyplexes, and carriers are often designed in such a way as to respond to these changes and release NAs under acidic conditions. Ros *et al*.[228] showed that the toxicity decreases on going from the poly(3-aminopropylmethacrylamide) carrier to poly(*N*,*N*-dimethylaminoethyl acrylate). The authors attributed this effect to 'charge shifting': hydrolysis converts the cationic propylaminoacrylate unit of the polymer chain into an anionic acrylate (Scheme 12).

A study of Dirisala *et al*.[229] illustrates well the integrated effect of charge on the transfection system. The authors proposed an original pathway for the charge-shifting hydrolysis, which somewhat differed from that described above. The formed PLO–mRNA polyplexes were coated with the pH-sensitive PAsp(DET-Aco) polymer (Scheme 13), which made the species anionic (and less toxic, and less sticky to the cell membrane) at the physiological pH. However, in an acidic endosomal medium, the species rapidly eliminated *cis*-aconitate, being converted to cationic form, PAsp(DET), thus initiating rupture of the endosomal membrane. Despite the fact that the anionic coating reduced the cellular uptake compared to that for the original cationic polyplexes, the total delivery of functional mRNA sharply increased due to endosomal escape. The coating that reversed the polymer charge increased expression by approximately an order of magnitude for the PLL system and by almost two orders of magnitude (approximately 80-fold) for the PLO system compared to the corresponding binary polyplexes. The control polyanion that was incapable of charge-shifting hydrolysis did not exhibit a similar effect.

The most interesting and well-studied mechanism of charge-shifting hydrolysis is characteristic of CART type copolymers. These copolymers, proposed as mRNA carriers in 2017, initially incorporated lipophilic alkoxycarbonyl-substituted poly(trimethylene carbonate) and cationic poly(morpholin-2-one) moieties (see Scheme 13).[230] Subsequently, the library of monomers was substantially expanded, but the key idea remained the same: using monomers based on α-amino acid derivatives, it is possible to obtain cationic polyesters that are stable in the protonated form and are rapidly fragmented *via* intramolecular ammonolysis upon deprotonation. In the cited

Scheme 12

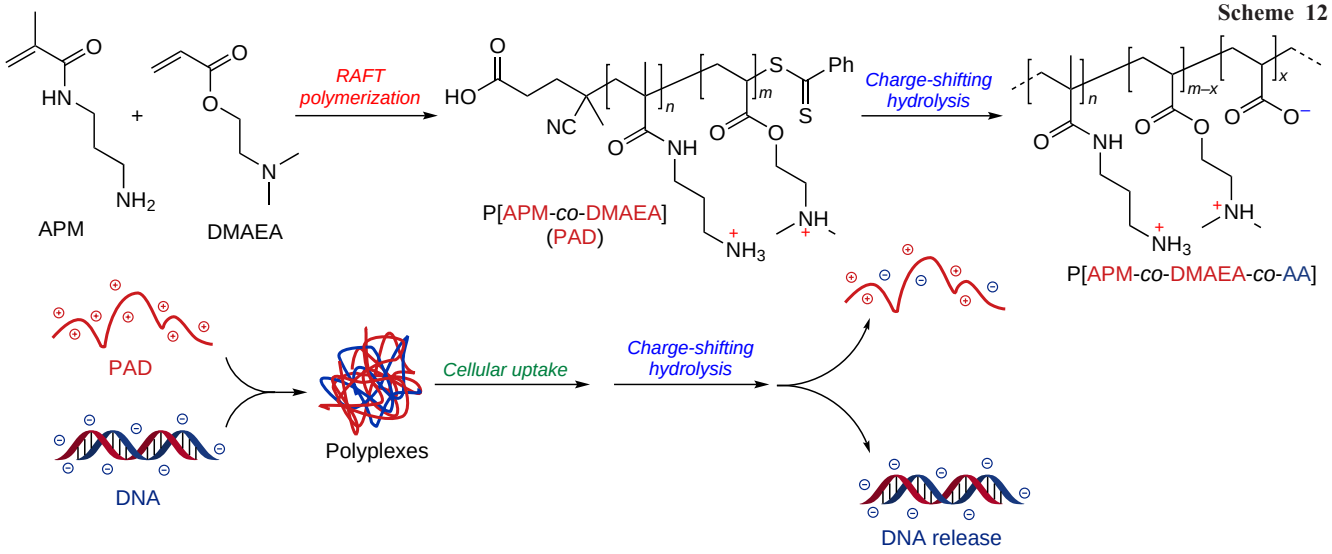

Scheme 13

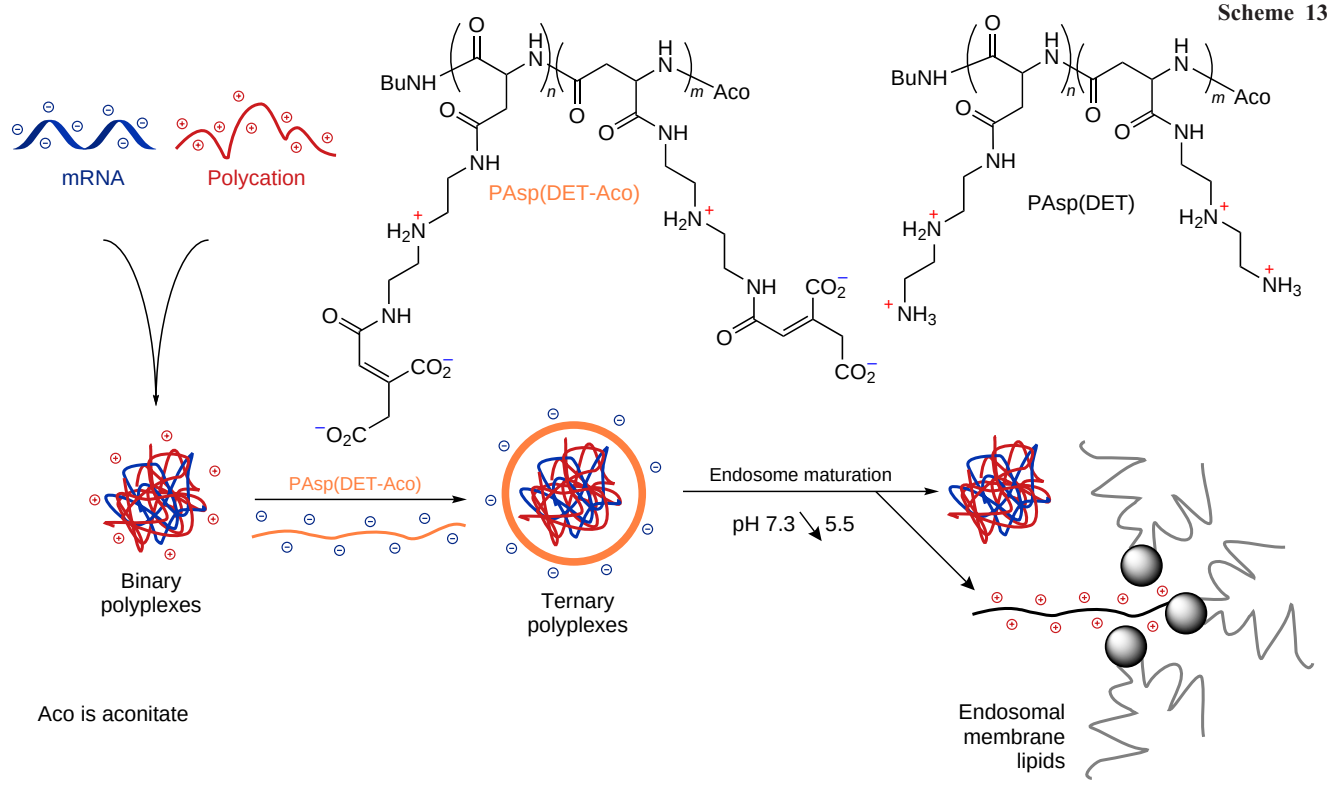

study, this mechanism, according to which cationic homopolymers and blocks within copolymers degrade to form substituted neutral diketopiperazines (DKP), was called charge-altering mechanism (Scheme 14).

This mechanism was studied in detail by Blake *et al.*,[231] who synthesized a series of structurally similar morpholinone type monomers (Scheme 15) and polymers based on them using the controlled organocatalytic ROTEP procedure. The ammonium polyesters formed after deprotection proved to be stable in an acidic medium; however at higher pH they were rapidly discharged. For the key **P1**$^+$ polymer, a study by ^{1}H NMR spectroscopy showed a sharp acceleration of degradation at neutral or weakly alkaline pH (half-life of a few minutes) and predominance of neutral diketopiperazine among the reaction products. A possible mechanism of degradation comprised a cascade of successive intramolecular 1,5- and 1,6-*O*→*N*-acyl shifts; in addition, stochastic modelling showed that the 1,6-shift proceeded faster than the 1,5-shift.

Minor changes in the polymer structure radically changed the decomposition pathway. The α-methyl-substituted **P2**$^+$ analogue degraded noticeably more slowly mainly *via* hydrolysis (giving *N*-hydroxyethylalanine instead of diketopiperazine); β-substituted **P**$^{3+}$ polymers degraded a few orders of magnitude more slowly to give mainly linear oligoamides;[k] and *N*-glycyl-modified **P4**$^+$ derivative showed a pronounced pH dependence and high selectivity in the hydrolysis to diketopiperazine (up to ~95% at pH ≈ 7). Finally, by copolymerization of rapidly hydrolyzable and slowly hydrolyzable units, it was possible to

[k] According to the logic of cyclization, instead of the 1,6-acyl shift, as was the case for **P1**$^+$, the statistically less likely and energetically less favourable 1,8-shift should have taken place.

Scheme 14

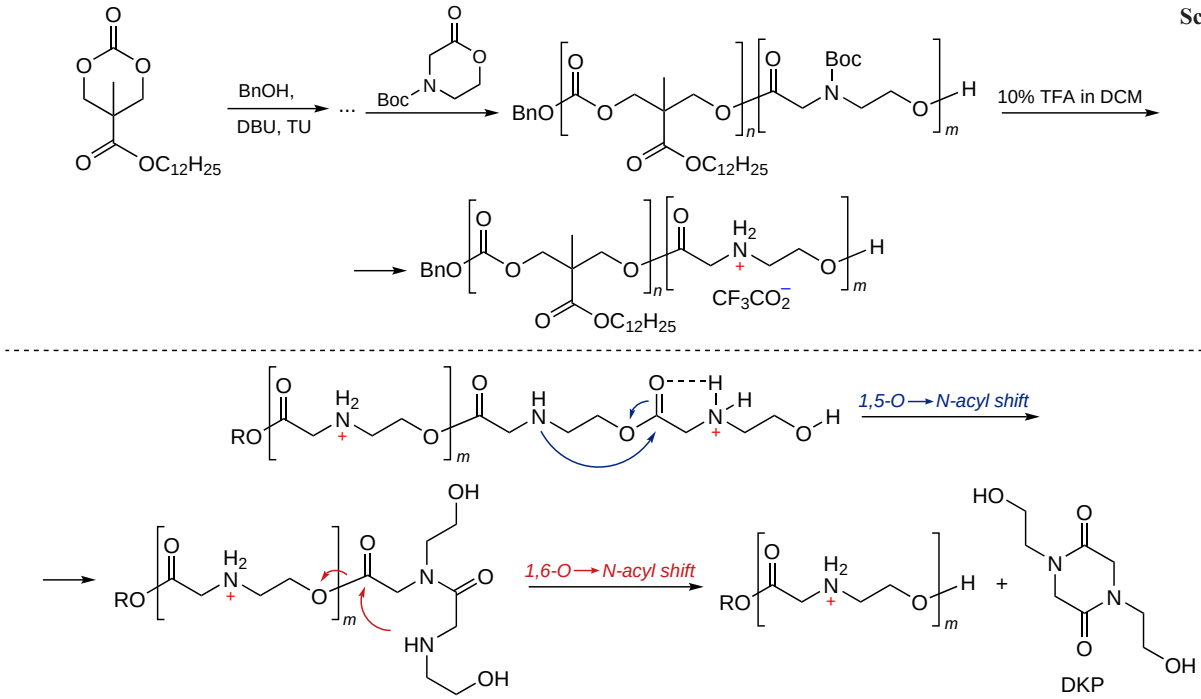

DBU is 1,8-diazabicyclo[5.4.0]undec-7-ene, TU is thiourea, TFA is trifluoroacetic acid, DCM is dichloromethane

Scheme 15

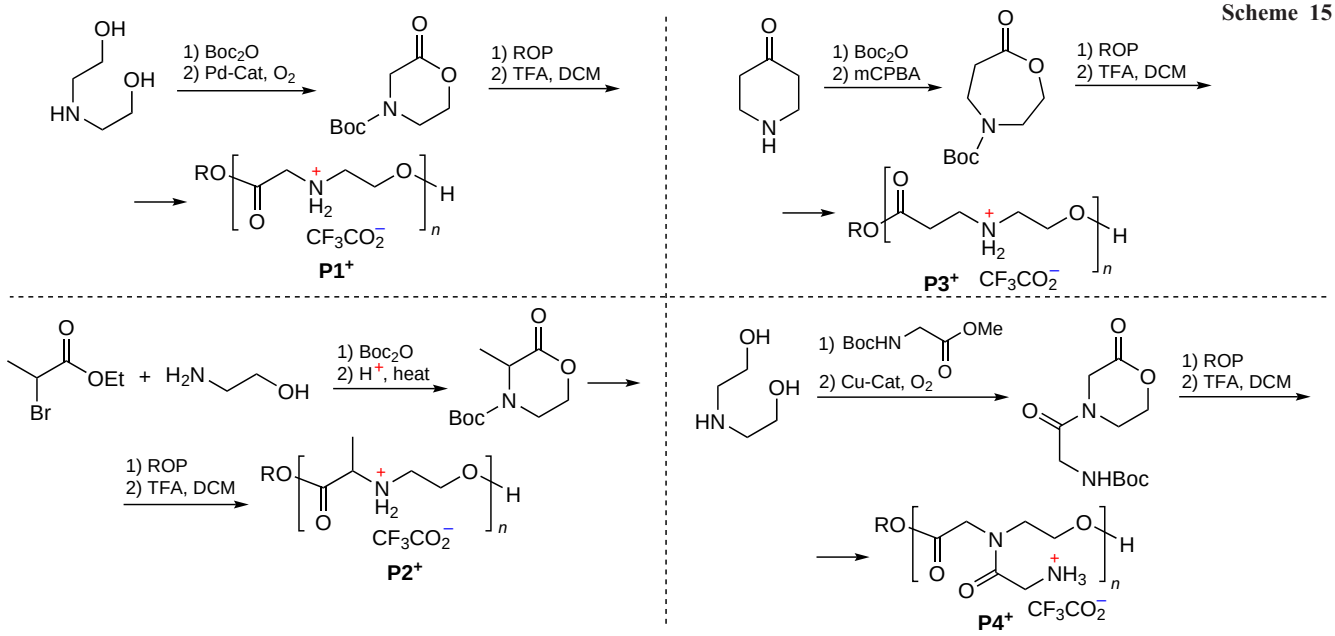

ROP is Ring-Opening Polymerization, mCPBA is *m*-chloroperoxybenzoic acid

achieve controlled tuning of the degradation time (ranging from a few minutes to a few hours). As a result, the following empirical rule was formulated for the design of these carriers: α-ammonium activation of ester groups and the appropriate distance to the nitrogen atom ensure a unique regime of controlled hydrolysis of the polymer chain with a charge loss, which relates the structure of the cationic block to the ability of the polymer carrier, first, to bind and then to release NAs.

Even the first study[230] devoted to CART demonstrated the high efficiency of the eGFP–mRNA delivery to HeLa cells (the fraction of the eGFP+ cells exceeded 99%) without considerable decrease in the cell viability. Meanwhile, the commercial Lipofectamine 2000 carrier provided only moderate expression and formation of ~50% eGFP+ cells. These polyplexes, which initially had a size of ~250 nm and a positive ζ-potential, gradually grew in the physiological medium, with ζ-potential being shifted to negative values over approximately two hours. This finding was interpreted as partial degradation of the cationic block, while maintaining stability for a therapeutically relevant period of time prior to intracellular breakdown. It was shown that the mechanism of cellular uptake of polyplexes is predominantly endocytosis-dependent (at 4°C, the uptake decreased by ~85%). However, it is the cargo escape rather than the uptake that is the key limiting factor: the analogues incapable of self-degradation provided a comparable level of intracellular delivery of labelled mRNA, but virtually did not induce expression, which attests to the importance and efficiency of the charge-altering mechanism. Finally, in *in vivo* experiments (on

mice), the fLuc–mRNA complexes provided a bright bioluminescence upon both the intramuscular administration (the peak was after ~4 h, and the signal was retained for up to 48 h) and intravenous administration (the early peak was after ~4 h and the signal was retained for up to 24–48 h), with the expression being mainly located in the liver and in the spleen.

In the subsequent studies, the Waymouth's research team demonstrated the efficiency of CART type copolymers for the delivery of pDNA,[232] mRNA,[233] and siRNA,[181] extended the range of lipophilic monomers by varying the lipid moiety of the starting trimethylene carbonate[234,235] and by using new type β-amidocarbonate monomers based on *N*-acyldiethanolamine,[236] and, what is more important, proposed several new monomers for the cationic part of NA carrier. In 2019, Benner *et al.*[237] described a new class of carriers, Serine–CART, the cationic block of which was based on oligoserine ester (Scheme 16). It has been shown that Serine–CART start to degrade when pH rises to 7.4 and are converted into neutral compounds within a few hours. Apart from the expected oligo(serine amides), this gives a considerable amount of the corresponding diketopiperazine (DKP, up to ~55% yield after 24 h), which emphasizes charge-altering nature of the cascade of the O→N acyl shifts as underlying the mechanism of charge loss.

In 2024, Waymouth and co-workers[238] reported guanidinylated CART based on serinol (GSer–CART), in which the authors rationally utilized too strong guanidinium–phosphate association owing to the charge-altering mechanism of polymer chain degradation (Scheme 17). Using a library of nine GSer–CART carriers and varying the lipid skeleton (carbonate *vs.* β-amidocarbonate moiety) and degree of polymerization, the authors achieved not only high expression of the reporter, but also virtually tunable binary

Scheme 16

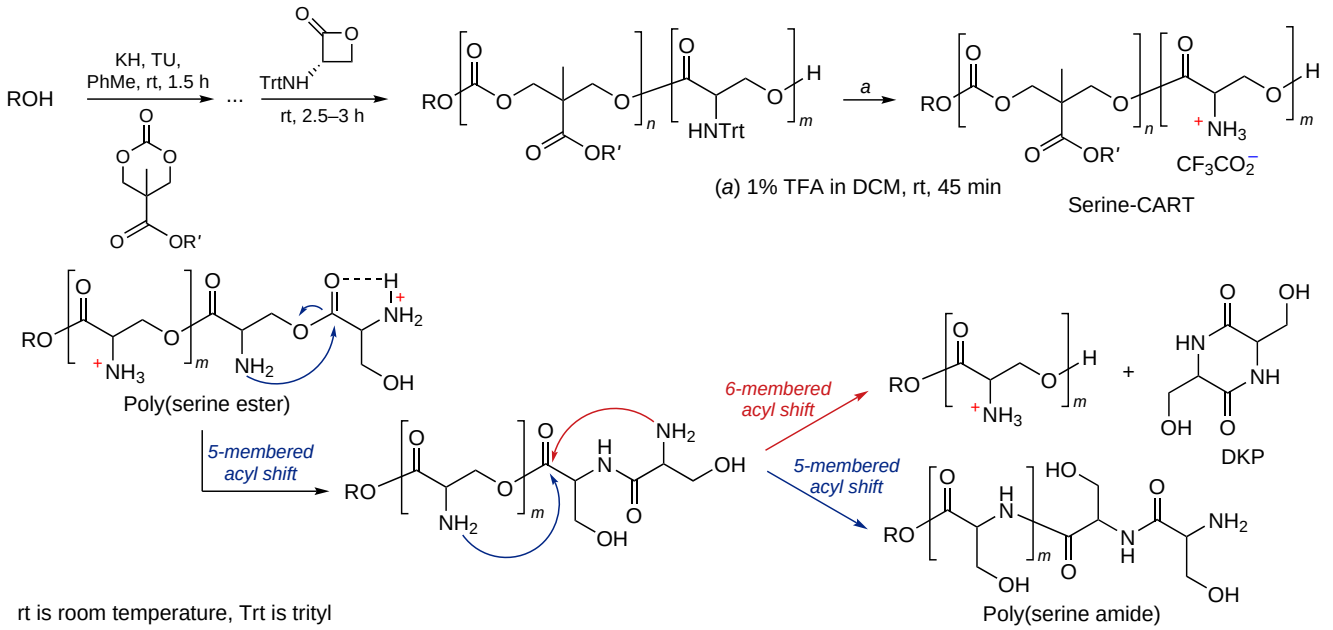

Scheme 17

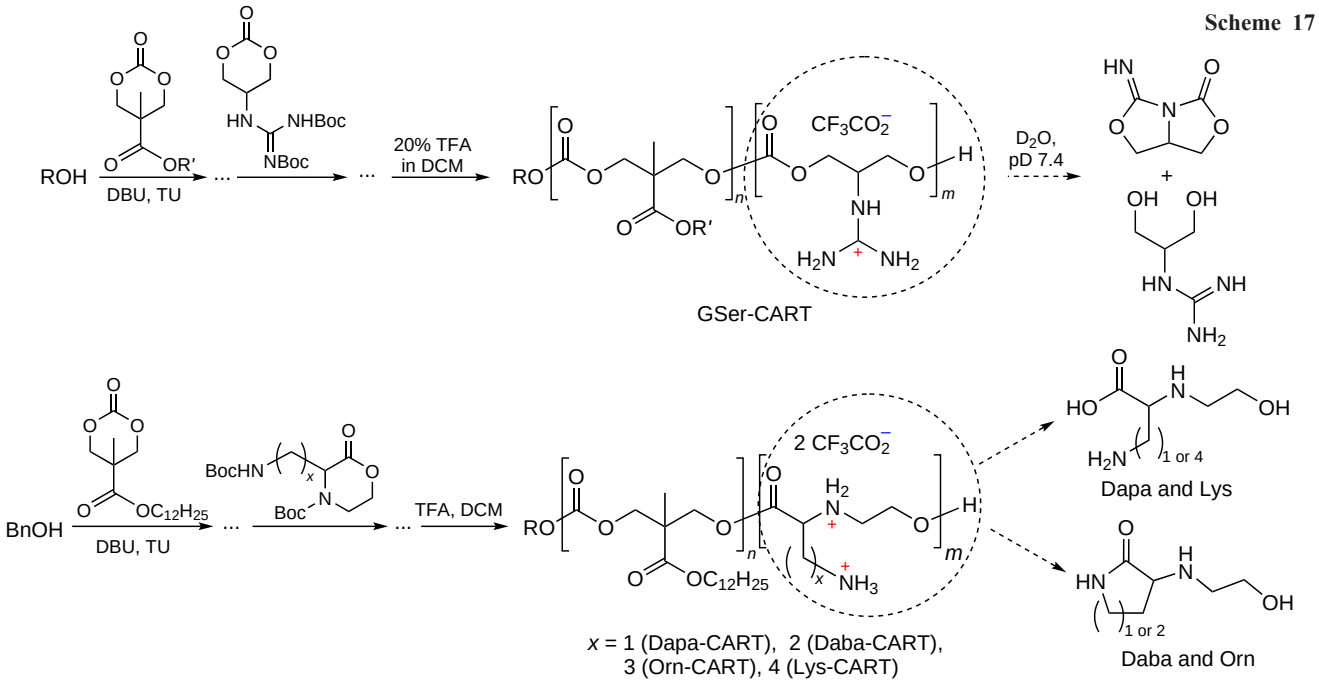

organotropism without using targeting ligands. The most effective formulations produced up to ~97% expression in the lungs or up to ~98% in the spleen, with the tropism being tuned solely by the guanidinium-to-phosphate charge ratio (high charge shifted the delivery toward the lungs, while low values shifted it toward the spleen). This effect was correlated with the biophysics of particles at pH 7.4 and especially in the plasma: the lung-tropic complexes rapidly increased in size up to the micrometre range, whereas the spleen-tropic complexes remained in the submicrometre range.

Finally, in 2025, Abd Elwakil[239] reported a series of monomers based on α-amino acids with an additional amino group in the side chain, two monomers based on natural lysine and ornithine and two monomers based on non-proteinogenic diaminobutanoic (Daba) and diaminopropanoic (Dapa) acids (see Scheme 17). It was found that for similar physicochemical characteristics of polyplexes (comparable sizes of ~180 nm and high degree of NA encapsulation), a slight change in the length of the diamine side chain crucially changed the outcome of the delivery. The Orn-CART carrier exhibited higher selectivity for the delivery to lungs compared to analogous Lys-CART and commercial PEI. The Daba-CART and Dapa-CART polymers ($n = 1$ and 2 in Scheme 17, respectively) increased the expression, but only the former preserved the selective delivery. The organotropism could be finely tuned by adjusting the N : P charge ratio (as in the previous study); at a 10 : 1 ratio, the expression was almost completely located in the lungs (>99%); at a 5 : 1 ratio, the spleen made a noticeable contribution; and at even lower ratios, the distribution was systemic.

While acknowledging the enormous contribution of the Waymouth's research group to the development of the concept of self-degrading polyester carriers for NAs, it should be noted that they are not the only developers of polymers that degrade with the loss of charge. For example, polymeric transfecting agents that completely meet the CART criteria, poly(4-hydroxy-*L*-proline ester)[210,240] and its block copolymer with dilactide,[241] were proposed for the first time for the pDNA delivery more than 25 years ago. There is no doubt that the potential of polyprolinate will be fully unlocked in the near future. Indeed, in 2025, Tian *et al.*[242] (evidently, inspired by the research of Waymouth's tram, but not concerned with the transfection as yet) reported the use of ROP to obtain homopolymers and random and block copolymers of *N*-acylated 4-hydroxyproline (Scheme 18).

Our research team also made a contribution to the development of CART. In 2022, we[243] proposed a new type of lipophilic monomers comprising monosubstituted glycolides, tyrosine derivatives acylated with fatty acids at the phenolic OH group (Scheme 19). The replacement of the polycarbonate block by a polyglycolide block made the carrier completely hydrolyzable under physiological conditions, as confirmed by a model *in vitro* experiment. Glycolidic CART also degraded *via*

Scheme 18

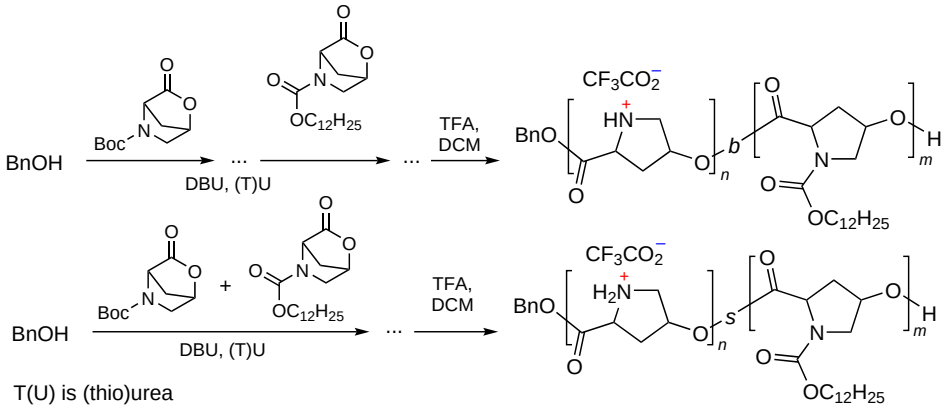

Scheme 19

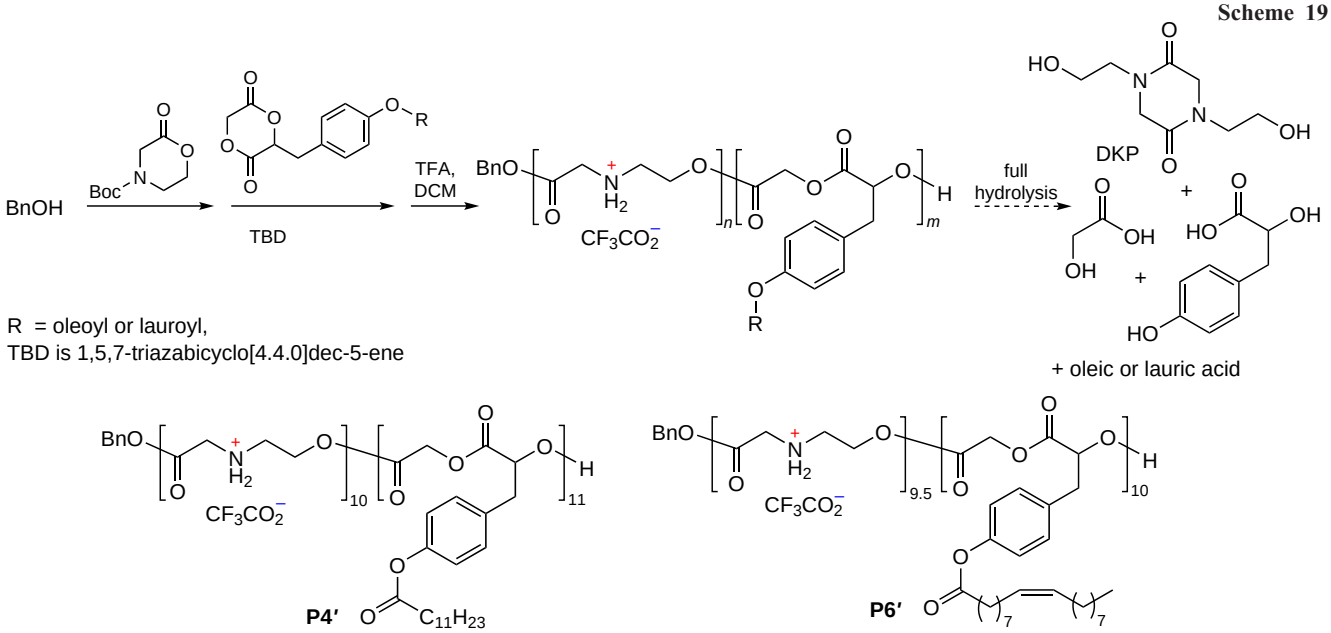

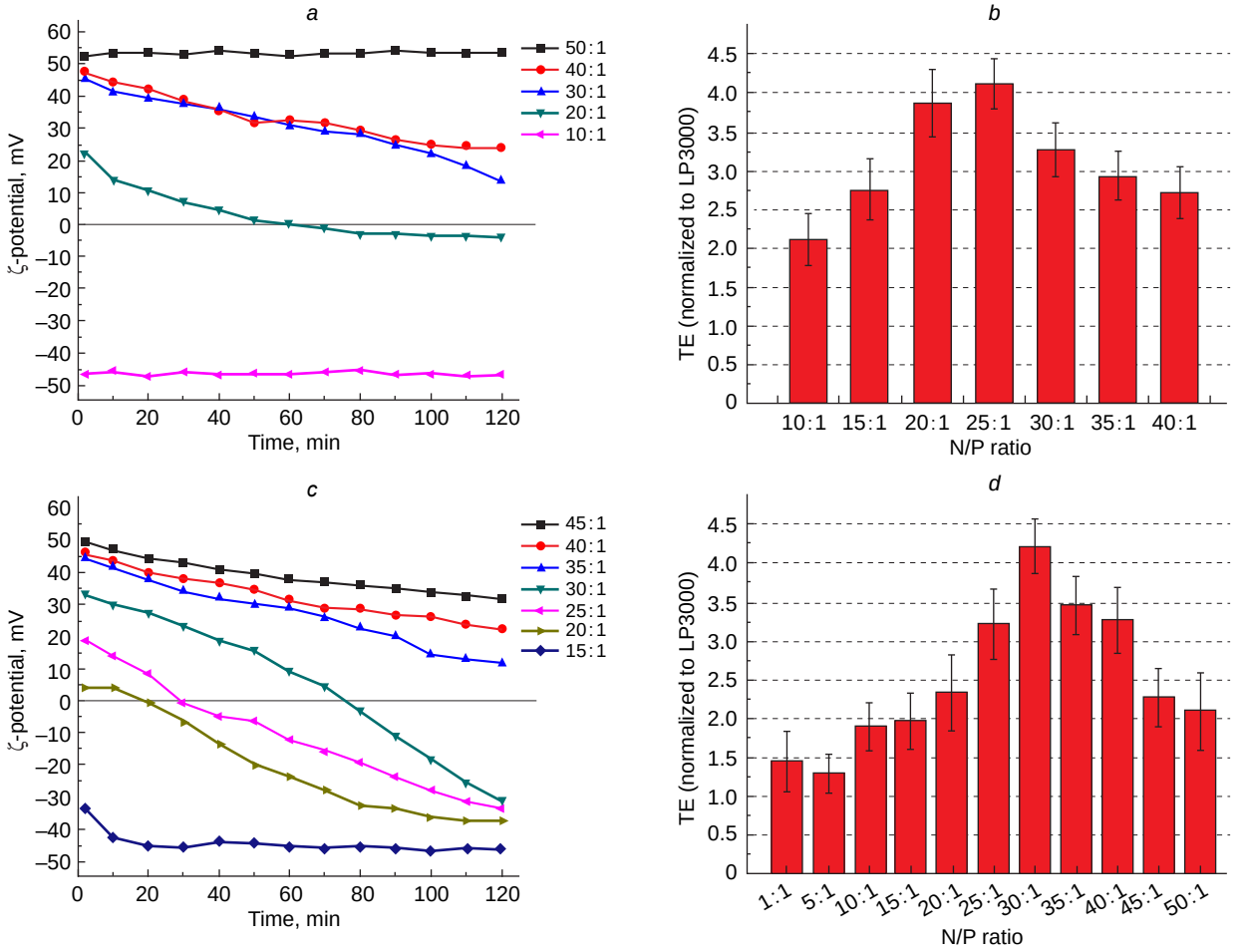

Figure 18. Time variation of the ζ-potential of eGFP polyplexes with **P4′** (*a*) and **P6′** (*c*) polymers at various N:P ratios (the starting pH = 6.5); transfection efficiency of HEK293T cells with the eGFP plasmid using **P4′** (*b*) and **P6′** (*d*) carriers normalized to the efficiency of Lipofectamine 3000 (LP3000) over a range of N : P ratios in the same experiment.[243] Copyright Elsevier 2022.

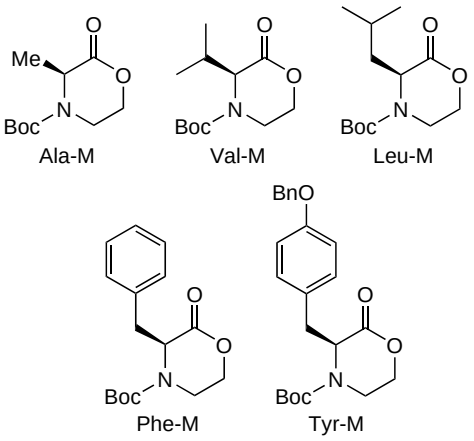

Figure 19. Structures of morpholin-2-one monomers based on natural amino acids.

a charge-altering mechanism, as confirmed by analysis of the hydrolysis products and by a change in the sign of the ζ-potential of the polyplex within ~1 h. Testing of the developed copolymers for pDNA delivery in HEK293T[1] cells demonstrated that they were 3–4 times superior in transfection to commercial agents. In relation to the **P4′** and **P6′** copolymers, which demonstrated the best results in the model transfection experiments, we identified a relationship between the efficiency of pDNA delivery and the physicochemical behaviour of the polyplexes (Fig. 18). The carriers with N : P ratios at which the ζ-potential decreased to zero in approximately 1 h proved to be most effective.

In 2024, Shaputkin *et al.*[244] developed a method for the synthesis of new monomers for the hydrophilic block of CART based on some natural α-amino acids (Ala, Val, Leu, Phe, Tyr) representing morpholin-2-one with the appropriate alkyl substituent in position 3 (Fig. 19).

4.2. Molecular weight

The molecular weight of the polymer also considerably affects the NA delivery. As a rule, transfection efficiency increases, along with toxicity, with increasing molecular weight; this tendency holds for both linear and branched polymers of various natures (PEI, PLL, PDMAEMA, *etc.*).[226] The studies of Blakney *et al.*[161,163] demonstrating the necessity of high-molecular-weight carriers to deliver relatively large cargo such as pDNA and saRNA have been mentioned above. The authors[161] synthesized a library of copolymers of poly(2-ethyl-2-oxazolines) (PEtOx) with PEI (M_n = 5–200 kDa) in which the

[1] HEK293T is a derivative of HEK293 cells, which steadily expresses large SV40 T-antigen.

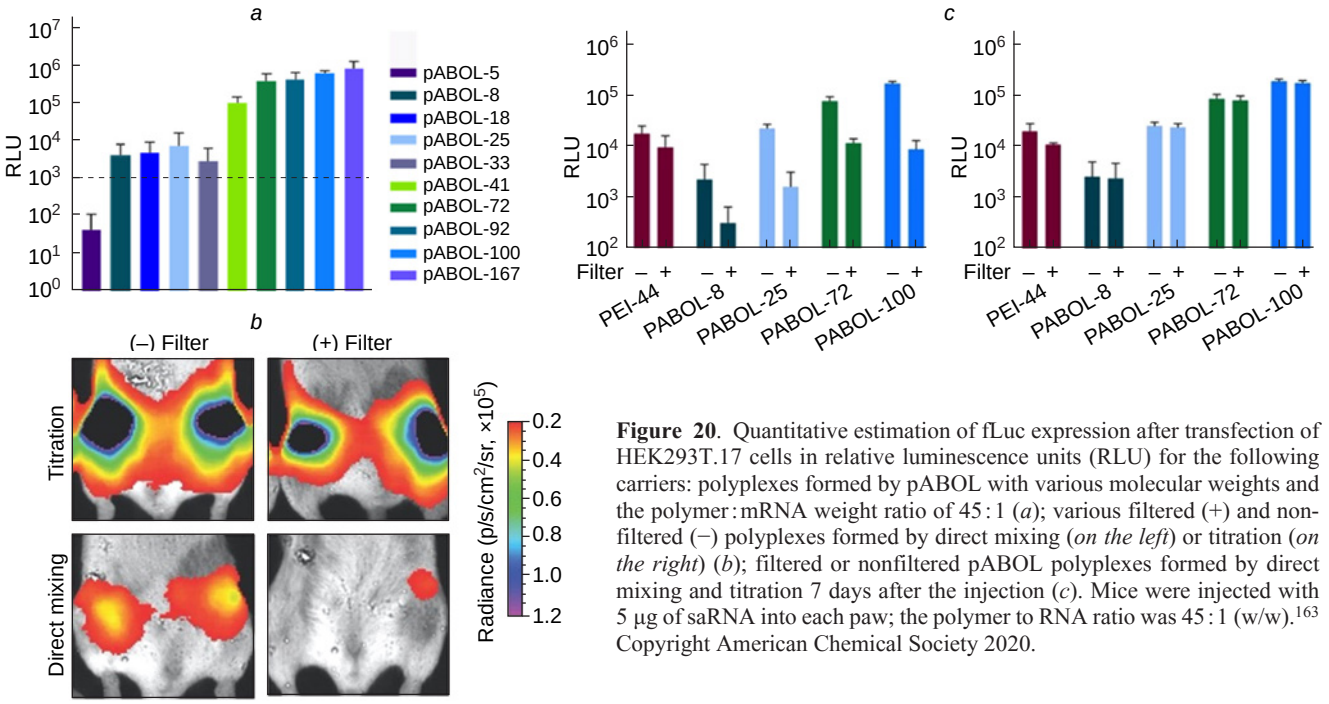

Figure 20. Quantitative estimation of fLuc expression after transfection of HEK293T.17 cells in relative luminescence units (RLU) for the following carriers: polyplexes formed by pABOL with various molecular weights and the polymer : mRNA weight ratio of 45 : 1 (*a*); various filtered (+) and non-filtered (−) polyplexes formed by direct mixing (*on the left*) or titration (*on the right*) (*b*); filtered or nonfiltered pABOL polyplexes formed by direct mixing and titration 7 days after the injection (*c*). Mice were injected with 5 μg of saRNA into each paw; the polymer to RNA ratio was 45 : 1 (w/w).[163] Copyright American Chemical Society 2020.

charge density (*i.e.*, frequency of amino-containing units) was varied through variation of the degree of hydrolysis (20–100% ethylenimine units) and compared these carriers in the delivery of pDNA (~7000 bp), mRNA (~2 kb), and saRNA (~9.5 kb) with the same fLuc reporter. High-molecular-weight polymers (83 and 72 kDa) provided the highest delivery efficiency for pDNA and large saRNA molecules, respectively, whereas in the case of mRNA, polymers with a lower molecular weight (45 kDa) showed the highest transfection efficiency.

The other study by Blakney *et al.*[163] was focused on saRNA. The role of the polymer molecular weight and the 'unpacking' mechanism was elucidated in relation to a biodegradable poly(amino ester): poly(cystamine bisacrylamide-*co*-1,4-amino-butanol) (pABOL) (Fig. 20). The transgene expression was enhanced by increasing the molecular weight of pABOL by more than an order of magnitude (from 5 to 100 kDa), which was achieved by adjusting the synthesis time. The carrier biodegradability played an important role for the efficiency of saRNA delivery: inhibition of cellular glutathione sharply reduced expression for pABOL but not for PEI, indicating the importance of disulfide reduction for the release of saRNA. The relationship between *in vivo* efficiency and molecular weight was non-monotonic (parabolic), which was attributed in this study to a trade-off between the NA binding and release rates.

4.3. Hydrophobicity

The hydrophobicity of polymer backbones or, alternatively, the introduction of additional hydrophobic side chains often increases the transfection efficiency, but, at the same time, causes cytotoxic effects.[226] Automated screening of the properties of polyplexes such as cytotoxicity, cellular internalization of the complexes, and transfection efficiency made it possible to study the structure–property relationships for a wide range of PEG-P(DMAEMA-*co*-AMA) amphiphilic copolymers (AMA is alkyl methacrylate) (Fig. 21 *a*). It was shown that the efficiency of mRNA delivery is determined by a 'hydrophobicity window' determined by two independent parameters: the length of the alkyl side chains (C_2–C_{12}) and the proportion of hydrophobic units (~20–60%).[136] The elongation of the side groups by itself does not induce a monotonic improvement of the performance: nanoparticles are formed throughout the whole range of structures (most often < 250 nm), but the most compact particles exist at intermediate alkyl lengths (approximately C_8–C_{10}) and moderately high proportion of hydrophobic units. Further increase in the hydrophobicity impairs the key early stage, that is, the electrostatic binding of mRNA to the carrier, since bulky hydrophobic substituents shield the cationic centres. The polymer with the lower molecular weight showed the best results and provided a higher transfection compared to PEI, according to the flow cytometry and mean fluorescence intensity. The minimum cytotoxicity was observed for PDEAEMA–butyl methacrylate polyplexes during 18 h after administration, irrespective of the length of the PEG moiety.

pABOL structure

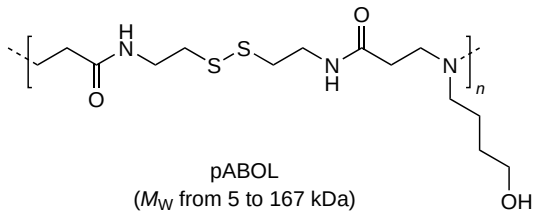

pABOL
(M_W from 5 to 167 kDa)

A modular strategy for tuning the amphiphilicity of poly(β-amino ester) carriers was proposed by Shi *et al.*[245] Hydrophobic and hydrophilic PβAE polymers based on a glycerol derivative of bisphenol A were synthesized separately, since changing the amphiphilicity of PβAE through copolymerization with hydrophobic monomers is a laborious and, to some extent, uncontrollable process.

Then l-PβAE and h-PβAE were used as the hydrophobic and hydrophilic modules, respectively, being co-condensed with DNA. This gave ternary polyplexes with a controlled ratio of the modules. The ternary polyplexes form smaller polyplexes compared to DNA–hydrophilic PβAE binary polyplexes and show a more pronounced decrease in the ζ-potential over time;

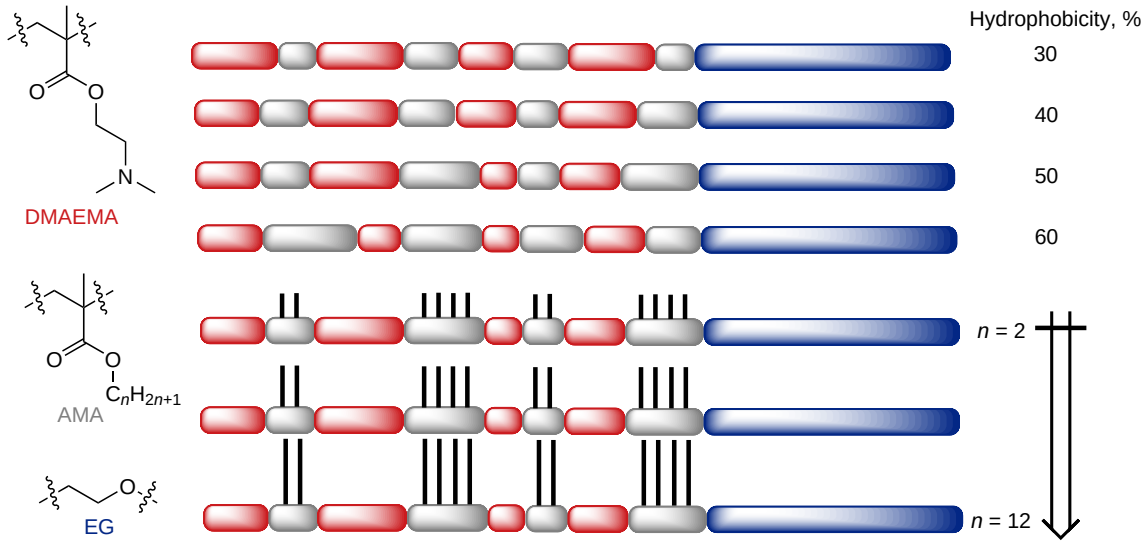

Figure 21. Schematic image of polyacrylate–PEG copolymers in which the hydrophilic–lipophilic balance can be tuned by controlling the ratio of the monomers DMAEMA (or ethyl homologue DEAEMA) and AMA with the C_2–C_{12} alkyl substituent in the ester group.[136] Copyright American Chemical Society 2021.

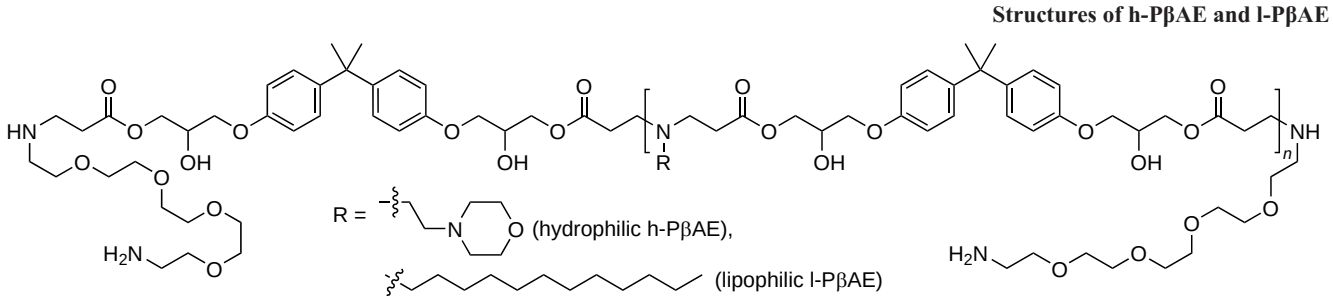

as the proportion of the hydrophobic component is increased, the cytotoxicity increases (Fig. 22). It was shown that particularly the balance between the hydrophilicity and hydrophobicity determines the size, stability, and functional transfection of the carrier.[245] As the proportion of hydrophobic module increased, the particle sizes varied non-linearly: the most hydrophobic polymers (and one ternary composition) formed small particles (25–28 nm), intermediate ternary systems formed ~170–270 nm particles, while the hydrophilic polymer gave large aggregates (>400 nm). In addition, the introduction of a hydrophobic component improved the colloidal stability of the particles and the retention of DNA in the presence of serum proteins. In experiments using HeLa cells, the best results were achieved with a formulation containing equal amounts of hydrophilic and hydrophobic components: it showed high cellular uptake and perinuclear distribution, with the delivery efficiency being only slightly inferior to that of the commercial jetPEI carrier. The applicability of this system was demonstrated for difficult-to-transfect HepG2 (human hepatocellular carcinoma) and B16.245 cells.

The modulation of the hydrophilic–lipophilic balance of the NA carrier is not limited to variation of the hydrocarbon substituents; another line of research is the introduction of fluorinated groups. Fluorinated derivatives of PEI,[246] PPI,[247] 2-hydroxy-PPI,[248] PLL,[249] PAMAM,[250,251] and PβAE[252] have already been studied as agents for NA delivery. Fluorination

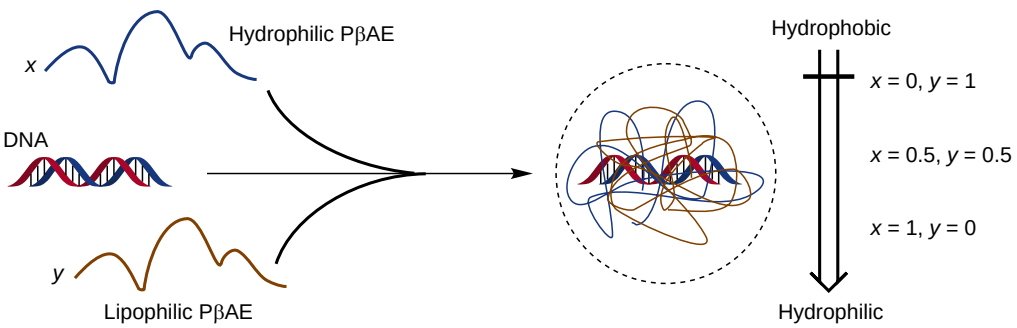

Figure 22. Modular strategy for the control of the amphiphilicity of the PβAE–DNA polyplexes.[245]

Scheme 20

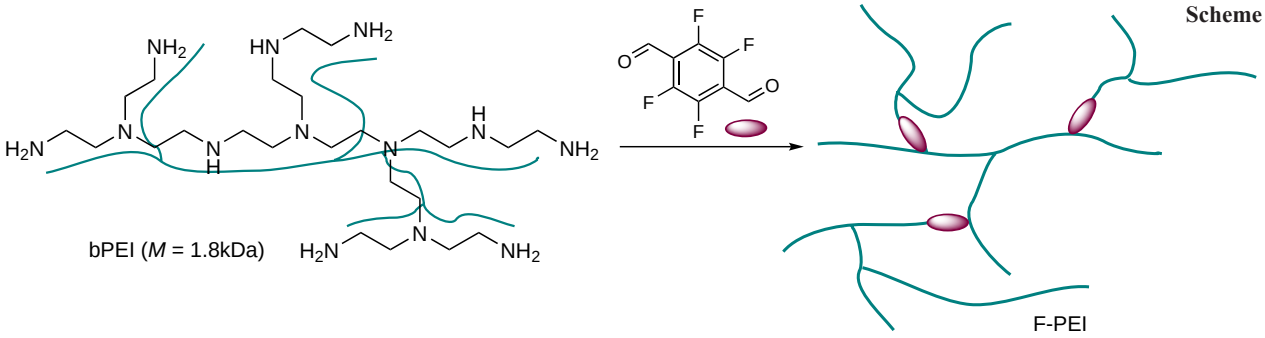

provides the carrier with both hydrophobicity and lipophobicity and also affects the basicity of the amino groups.

This can be illustrated by a study by Jin *et al.*,[253] who developed a fluorine-containing low-molecular-weight PEI (Scheme 20). The F-PEI carrier condensed DNA even at a very low polymer:NA ratio and formed particles with a size of ~200 nm. Furthermore, in the presence of serum, no displacement or leakage of nucleic acid was observed for 48 h, which was attributed to the hydrophobic and lipophobic properties of the fluorinated moiety and weakening of its nonspecific interactions with proteins and lipids. In cellular assays, the developed carrier had a markedly milder toxicological profile than the non-fluorinated analogue, PEI with $M_n \approx 25$ kDa: ~80% cell viability after 72 h at high doses and highly increased cellular uptake. According to flow cytometry, up to 60% of the polyplexes *vs.* ~10% for the control PEI entered the cells. A confocal microscopy examination showed pronounced endosomal escape and subsequent penetration of labelled pDNA into the nucleus after 4 h. Against this background, the transfection itself also improved: for the GFP reporter, the polyplexes with polymer:pDNA = (40–50):1 (w/w) surpassed PEI with $M_n \approx 25$ kDa, with the optimal system with a ratio of approximately 50:1 (w/w) proved to be ~1.5 times more efficient than the control. In an *in vivo* H1299 xenograft model, repeated introduction of the F-PEI–plasmid polyplex resulted in a statistically significant retardation of the tumour growth without a decrease in the body weight or lethality. In the tumour tissue, an even more pronounced decrease in the expression of vascular endothelial growth factor (VEGF) was observed; the microvascular density assessed by the CD31 and CD34 markers[m] decreased, while CD8+ T-cell infiltration simultaneously increased. A histological examination of the major organs revealed no obvious cellular damage.

Deng *et al.*[252] proposed a way to solve the problem of NA delivery to difficult-to-transfect cells. It was shown that fluorination of poly(β-amino ester) markedly 'raises the ceiling' for nonviral delivery of plasmid DNA particularly in adherent HepG2 cells and suspension Molt-4 cells.[252] The F-PβAE fluorinated polymer (Scheme 21) obtained by the authors formed spherical cationic polyplexes with a more compact size and a higher ζ-potential compared to the non-fluorinated analogue. This was in line with the sharp increase in the fraction of the GFP+ cells up to ~87% in HepG2 (*vs.* ~30% for Lipofectamine 3000) and up to ~55% in Molt-4 (*vs.* ~5% for Lipofectamine 3000), with the cell viability being admissible. An important issue of the study was the finding that in the delivery of Bcl-xL pDNA, the F-PβAE polymer provided markedly better protection of HepG2 cells against induced apoptosis: the proportion of apoptotic cells decreased to approximately ~10% *vs.* ~22% for Lipofectamine 3000 and >33% in the control experiment. However, the delivery of pDNA encoding PKCβII with this polymer considerably enhanced the cell sensitivity to ferroptosis (the cell death amounted to ~52% *vs.* ~25% for Lipofectamine 3000), as confirmed by Fe^{2+}-initiated lipid peroxidation markers and protein expression. The results of the cited study[252] indicated that local fluorination of PβAE may serve as a simple tool to overcome the key intracellular barriers and expand the scope of

[m] CD31 and CD34 are protein markers used in immunohistochemical or immunofluorescence staining to visualize the vascular endothelium in tissue sections.

Scheme 21

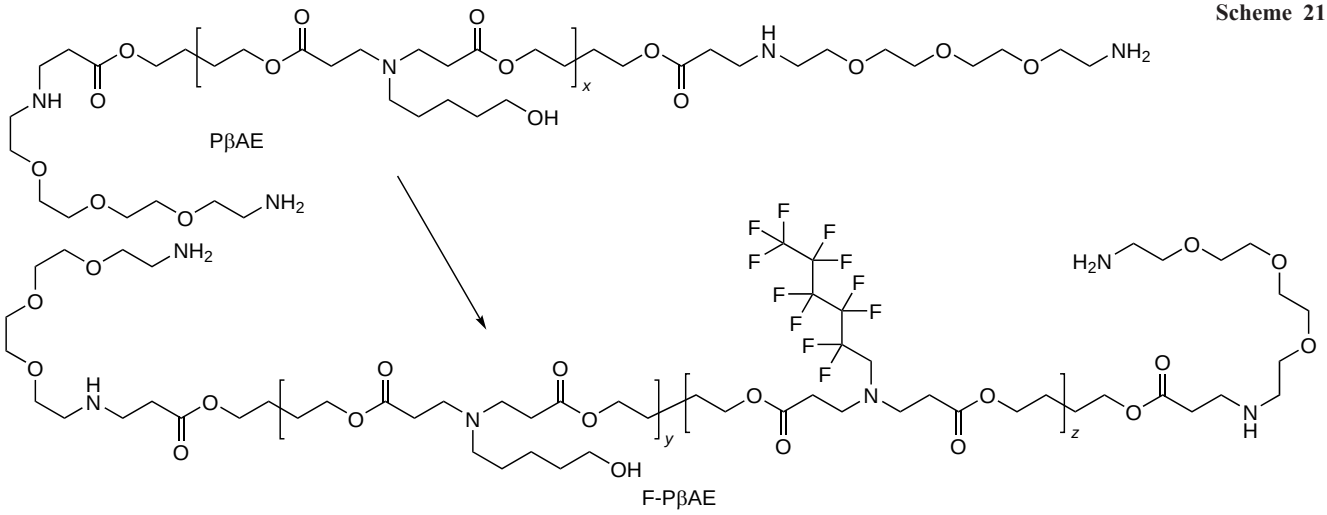

Scheme 22

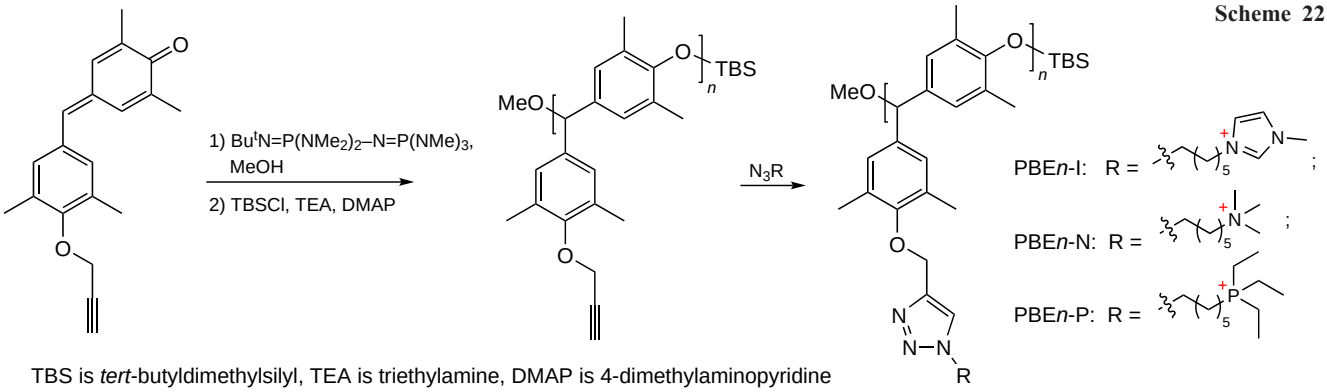

TBS is *tert*-butyldimethylsilyl, TEA is triethylamine, DMAP is 4-dimethylaminopyridine

applicability of polymer vectors in cellular systems in which conventional agents are of low efficiency.

4.4. Polymer chain rigidity

The rigidity of the polymer chain affects binding to or interaction with NAs, as well as potential biological functions such as endosomal escape[134] and, consequently, the efficiency of transfection. The stiffness of nanoparticles may not only be responsible for the general efficiency, but also dictate the cellular uptake pathway. This relationship was demonstrated by Gurnani *et al*.,[254] who used the glass transition temperature of the polymer to characterize the rigidity of nanoparticles.

Despite numerous studies on the role of NP rigidity, contradictory results have been obtained in some cases. Thus, relying on the idea that the structural rigidity of rod-like polycations enhances the membrane activity, Liu *et al*.[255] designed a new class of rigid polybenzyl ethers (PBE) with various cationic side groups, including imidazolium, quaternary ammonium, and phosphonium ions (Scheme 22). In relation to these compounds, the authors demonstrated that polyplexes are capable of direct translocation through the cell membrane, which makes it possible to circumvent the endosomal uptake problem, while the introduction of imidazole into the side chain ensures higher transfection performance for the PBE100-I carrier compared to PEI25k.

The authors planned to combine pronounced DNA condensation with endocytosis-independent uptake and thus circumvent the endosomal escape, which is a bottleneck of transfection. In experiments, the whole PBE*n* family formed stable 200–300 nm polyplexes even at low N:P ratios ($\geqslant 4$), thus providing a positive ζ-potential (>25 mV). The imidazolium analogue of PBE100-I was distinguished by the highest ζ-potential (~30 mV) and especially high degree of DNA condensation (>85% even at N:P = 4, which is comparable with the PEI25k polymer). The researchers attributed this finding to the possibility of aromatic stacking of the imidazole moieties and the nitrogenous bases of NA. In addition, PBE demonstrated much better biocompatibility compared to PEI25k (for most polymers, cell viability exceeded 97% at a concentration of 32 μg mL^{-1}).

The experimental results confirmed the initial hypothesis: the polyplex uptake was fast and little dependent on the serum type, and it was only slightly suppressed by the conditions of endocytosis inhibition. Meanwhile, fluorescence-labelled PBE100-I exhibited low colocalization with lysosomes, which is consistent with partial bypass of the endo- or lysosomal pathway and accounts for the observed high transfection performance of exactly the combination of a rigid aryl backbone and cationic side groups, since it reduces the required charge density without compromising the condensation.

Meanwhile, Miyazaki *et al*.[256] performed a comparative study of mRNA delivery using two different types of cationic PEG block copolymers with poly(glycidylbutylamine) (PGBA) and with PLL (Fig. 23), differing in the chain rigidity. It was shown that PEG-PGBA comprising more flexible polyether backbone produced polyplexes involving 50 times stronger interaction with mRNA molecules compared to PEG-PLL, which contains rigid peptide bonds. The enhanced binding of mRNA to PEG-PGBA improved the biological characteristics of polyplexes, such as NA protection against enzymatic degradation, protein hyperexpression, and bioavailability both *in vitro* and *in vivo*, compared to those of PEG-PLL.

The apparent contradiction in the results of the above studies stems from the fact that the rate-limiting stages of NA delivery are different. In the study by Liu *et al*.,[255] this is overcoming the endosomal barrier, since the rigid polymer backbone enhances the direct membrane translocation. Meanwhile, in the publication of Miyazaki *et al*.,[256] the rate-limiting stage is the assembly of PIC micelles under physiological conditions: more flexible polycationic chain is better adapted to mRNA and provides more effective binding. Thus, the rigidity is beneficial when penetration through the membrane is the bottleneck, while flexibility is useful when the critical issue is packing, retention, and protection of NA.

It is noteworthy that NA itself also contributes to the total rigidity of the system (the difference between siRNA and ssRNA

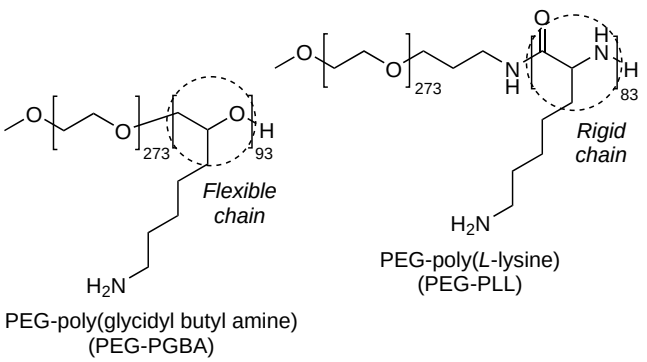

Figure 23. Cationic block copolymers with varying flexibility of the charged segments based on poly(glycidylbutylamine) (flexible) and poly(*L*-lysine) (rigid).[256] PEG-PGBA provides for more than a 50-fold increase in the mRNA binding strength compared to that of PEG-PLL, which results in the formation of mRNA polyplexes with enhanced protection against enzyme attack.

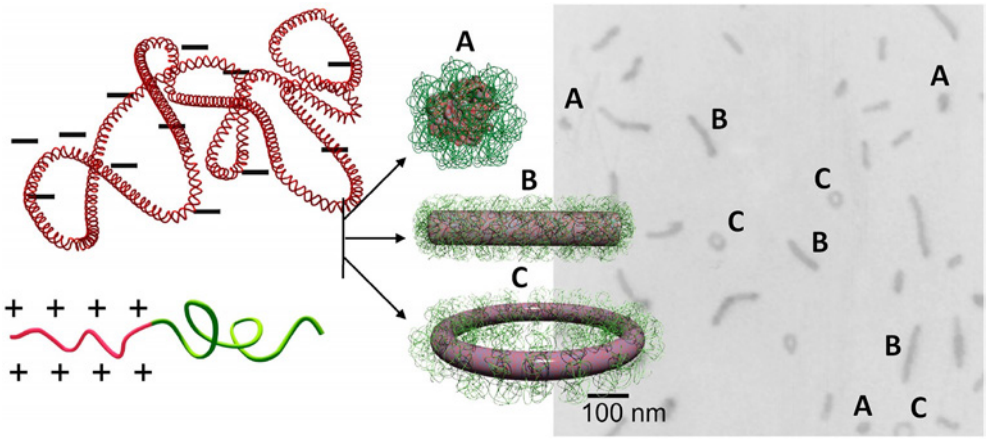

Figure 24. Morphology of polyplexes formed by pRSVLuc and mPEG-*b*-PAMAM copolymer[259] and transmission electron microscopy (TEM) image confirming the morphology. Adapted from Osada *et al*.[258] under the CC-BY 4.0 license.

binding to polyplexes was discussed in Section 2.2.3): the longer and the less flexible NA, the lower the energy benefit of binding to the polycation.[257] It is known that the persistence length of double-stranded DNA is approximately 50 nm (*i.e.*, when the length is less than 150 bp, it can be considered to be a rigid rod), which results in a limited set of possible polyplex morphologies[258] (Fig. 24).

Using molecular dynamics simulation, Bae *et al*.[260] found that even a minor difference in the flexibility of double-stranded DNA can crucially change the scenario of complex formation with a cationic nanoparticle of histone-like size. For fragments approximately 100 bp long with similar persistence lengths (l_p),[n] but still differing by ~10 nm, an increase in the NP charge progressively enhances bending of the DNA and leads to a transition from local contact without noticeable deformation to wrapping around the particle, with the transition threshold shifting because of rigidity. It was also shown that in the case of partial wrapping, NP can slide along the DNA (dynamic rearrangement of contacts), with the stability of a formed loop sharply decreasing with increasing ionic strength. This is consistent with the shielding of electrostatic interactions and an increase in the effective rigidity of double-stranded DNA. Thus, the total rigidity imparted to the polyplex by the nucleic acid and the carrier can serve as an additional tool for controlling the binding strength. If the efficiency of polyplex formation is low, a more flexible polymeric carrier should be selected for the delivery of this NA; conversely, if strong binding prevents the polyplex from leaving the endosome, a less flexible carrier would be more suitable.

4.5. Topology of the polymer backbone

The topology of polymers used in NA delivery can be linear, branched, cyclic, star-shaped, *etc.* The architecture of a macromolecule considerably influences the charge density and distribution and, hence, the functions such as NA compaction, stability of polyplexes, and crossing biological barriers.[77] It was reported that highly branched PEI provides more efficient release from endosomes by inducing a greater osmotic swelling compared to linear PEI.[134] Meanwhile, back in 2001, Wightman *et al*.[261] showed that transfection *in vitro* was more efficient for the DNA complex with linear PEI than with branched PEI. Despite the results of more recent studies (see below), which have demonstrated the advantages of cyclic, branched, and other complex architectures over linear polymers, linear PEI remains significant as one of the most studied and clinically validated reference polymeric carriers for nonviral NA delivery, although it has not been FDA approved for gene delivery.[262] Ahn *et al*.[263] chose linear PEI particularly as a clinically tested, industrially reproducible, and potentially scalable carrier for a drug to treat a syngeneic model of murine lung cancer. Using fast nanocomplexation technique, the authors achieved high-precision control of the size and composition of NPs, which also retained stability in the freeze-dried state. The study demonstrated a pronounced increase in median survival for both the orthotopic Lewis lung cancer (LL/2) model and metastatic B16F10 model. In addition, the authors noted the absence of pronounced systemic toxicity or statistically significant deviations in biochemical markers of liver function in the LL/2 model.[262,263]

It is believed that branched polymers have a higher potential for gene delivery owing to their improved buffering capacity, three-dimensional structure, and a multitude of terminal groups, which provide more effective interaction with cell membranes during intracellular transport, thus finally increasing the transfection efficiency.[82] A number of studies have demonstrated higher transfection efficiency achieved using branched polylysines, poly(β-amino esters),[264,265] whose synthesis is shown in Scheme 23, and poly(dimethylaminoethyl methacrylates) compared to their linear analogues.[77]

Currently, difficulties in preparation and purification still limit the development and application of cyclic polymers. A relatively small number of publications address this type of nonviral vectors for NA delivery. There are studies that report a higher performance of cyclic PEI (surpasses the linear analogue with the same length and is comparable with branched PEI in the transfection efficiency, while having lower toxicity),[266] cyclic amino acrylates [both parent PDMAEMA and sunflower PDMAEMA containing a poly(hydroxymethyl methacrylate) ring with polymeric petals],[267,268] and cyclic PβAE.[269]

The last-mentioned study states that cyclization of PβAE can markedly improve their characteristics as nonviral vectors: the precursors of the linear polymers (L-PβAE) were prepared by the Michael reaction, then they were terminated by butane-1,4-diol bis-acrylate and cyclized in the presence of azobis(isobutyronitrile) (AIBN) as a free radical initiator at high dilution (Scheme 24). As compared with the linear analogue,

[n] The more flexible $(AT)_{50}/(AT)_{50}$ chain has $l_p \approx 75$ nm, while for more rigid $(AC)_{50}/(GT)_{50}$, l_p is approximately 84 nm.

Scheme 23

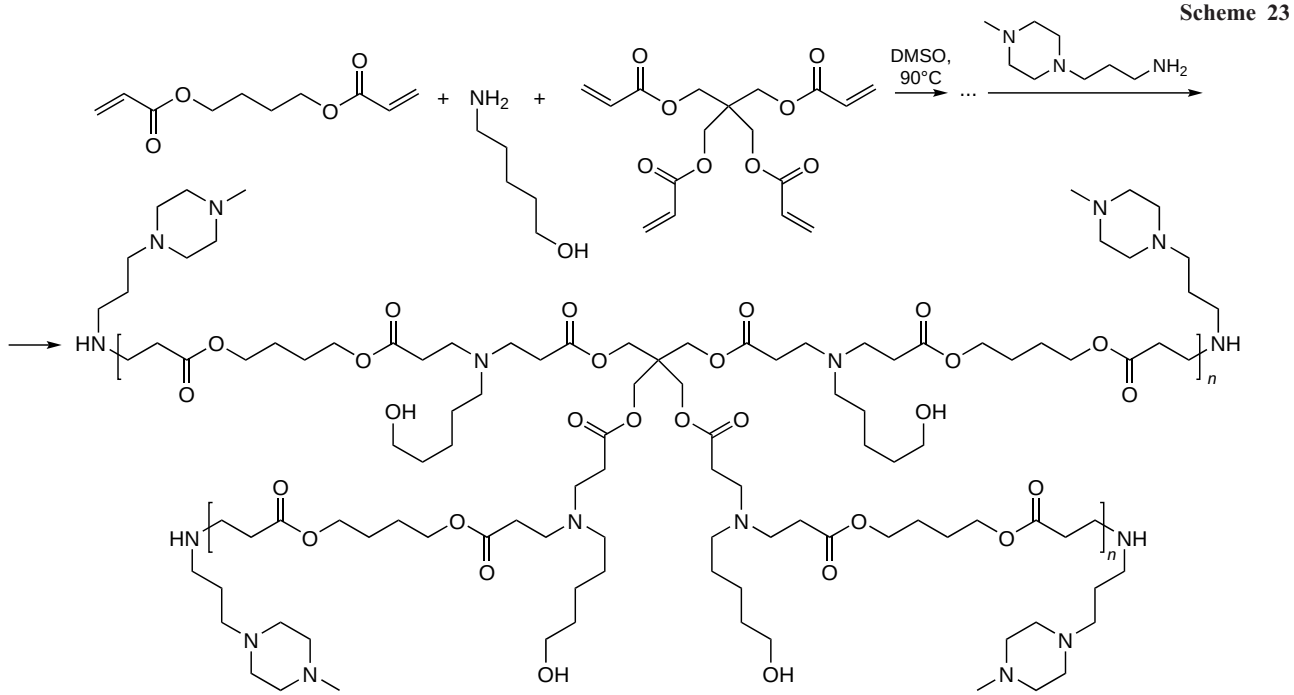

Scheme 24

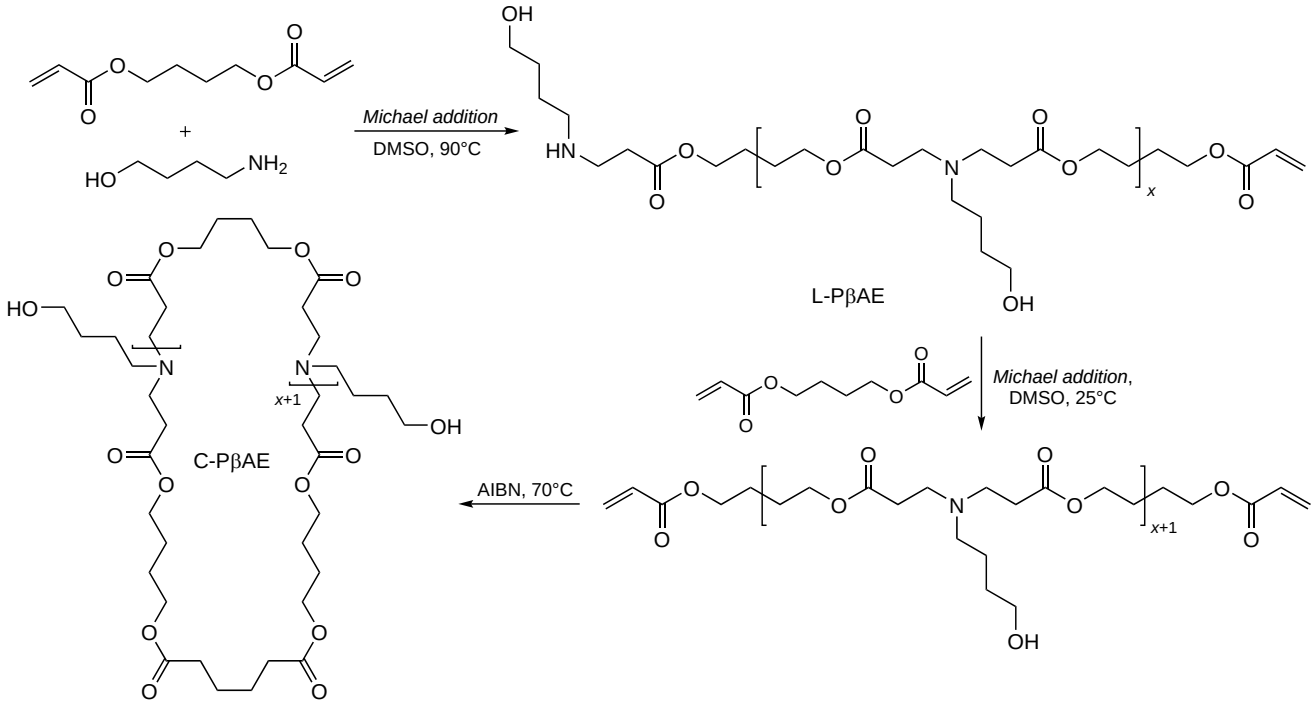

cyclic poly(amino ester) (C-PβAE) condensed DNA more efficiently (~55% *vs.* ~35%) and had a higher ζ-potential, which is consistent with the higher effective charge density corresponding to more compact topology. These structural features provided more efficient transfection of HEK293T cells. Cyclic poly(amino ester) ensured the formation of a much larger number of GFP+-cells and an approximately 10-fold gain in the secreted *Gaussia* copepod luciferase (gLuc) at optimal polymer : pDNA ratio in comparison with linear poly(amino ester). In addition, it had lower cytotoxicity: cell viability was above 75% even when the carrier to the cargo ratio was 150 : 1 (w/w), whereas in the case of the linear analogue, the cell viability was <45% even at a ratio of 50 : 1 (w/w).

Dalal *et al.*[270] and Floyd *et al.*[271] also showed that the use of graft polymers (*e.g.*, bottlebrush copolymers with a large number of side groups connected to the backbone) increases the efficiency of transfection and decreases cytotoxicity. Thus, poly(cyclooctene-*graft*-oligolysine) exhibited higher transfection efficiency in COS-1 cells (increase in the GFP expression) compared to linear poly(*L*-lysine).[272]

In some bottlebrush polymers, PEG chains act as numerous short-chain substituents[273–275] stabilizing the colloidal system. An additional benefit of this type of architecture is its efficiency in the cargo delivery to lung tissue. He *et al.*[276] described the synthesis of bottlebrush-PEG with a high density of grafted short (~1 kDa) PEG segments. The authors compared polymers

containing ~1000 and 750 side chains using a model of primary human bronchial epithelial cells in a system simulating the air/liquid interface (with endogenous mucus and a periciliary layer). It was shown that PEG with a higher density of grafted side chains passed through the mucus and the periciliary layer within a minute and was rapidly internalized by the cells; after incubation, the particle distribution became uniform for apical and basal cells. A decrease in the degree of branching decreased the cellular uptake by an order of magnitude, indicating that the bottlebrush geometry and high density of PEG grafting play a crucial role in the platform for drug delivery through mucous membranes.

Linear block copolymers are widely represented among promising NA carriers. Quite a few PEGylated polymers belong to this class, and the block structure provides the possibility of circumventing the PEG dilemma. According to a study of PEI and PEG copolymers with different block lengths,[277] an increase in the length of the PEG block regularly decreases the size and ζ-potential of the particles and crucially increases their colloidal stability, at the cost of a sharp decrease in the transfection efficiency compared to the PEI homopolymer. This was especially noticeable when the PEG concentration was > 50% where small (<150 nm), virtually neutral, and stable polyplexes were formed. The introduction of a redox-cleavable disulfide linkage between PEG and PEI increased transfection efficiency 1.2- to 4.5-fold compared to non-cleavable analogues.[277]

It is evident that any study dealing with the development of a block copolymer-based NA carrier necessarily includes optimization of the length of each block and that fine-tuning of the degree of polymerization of the cationic part is of fundamental importance. In a study by Hayashi *et al.*,[182] which was already mentioned above, the authors established the formation of very small uPIC complexes consisting of one siRNA molecule and one PEG-PLL copolymer molecule. The latter contained a polycation segment that exactly corresponded to the length of NA (Scheme 25).

The subsequent studies demonstrated the possibility of introducing siRNA and ASO into the blood without preliminary binding to the carrier. The uPIC complexes were formed in the blood stream, which was confirmed by 20-fold increase in the circulation time of siRNA. Furthermore, the obtained polyplexes exhibited 15-fold higher siRNA accumulation in the pancreatic tumour and the ability to cross the blood–brain barrier (BBB), resulting in a 90% reduction in target gene expression.[278] It was also shown that NA exists in a dynamic equilibrium between its free and uPIC-bound forms; that is, the presence of excess polymer can further prolong the blood circulation.[279] Consequently, the number of carrier molecules is clearly determined by the NA charge.[280]

Taniguchi *et al.*[281] and Chaya *et al.*[282] reported uPIC complexes with the composition polymer : double-stranded NA = 2 : 1 (see the lower reaction in Scheme 25),[o] which effectively delivered material to triple-negative breast cancer tissue. This suppressed tumour growth and reduced metastatic burden in the lungs. The average survival time of the animals was up to 87.5 days compared with 34 days in the control group. In addition, these systems were used for the delivery to inflamed muscle tissue: ~80% knockdown was achieved for the MALAT1 target in the quadriceps at an N : P ratio of 2. This is a nontrivial result, since it requires penetrating the continuous endothelium, which becomes possible exactly due to the drastic reduction in the size of the uPIC complex compared to LNPs.

A nontrivial question regarding the structural features of copolymers was raised by Lawson *et al.*[283] As a rule, a single study focuses on either statistical copolymers or block copolymers, but perhaps, intermediate, gradient structures would offer certain advantages as NA carriers. It was shown that copolymers of different microstructures, statistical (S), block (B), and gradient (G1–G3) ones, but with the same length and monomer composition, form spherical polyplexes of comparable size (~50 nm) crucially differing in the 'capacity' and NA binding strength. Copolymer B and the most block-like polymer G1 carried more pDNA molecules per particle and showed the strongest retention (the dissociation constant of B and NA polyplex was ~0.7 μM). The former condensed pDNA with minimum change in its native conformation, while copolymer S and more 'statistical' gradient polymers required considerable conformational rearrangements in pDNA for binding. In a protein–salt solution, the microstructure determined the colloidal behaviour. Copolymers S and G3 aggregated in serum, whereas the G1 and G2 materials remained stable (the aggregation occurred at high N : P ratios). Paradoxically, copolymer B lost pDNA more significantly (*via* serum-induced release), despite its high dimensional stability, whereas polymer G1 combined resistance to aggregation with more favourable retention of the cargo. This directly determined the results of testing on the HEK293T cell line. The macromolecule S provided the highest transfection efficiency, but this was accompanied by a sharp increase in cytotoxicity; copolymer B was well tolerated, but almost did not express the transgene, while polymers of series G showed intermediate results. Among the gradient copolymers, material G1 provided the best balance between pDNA delivery efficiency and viability of HEK cells. From the mechanistic standpoint, the differences were mainly manifested in the cellular uptake (in the series S > G1 > G2 > G3 ≫ B), whereas the intracellular locations of the polyplexes already taken up (cytoplasm or nucleus regions; colocalization with lysosomes) were similar and depended only little on the microstructure.

[o] The numbers in parentheses next to a polymer name indicate the number of lysine residues; for siRNA, they indicate the length in nitrogenous base pairs.

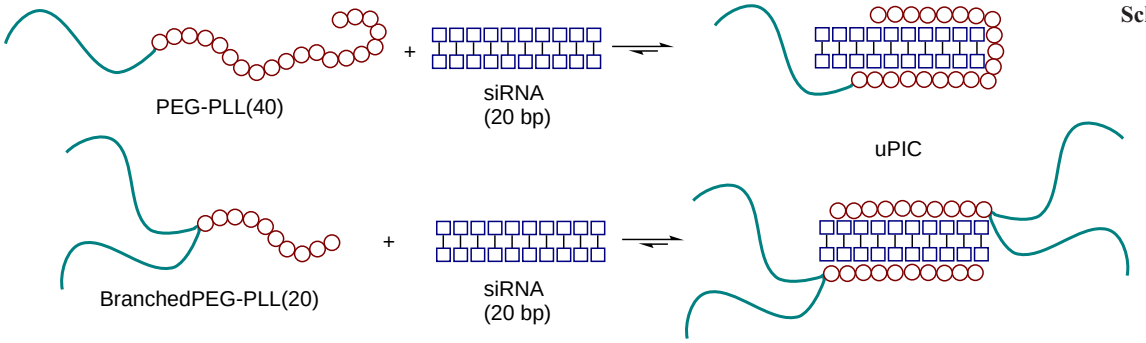

Scheme 25

4.6. Morphology and colloidal properties of polyplexes

4.6.1. Morphology of polyplexes

The size and surface charge of the nanoparticles formed by NA and the carrier have a crucial effect on the actual mechanism of endocytosis; however, other factors are also important. The structural factors (if it includes not only particle size and ζ-potential, but also internal architecture, surface composition, and other parameters) influence phase stability in the blood stream, the specificity of delivery to organs and tissues, and the efficiency of endosomal escape.[226,284,285]

The architecture of the polymeric NA carrier plays a decisive role in the morphology of the polyplexes.[226] Linear and branched cationic polymers (*e.g.*, PEI) are dissolved in an aqueous medium and form polyplexes, that is, complexes with plasmid DNA. Copolymers behave in a similar way if both types of monomer units are charged.[286] Polyplexes formed by block copolymers of the 'cationic block+hydrophilic uncharged block' type (PEI-PEG, PLL-PEG, *etc.*) show a pronounced compaction of plasmid DNA and increase the colloidal stability in biological media, which results in high transfection efficiency.[287] Meanwhile, the architecture of the colloidal system depends appreciably on the type of NA incorporated into the polymer.

The condensation of the PLL-PEG copolymer with DNA resulted in the formation of polyelectrolyte complex micelles (PCMs, Fig. 25).[288] Double-stranded DNA complexes with PLL-PEG block copolymers formed cylindrical micelles with a polyelectrolyte core and a PEG shell, whereas single-stranded DNA formed spherical micelles under the same conditions. The lengths of the Kuhn segments, which describe the bending stiffness of double-stranded PCMs, ranged from 45 to 60 nm, which was close to the persistence lengths of pure double-stranded DNA.[288]

Amphiphilic block copolymers of the 'cationic block+hydrophobic block' type self-assemble into micelles in solution (provided that the hydrophobic block is sufficiently long), and upon the addition of plasmid DNA, they form micelleplexes (Fig. 26).[289] Micelleplexes have a beads-on-a-string structure, in which DNA strands wrap around and connect a multitude of polycationic micelles. These particles provide a higher (by a factor of more than four) transfection efficiency than polyplexes, with a comparable level of cytotoxicity. The D and OD polyplexes form large aggregates and globular structures, respectively, with plasmid DNA condensed in the core.

Studies that compare polyplexes and micelleplexes are relatively rare and their results are contradictory. Sharma *et al.*[290] described a comparative study of the efficiency of plasmid DNA binding to three carriers: PDMAEMA homopolymer, PDMAEMA-PBA block copolymer [PBA stands for poly(n-butyl acrylate)], and PEG-PBA-PDMAEMA block terpolymer.[290] According to experiments, micelleplexes exhibited lower transfection efficiency than polyplexes. In the authors' opinion, this is potentially due to the higher binding affinity of plasmid DNA in the complex core. Conversely, micelleplexes of the same composition containing siRNA surpassed block copolymers in terms of efficiency;[291] the authors attributed the observed difference to different internalization mechanisms.

A direct comparison of pDNA assembly into polyplexes and micelleplexes with identical chemical composition of the blocks was conducted in 2019. Tan *et al.*[289] confirmed the formation of PDMAEMA and PEG-PDMAEMA polyplexes with pDNA condensed in the core. Polyplexes based on homopolycations

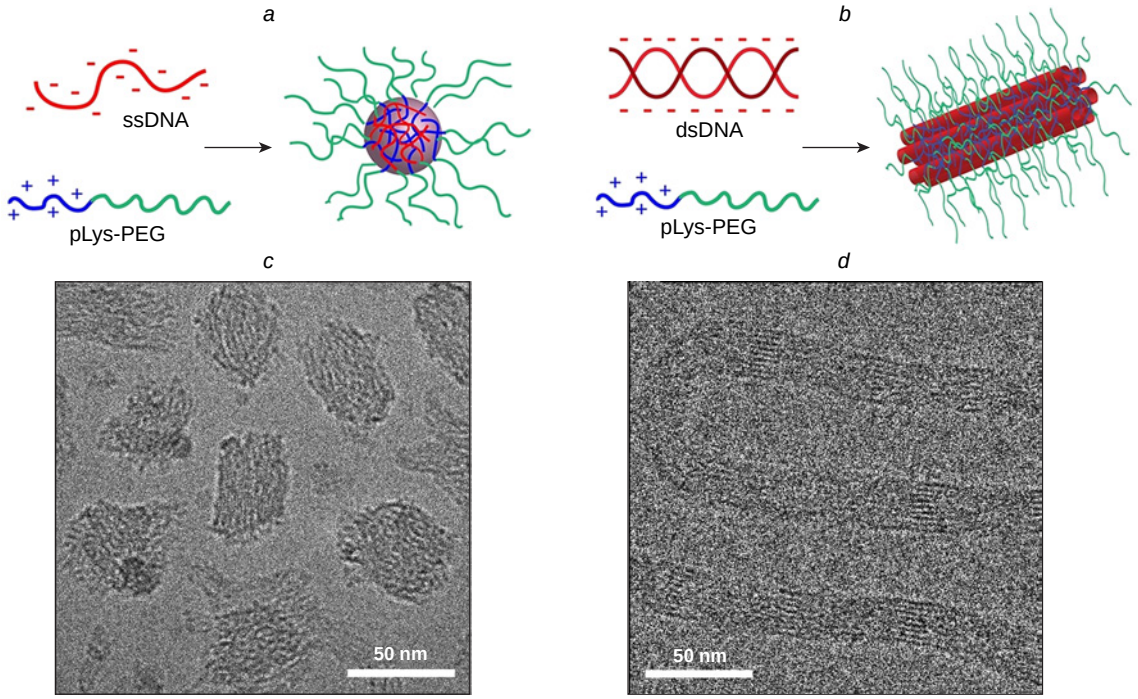

Figure 25. Diagrams of self-assembly of polyplexes: formation of spherical PCM nanoparticles with a minimum internal ordering from single-stranded DNA (22 nucleotides) and Lys(50)-PEG(5k) block copolymer (*a*) and formation of long (⩾ 1 μm) flexible PCM with parallel ordering of DNA helices from double-stranded DNA (22 bp) and Lys(50)-PEG(20k) block copolymer (*b*); and cryo-TEM images of the spherical (*c*) and cylindrical (*d*) polyelectrolyte micelles.[288] Copyright American Chemical Society 2018.

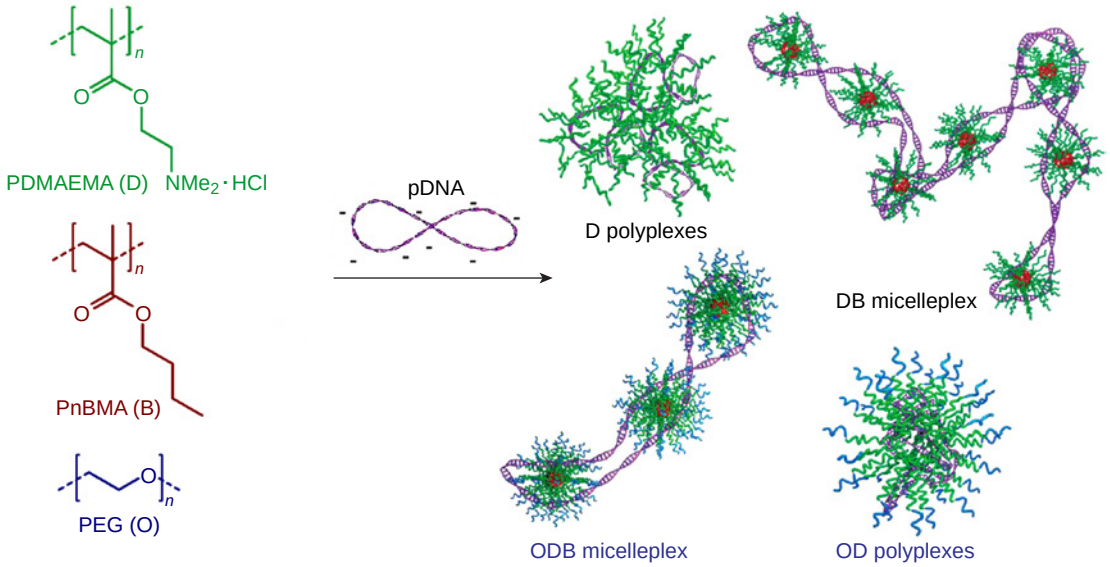

Figure 26. Schematic image of the interaction products between cationic polymers (D, B, O) and plasmid DNA: the D and OD polymers form complexes and polyplexes, while amphiphilic block copolymers DB and ODB are self-assembled into spherical micelles and form micelleplexes with plasmid DNA.[289]

were eventually transformed into large aggregates, while PEGylated polyplexes were stable for a week. In addition, the authors observed the formation of PBA-PDMAEMA and PEG-PBA-PDMAEMA micelleplexes with a beads-on-a-string structure. They showed that micelleplexes were more than four times superior to polyplexes in the transfection efficiency, with the cytotoxicity levels being approximately equal. They also found that micelleplexes are internalized by the CvME mechanism more efficiently than polyplexes. The inclusion of a greater number of amino groups (and a decrease in pK_a due to the close proximity of neighbouring polymer chains) into each micelleplex could potentially facilitate the release of NA from the endosome. More importantly, the beads-on-a-string in the packing of micelleplexes mimic the way cells wrap DNA around histones in chromatin and preserve the native B-DNA helix. Tan *et al.*[289] assumed that this structural preservation of DNA can provide much more effective protein expression compared to DNA condensed in polyplexes and possessing a substantially changed secondary structure.

It should be noted that not all amphiphilic block copolymers are capable of forming micelleplexes. In the studies mentioned above, the number of lipophilic units was several dozen and, in some cases, about a hundred. However, if the hydrophobicity of the block copolymer is insufficient for self-assembly to micelles, the formation of colloidal polyplex particles occurs only upon the addition of NA. The research team headed by Waymouth[292] found that complexes of CART block copolymers (Fig. 27) with RNA form coacervate nanoparticles with a clearly defined internal phase organization.

In the case of low-molecular-weight CART, in which the total number of units (both hydrophobic and cationic) does not exceed 24, mixing with mRNA results in the formation of particles with sizes of ~140–220 nm, a positive ζ-potential, and a characteristic bicontinuous worm-like morphology. In these NPs, the hydrophobic (lipid) domains and aqueous or coacervate channels run through the whole particle. This conclusion was supported by images obtained using cryo-electron microscopy (cryo-EM) and its tomographic version (cryo-ET), as well as scattering data (SAXS, SANS), which make it possible to estimate a characteristic period of ~6–8 nm domains. In

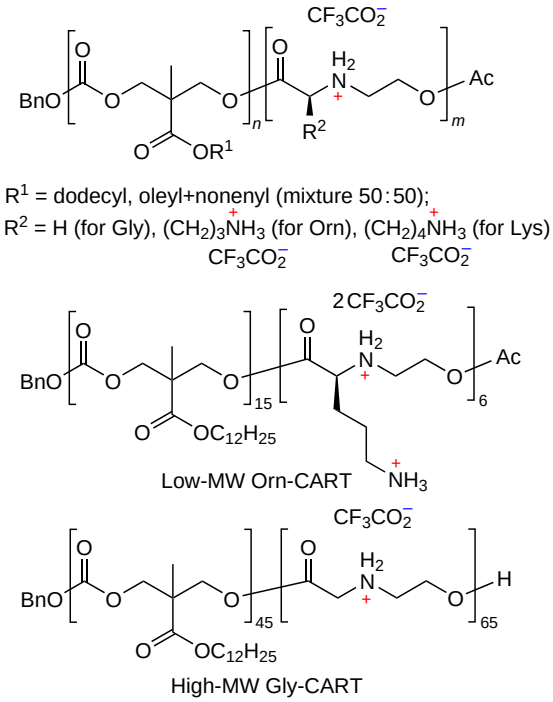

Figure 27. Structures of CART copolymers.[292]

addition, the particles were shown to be relatively stable to the variation of the N:P ratio in the range in which the particles are clearly detected. The type of RNA influences also the degree of ordering. For example, in the case of siRNA, apart from the bicontinuous morphology, more regular lamellar regions and a multilayer upper shell are detected; this is reflected in sharper SAXS peaks. The chemical structure of CART (the type of cationic block and features of the lipid moiety, including unsaturation) systematically shifts the domain distances, whereas neat polymers, without RNA, form unstructured emulsions. This points to the key role of RNA as a driver of morphogenesis through a combination of coacervation and

hydrophobic segregation. Finally, an increase in the molecular weight changes the type of self-assembly. High-molecular-weight CART (totally ~100 units) form aggregated micelle-like structures with a diameter of 10–20 nm, instead of bicontinuous particles, thus indicating that the polymer architecture and size determine the internal morphology. From a biological standpoint, the bicontinuous architecture proved to be the most effective for *in vitro* delivery of mRNA. All low-molecular-weight CARTs with this type of structure provided the delivery or expression in A549 cells (to varying degrees depending on their structure), whereas the only high-molecular-weight polymer without a bicontinuous morphology was ineffective. However, in *in vivo* experiment, gene expression was also observed after intramuscular administration of formulations containing high-molecular-weight CART. For this reason, the relationship between phase behaviour and delivery efficiency is considered to be likely for cell transfection, but not yet sufficiently studied at the organism level.[292]

4.6.2. Colloidal properties of polyplexes

While switching from a discussion of the internal structure of NA–carrier nanoparticles to their colloidal properties, we would like to note that precisely the colloidal characteristics of the particles, first of all, the average size, dispersity, and surface charge, have been identified as critical quality parameters in the production of RNA vaccines. Although the optimal size of the NP carrier remains a matter of debate and varies depending on the administration method, the target size is usually less than 200 nm and the polydispersity index (PDI) is less than 0.3.[285]

Sekar *et al*.[293] attempted to distinguish between the transfection dependence on the polyplex size and on the polycation chemical structure, which are studied in parallel in most works. The authors developed a method for the production of polyplexes of P(DIPAEMA$_{56}$-*st*-HEMA$_{48}$) [DIPAEMA is 2-(diisopropylamino)ethyl methacrylate, HEMA is 2-hydroxyethyl methacrylate] greatly varying in size with pDNA with a hydrodynamic radius of 40 to 827 nm. First, the complexes were formed at low pH and low ionic strength of the solution; then, their controlled aggregation was initiated through deprotonation of the polycation and Debye shielding and then it was arrested at the desired stage by acidification of the solution. As a result, it was established how the morphology of the complex changes with increasing size. The small polyplexes had a nearly spherical shape, whereas the larger ones had a fractal-like morphology characteristic of diffusion-limited aggregation. The latter not only contained more pDNA, but also packed it progressively less densely (according to static light scattering, SLS, data)[p] following increase in the hydrodynamic volume. According to biological experiments, the optimal size varied depending on the cell type: in the case of HEK293, polyplexes of 85–136 nm size provided the best results; for ARPE-19, a wider range of 85–349 nm proved to be efficient; while for RAW macrophages, the size was generally much less significant, except for the decrease in the efficiency of transfection for the largest particles. Thus, by merely tuning the polyplex size, it is possible to deliberately move along the scale of efficiency and toxicity without replacing the polymer. Simultaneously, it was shown that hemolysis mainly depends on the composition of the carrier rather than on the size of the polyplex. Hence, polyplexes of all sizes were less prone to cause hemolysis (8–12% lysed blood cells) than Lipofectamine 2000 (18%) or jetPEI (23%).

The significant contribution of the properties of the medium to the colloid behaviour of NPs is also illustrated by the study of Coelho *et al*.[294] The authors showed that the method used to prepare solutions with a physiologically relevant ionic strength considerably affects the size and the colloidal stability of the polycation–DNA complexes. Meanwhile, the final composition of the complexes is formally identical. The authors used two assembly protocols: mixing of NA and the carrier in water followed by the addition of a buffer solution (path I) and component mixing in a ready buffer solution (path II). A comparison indicated that even at NaCl concentrations of ~70 mM, the polyplexes formed according to path II were, as a rule, larger and less stable and also had a wider aggregation regions near the isoelectric point. Path I resulted in the formation of smaller and more stable particles. This effect is attributable to the kinetics of complex formation: in water, the structures are fast stabilized in a dense, excess charge state even after the addition of a salt, whereas in the presence of a salt in the initial solution, complex formation proceeds more slowly and leads to optimal charge neutralization, which facilitates NP aggregation. The PLL polymer forms the most stable and relatively small particles, PEI induces a more pronounced aggregation and gives larger aggregates, and biodegradable bPLL [Cys-(Lys)5-Cys heptapeptide cross-linked to form poly(disulfide) under the action of DMSO] is aggregated especially easily in the presence of salts and virtually does not form stable phases. In A549 cell cultures, the structural differences have almost no effect on transfection: PEI provides higher GFP expression than PLL, despite the lower cellular uptake of NPs. This is in line with better endosomal escape or release of NA in the case of PEI, whereas PLL exhibits high cellular uptake at low expression levels, and bPLL shows neither pronounced uptake nor transfection. The only consistent biological difference between the two protocols of polyplex assembly is the decrease in the cellular uptake of PEI upon assembly in the salt (path II) compared to that for path I, with the overall transfection efficiency being comparable; and no significant cytotoxicity was observed under any conditions with the selected parameters. Thus, subtle variations in the assembly protocol substantially change the physicochemical characteristics of the polyplexes and could potentially become critical in more complex *in vivo* scenarios.

4.6.3. Protein corona

Yet another important feature of the NP surface is the protein corona formed in a physiological medium. In the case of lipid nanoparticles, the protein (or, more broadly, biomolecular) corona transformed from a secondary colloidal and biological issue into a central concept used to interpret the behaviour of LNPs *in vivo*. Whereas Francia *et al*.[295] noted in their review of 2020 that the number of direct studies of the corona effects for LNPs is moderate, in the subsequent years this topic rapidly became a mechanistic issue. It was shown that the adsorption of ApoE (apolipoprotein E is a blood plasma protein involved in the lipid transport and recognition of lipoprotein particles by cellular receptors) is not only related to the liver tropism of LNPs, but is also able to rearrange their internal organization and composition.[296]

This reasoning was followed most consistently in the studies of Siegwart's research team.[297,298] Using the SORT-LNP

[p] SLS (static light scattering) is a method based on measurement of the intensity of light scattered by particles at different angles and concentrations followed by calculation of the molar (or molecular) weight of the aggregates and the radius of gyration using these data.

models,[q] the authors demonstrated that a change in the chemical structure of the supplemental lipid changes the composition of the protein corona and thus influences the organ specificity of the delivery.[297] In particular, Dilliard *et al*.[298] described a corona for lung-tropic systems that had a lower contribution of ApoE and a higher contribution of vitronectin and other proteins compared to those of conventional liver-tropic four-component LNPs.[298]

The subsequent studies have shown that not only apolipoproteins such as ApoE, but also high-density lipoproteins may be functionally significant components of the corona, and the research area has reached a new methodological level, owing to the emergence of special approaches for isolation and analysis of the corona directly on LNPs.[299] In contemporary studies, the corona is considered not merely as a factor of cellular uptake, but also as a factor of effective delivery: it may enhance binding of particles to cells, but simultaneously reduce the efficiency of mRNA release and expression.[300] The protein corona should be regarded as a separate design tool, as it alters not a single parameter, but the whole identity of the carrier, including size, aggregation behaviour, effective surface charge, stability in salt solutions, and, finally, the expression level of the delivered NA.

Evidently, corona effects are equally important for polyplexes. Using the classic PEI–pDNA model, Zhu *et al*.[301] showed that the adsorption of BSA and serum proteins modifies the hydrodynamic size, ζ-potential, morphology, and salt sensitivity of PEI polyplexes. The next study of the same research group[302] additionally demonstrated that the BSA corona effect cannot be adequately described by only the reporter signal averaged over the cell population, since corona changes both the expression kinetics and heterogeneity at a single cell level. In the case of PEI systems, albumin has a dual behaviour: it can shield excess cations, but for certain incorporation routes, it increases the cellular uptake and transfection. Syga *et al*.[303] demonstrated that even the order of albumin introduction into the complex plays a crucial role for the L-PEI–pDNA particles, while Carrabino *et al*.[304] attributed the enhancement of PEI-mediated gene delivery in models of respiratory epithelium to facilitation of cellular uptake for albumin-containing complexes.

It is worth noting that the corona of polymer carriers can already be programmed. Zhang *et al*.[305] reported retinol-conjugated PEI that selectively accumulated retinol-binding protein in the corona, thus directing ASO-loaded particles to the hepatic stellate cells and reducing the type I collagen expression in two models of hepatic fibrosis in mice, induced by CCl_4- and bile duct ligation. Proteomic evidence indicates that this effect appreciably depends on the hydrophilic–lipophilic balance of the polymeric carrier. For example, Hartl *et al*.,[306] who compared bPEI and polyamidoamine $NM_{0.2}$–$CP_{0.8}$, found compositional differences between the dense inner corona, first of all, higher amount of HABP2 in $NM_{0.2}$–$CP_{0.8}$ polyplexes and decrease in ApoB[r] at comparable albumin, transferrin, and ApoE levels.

Structure of $NM_{0.2}$–$CP_{0.8}$

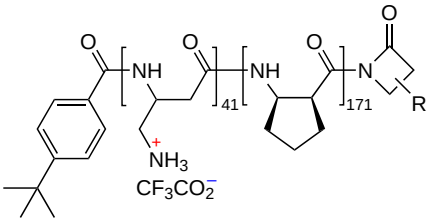

The authors revealed different sets of functionally significant proteins that may potentially influence the direction and efficiency of transfection.

Finally, as illustrated by new polymer-based mRNA delivery systems, it is clear that the formation of a useful protein corona can be deliberately stimulated, while the formation of an undesirable one can be suppressed. For example, in 2025, while studying fluorinated PAMAM, Fan *et al*.[307] showed that mRNA polyplexes form a serum albumin layer, which facilitates the uptake through receptor-mediated endocytosis. Meanwhile, in another publication of the same year,[308] the F-PEI–mRNA–heparin ternary polyplex with an mRNA:heparin ratio of 1 : 1 retained 89% encapsulation efficiency and stable small size (average diameter of ~40.5 nm) for more than three weeks in a serum medium. The authors attributed this fact to inhibition of excessive adsorption and prevention of large aggregation of serum proteins. Altogether, these results indicate that in the context of polymeric delivery systems, the protein corona is not a secondary artifact but rather a tunable module that can either hinder NA delivery due to destabilization of polyplexes and unproductive cellular interactions, or, conversely, facilitate the selective uptake of NAs by cells in particular organs.

4.7. Thermal sensitivity

One tool for improving the performance of polymeric NA carriers is to design thermosensitive colloidal systems formed by an amphiphilic polymer and NA. The design of the corresponding copolymers plays a key role in the development of such systems, as particularly the ratio of lipophilic, hydrophilic, and (poly)cationic moieties, together with the hydration characteristics of all structural segments of the macromolecule determine the structure and relative stability of the associates upon variation of the temperature. The colloidal behaviour of amphiphilic polymers in aqueous solutions is described by two parameters. The first one is the critical micellization temperature (CMT), or Krafft point, characteristic of ionogenic surfactants, that is, the temperature above which the solubility of an ionic surfactant is sufficient for micelle formation. Below this temperature, the crystalline phase predominates. The second parameter is the lower critical solution temperature (LCST), a more general parameter applicable to two-phase solutions and typical of various amphiphilic copolymers. This is the temperature above which the polymer solution undergoes phase separation due to dehydration and chain collapse; for amphiphilic block copolymers, this may be accompanied by micelle formation.

The foundations for the use of thermosensitive (thermo-responsive) polymers for NA delivery were laid in 2000 by Kurisawa *et al*.[309] The main idea of this study was to find a balance between the stability of the NA–polymer complex in an external environment and its dissociation within the cell by using an external physical signal, that is, temperature. The authors synthesized a thermo-responsive cationic copolymer

[q] SORT-LNP (selective organ targeting lipid nanoparticles) is an approach designed for LNP retargeting after intravenous administration. A fifth component, SORT molecule, is added to the conventional four-component LNP formulation; the chemical nature of this molecule changes the composition of the adsorbed protein corona and thus it can switch the predominant mRNA delivery from liver to other organs, including lungs and spleen.

[r] HABP2 (hyaluronan-binding protein 2) is a serine protease of blood plasma capable of binding hyaluronic acid; ApoB (apolipoprotein B) is the protein component of blood lipoprotein particles, first of all, low-density lipoproteins, which are involved in the receptor-mediated lipid transport.

P(NIPAAm-*co*-DMAEMA-*co*-BMA) (NIPAAm is *N*-isopropylacrylamide), the plasmid complex of which was tightly held above LCST and partially dissociated at lower temperature. Using the COS-1 model (African green monkey kidney cells) with the pCMV-lacZ plasmid, the authors showed that a short-term cooling of this copolymer after incubation at 37°C increased the gene expression, which is not the case for conventional PDMAEMA. Thus, gene expression can be controlled through the temperature-dependent formation and degradation of the polyplex, that is, not merely DNA delivery, but also the instant of DNA release can be tuned.

A review by Bikram and West[310] published in 2008 put forward a more general concept: temperature is a very convenient external trigger for controlled drug release. This is due to the fact that systems of this type can be tuned for the physiological range, utilized for local hyperthermia, and administered almost non-invasively, *e.g.*, as solutions that are converted into a gel or change the structure in the body. The behaviour of PNIPAAm, the main object of this review, and related materials was shown to be determined by LCST and the balance between the hydrophilic and hydrophobic segments. By varying these parameters, it was possible to produce hydrogels, micelles, liposomes, and other carriers that switch on or off the release of the cargo in response to changes in temperature. The limitations of the method are related to moderate mechanical properties of PNIPAAm hydrogels and potential issues with the long-term biocompatibility of the degradation products of this polymer. The review proposes the following evolutionary path for the development of thermosensitive carriers: from simple PNIPAAm systems and more complex platforms: thermo-responsive PEG analogues, biodegradable thermogels, elastin-like polypeptides and liposomes, and combined systems in which the effect of temperature is accompanied by a change in pH or irradiation for more precise control of the release. To date, thermo-responsive polymers have carved out their own niche of smart NA carriers.[311–314]

Apart from the sharp and visible solution ⇆ associate transitions, temperature variations may also accompany less pronounced morphological changes in thermosensitive colloidal particles. For example, changes of this type at physiological temperatures (~37°C) were reported by Ma *et al.*[180] for micellar siRNA polyplexes and mixtures of cationic AB diblock and ABA triblock copolymers, as well as a polyanionic component, homopolyanion (Scheme 26). The latter counterbalanced the total charge thus providing the compatibility of cationic copolymers with a flexible chain and rigid siRNA.[315]

The following values were used as variable parameters characterizing the component ratios:

— f_{tri} is the molar ratio of the number of positive charges in the ABA polymer to the total number of positive charges,

— f_{miRNA} is the molar ratio of the number of negative charges in siRNA to the total number of negative charges.

At the optimal ratios $f_{tri} = f_{miRNA} > 0.5$ and a balanced charge, micelles with a diameter (d) of ~70 nm formed hierarchical coacervate microparticles ($d > 200$ nm). In combination, they formed a cross-linked network of cylindrical micellar domains

Scheme 26

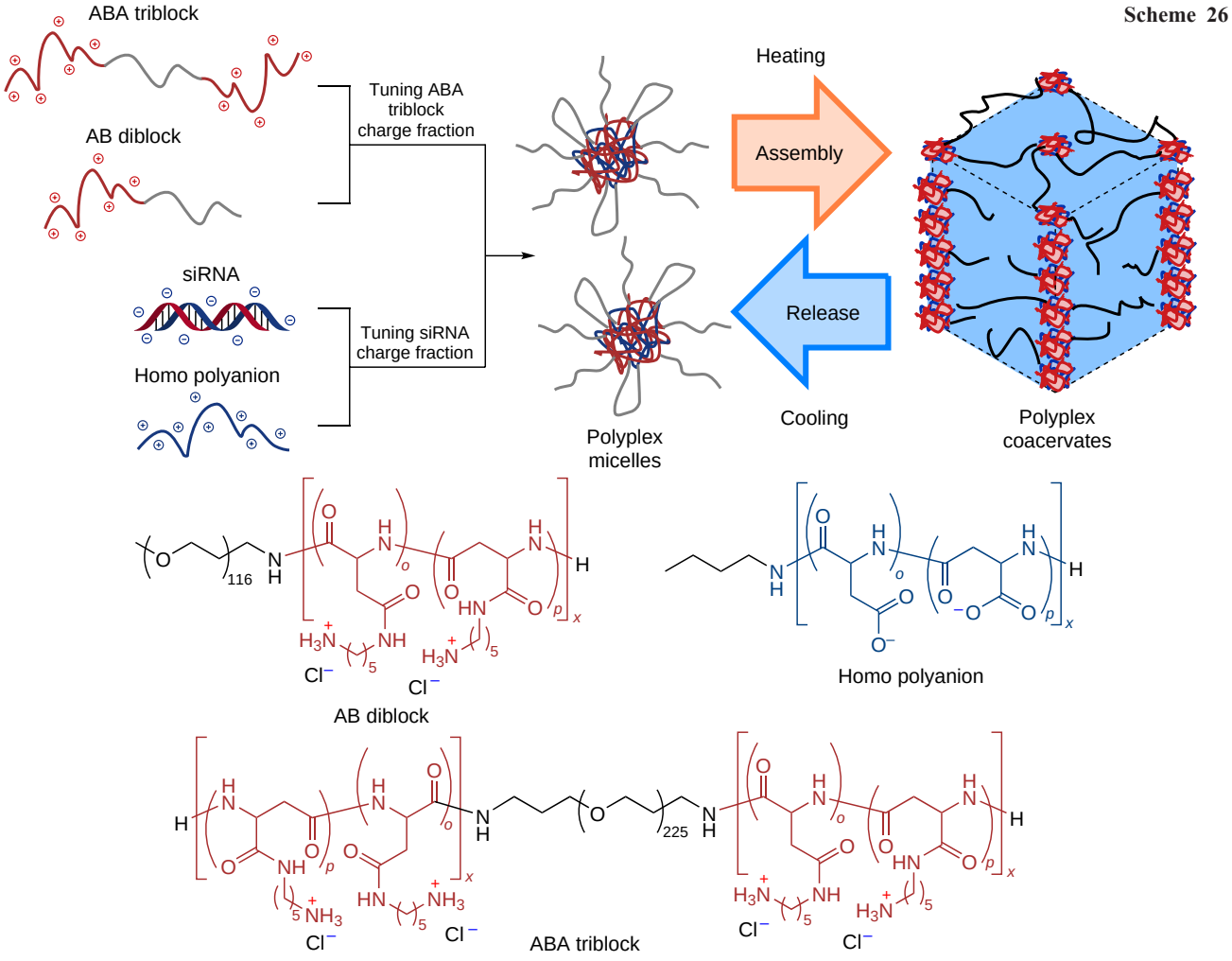

(see Scheme 26) capable of releasing siRNA at 37°C and at a constant rate for a long period of time (~10 days), primarily as PIC structures. The kinetics of NA release was nonuniform: in the early stage, small polyplexes (up to the uPIC level) were mainly released into the solution; the release of full-sized micelles was delayed for ~72 h. In cellular assays, the coacervate formulation provided a higher siRNA accumulation compared to conventional micelles of the same composition and induced a statistically significant reduction of the expression of the target gene. The cytotoxicity measured against CT26-Luc cells at concentrations of up to 7.5 mM after 24 h was virtually absent. However, after 72 h, a concentration of 2.4 mM was already found to be toxic (a 90% decrease in cell viability compared to the control). The results of the experiments on NA delivery into cells are ambiguous due to their short duration, which was 3 days. It was shown that a coacervate can be used for the gradual release of siRNA-carrying polyplexes; however, further research is needed to improve the efficiency of polymer-based delivery systems of this type.

Hossainy *et al.*[316] chose poly[ethoxydi(ethylene glycol) acrylate] (PDEGEA) with LCST ≈ 13–15°C as a polymeric carrier. At low temperatures, PDEGEA was hydrated and was stable in aqueous solution; a temperature rise led to a decrease in hydrophilicity and initiated the formation of polymersomes (Scheme 27). At ~4°C, solutions were prepared for a series of RAFT copolymers with a thermosensitive PDEGEA130 block in combination with either neutral poly(2-hydroxyethyl acrylate) (PHEA70) or cationic poly[2-(trimethylammonio)ethyl acrylate] (PTMAEA25) blocks in various ratios; micelle-forming copolymers were tested for NA delivery. The lengths of the neutral and cationic hydrophilic blocks were selected relying on the results of earlier studies[317] on the stability of similar colloidal systems. The developed polymersomes demonstrated more pronounced suppression of mRNA targets (~60% for siVEGF-A and ~50% for siBcl-2) compared to Lipofectamine 2000. In a subcutaneous xenograft model of MCF-7 (human breast adenocarcinoma), the intratumorally administered polymersomes retarded the tumour growth and increased the survival of laboratory animals (mice) to a larger extent.

This work is an example of a well-planned comparative study: the efficiency of polymersomes was evaluated not only in relation to free siRNA and unloaded carrier, but also in comparison with LNP formulations similar to the clinically used Alnylam systems. Thirty five days after inoculation of MCF-7 tumour cells and a series of intratumoral injections at the same siRNA dose, the average tumour volume was approximately 500–580 mm^3 for LNP carriers and approximately 300–330 mm^3 for polymersomes containing either siVEGF-A or siBcl-2.

5. Current approaches to the development of polymeric NA delivery systems

The most recent advances in the development of innovative polymeric carriers can be illustrated by particular examples of polymers of various classes that have been introduced in recent years, in comparison with popular low-molecular-weight transfection reagents.

5.1. Poly(β-amino esters)

Bo *et al.*[318] performed a comparison of PβAE with commercial polymeric (jetPEI) and lipid (Lipofectamine 3000) carriers. Star-shaped poly(amino esters) (SPAE) were found to be generally superior to both reagents. All eight SPAE–DNA polyplexes exhibited higher transfection efficiency in experiments with HeLa cells at a 40 : 1 ratio (w/w); the best results were obtained for SPAE-4 and SPAE-3 samples (96.1 and 90.4% GFP-positive cells, respectively). In the case of difficult-to-transfect human HaCaT normal skin cells (keratinocytes) and NHF cells (fibroblasts), the SPAE-4 delivery vector provided 20 and 16% GFP+ cells, respectively, which was ~2 times superior to the performance of Lipofectamine 3000. Similar results were obtained for HepG2 and HCC-LM3 cells (human hepatocellular carcinoma) and A2780 cells (human endometrioid ovarian carcinoma). Thus, the superiority of new-generation polymeric carriers over both the classic lipid-based formulation and the basic polymeric carrier was demonstrated in relation to a wide range of cell lines. The viability of HeLa cells after transfection with SPAE was > 86% for mass ratios ranging from 20 : 1 to 60 : 1, thus exceeding that observed for jetPEI.

A direct comparison of the PEG-PβAE polymeric carrier with a lipid system similar to the Comirnaty platform (the base of the COVID-19 vaccine developed by Pfizer and BioNTech) demonstrated an obvious advantage of the former for targeted delivery of mRNA to the brain.[319] For similar sizes (~65–70 nm), the polymer nanoparticles were more uniform: PDI was 0.19±0.04, compared with 0.39±0.03 for LNPs. The former had a nearly neutral surface charge, which resulted in a fundamentally different pharmacokinetics: in four hours after intravenous administration, approximately 30% of the dose remained in the blood stream for PEG-PβAE–mRNA, but only

Scheme 27

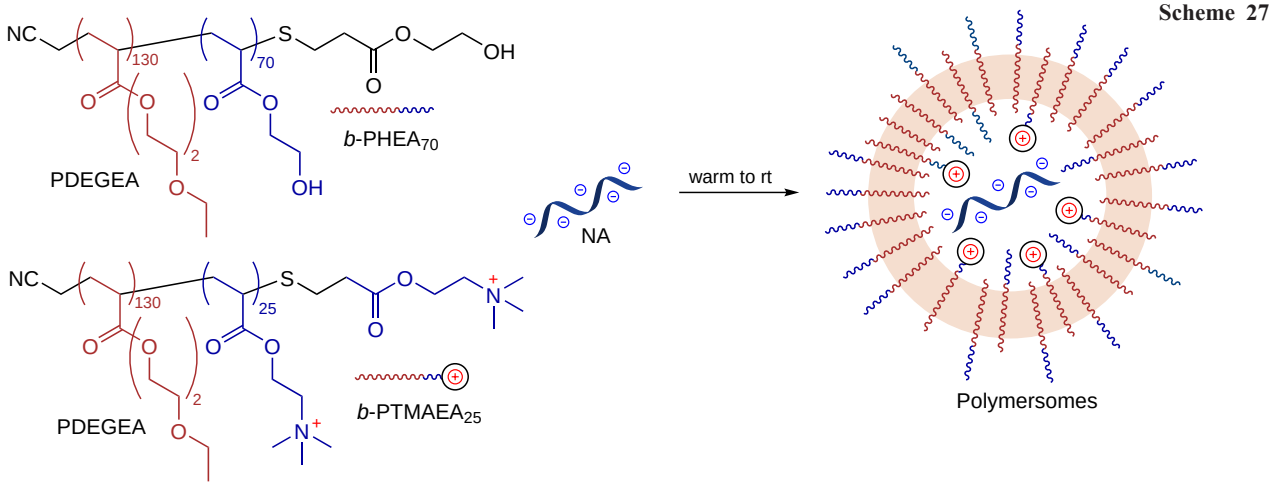

1% for the LNP system. Furthermore, following focused ultrasound (FUS)-mediated opening of the blood–brain barrier (BBB), only the PEG-PβAE–mRNA system ensured truly effective reporter expression in the treated brain region: luciferase activity was approximately 6–8 times higher than that observed in the lipid system. In other words, in this study, the advantage of the new polymeric reagent over the commercial lipid carrier was provided by a combination of prolonged circulation of the polyplexes, low retention in the liver, and the ability to effectively deliver mRNA to the brain parenchyma. Despite clinical validation for other routes of administration, the use of LNPs for this purpose proved to be ineffective.

It is noteworthy that competition between high- and low-molecular-weight delivery systems does not always mean complete abandoning of one system and switching to another one. Cao *et al.*[320] demonstrated the beneficial effect of combining polymer and lipid carriers within a five-component transfecting system (five-element nanoparticles, FNPs). The authors showed that the addition of the PβAE polymer to the basic lipid system crucially increased the functional efficiency of mRNA delivery to lungs. The best five-component formulation administered intravenously (i.v.) in a dose of 0.3 mg kg^{-1} provided a luciferase signal in lungs approximately two orders of magnitude higher than that obtained with the basic formulation: 1,2-dioleoyl-3-trimethylammonium-propane (DOTAP) with LNPs. Approximately the same difference in the efficiency of five- and four-component systems was also observed in *ex vivo* experiments. In addition, according to the confocal microscopy data, at the cellular level, the uptake of the mRNA molecule chemically conjugated with the Cyanine 5 fluorescence dye (Cy5–mRNA) complexed with the best FNP was detected 6–8 times more often than for DOTAP–LNPs. In other words, in this study, PβAE as a part of FNP acted not only as an additional stabilizer, but also as a key element that, in combination with DOTAP, gave a clear-cut synergistic gain of the NA delivery to lungs compared to the basic purely lipid DOTAP–LNP carrier.

5.2. Polyethylenimines

Ye *et al.*[321] compared PEI modified with cyclic disulfides (CD*n*-PEI, where *n* is the number of disulfide bridges) with the commercial Lipofectamine carrier.

All CD*n*-PEI–mRNA complexes had similar physicochemical characteristics: approximately 50–70 nm size, positive ζ-potential, and encapsulation efficiency of > 95%. However, the CD17-PEI agent based on PEI1800 with 17 disulfide groups proved to be most effective for transfection. The transfection efficiency of HEK293T cells with the use of CD17-PEI was ~97% (for the polymer dose of 12.3 μg mL^{-1}); the polymer did not exhibit a noticeable cytotoxicity in concentrations of 6.15–18.45 μg mL^{-1}. It was particularly important that the advantage of the new polymer was enhanced in difficult-to-transfect immune cells. For a set of cells comprising L929, LLC, 4T1, MC38, RM1, B16F10, U87, HEK293T, DC2.4, RAW264.7, and Jurkat,[s] the CD17-PEI carrier was superior to Lipofectamine almost in all cases, and for the DC2.4, RAW264.7, and Jurkat cells, it provided an almost fourfold increase in the transfection, which was particularly highlighted as an important benefit for antigen-presenting cells. A qualitative mechanistic difference was also found between the behaviours of CD17-PEI and Lipofectamine. Thus, treatment of CD17-PEI with bafilomycin A1 (an inhibitor of vacuolar H^+-ATPase) resulted in the suppression of transfection, whereas in the case of Lipofectamine, there was hardly any effect. This indicates that endosomal escape mediated by the proton sponge effect is implemented for the new polymer. In addition, the CD17-PEI–mRNA complex retained the size, ζ-potential, and transfection activity when stored for up to 28 days at 4°C and remained active after incubation in a fetal bovine serum (FBS) with a concentration of 10 and 30%.

Structure of CD*n*-PEI

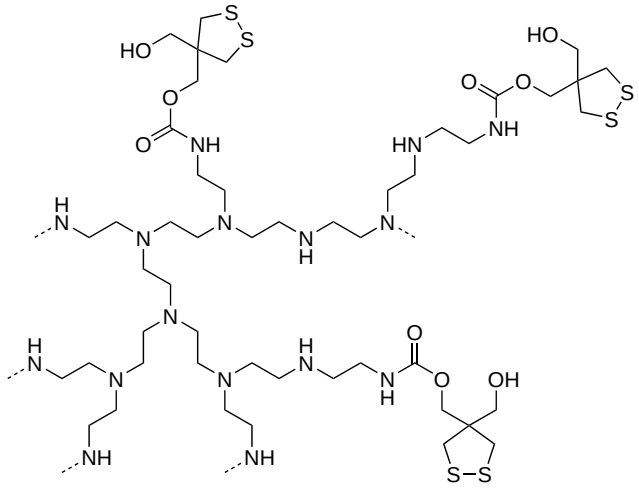

Lin *et al.*[322] described phospholipidated and alkylated polymers (PAP), the synthesis of which is depicted in Scheme 28. The representatives of this system, CP-EP*n*–*x*PO,[t] showed an obvious advantage simultaneously at several levels when directly compared with commercial lipid systems. For example, in *in vitro* experiments, optimized PAP polyplexes provided a 7500-fold increase in expression compared to non-modified parent polycations. For the best-performing samples, the mRNA translation levels were approximately an order of magnitude higher than those for commercial LNPs, DLin-MC3-DMA and SM-102. In addition, in the presence of serum, the BP1-EP4-0.5PO carrier maintained high activity at 10, 30, and even 50% FBS concentrations, whereas the Dlin-MC3-DMA LNPs rapidly lost the efficiency with increasing serum concentration. This advantage became even more significant in *in vivo* experiments: PAP provided a 30–500 times higher mRNA expression in spleen than the non-modified polymers. The most effective carriers, BP1-EP4-0.5PO and PA-EP8-0.33PO, exhibited expression selectivity in the range of 10^2–10^4. In the B16-OVA melanoma model, the intravenous administration of mRNA encoding ovalbumin (OVA) with the PA-EP8-0.33PO carrier induced a faster and more pronounced antitumour response compared to that of SM-102 LNPs. The difference in the tumour volume relative to the control was already noticeable by the 17th day, whereas no such effect was observed for SM-102 LNPs. In addition, the proportion of CD8+ T-cells in the tumour

[s] Cell lines: L929 are mouse fibroblasts, LLC are Lewis lung carcinoma cells, 4T1 are mouse mammary carcinoma cells, MC38 are mouse colon adenocarcinoma cells, RM1 are mouse prostate cancer cells, B16F10 are mouse melanoma cells, U-87 are glioblastoma cells, DC2.4 are mouse dendritic cells, Jurkat are human leukemic T-lymphocytes.

[t] CP means cationic polymer, which included branched and linear PEI and zero-generation PAMAM; EP*n* is an alkyl-substituted oxirane with *n* carbon atoms; PO is 2-nonyloxy-1,3,2-dioxaphospholane 2-oxide; *x* is the molar ratio of PO and active amino groups in the CP-EP*n* carrier.

Scheme 28

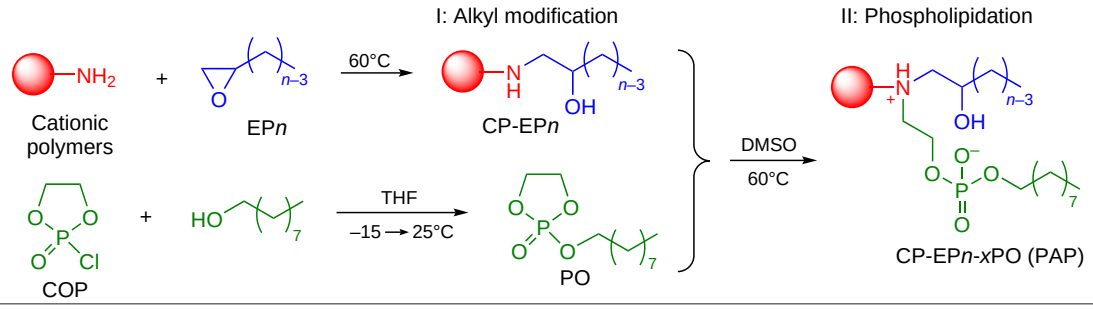

microenvironment increased from 6% in the control group to 46% in the group receiving the PA-EP8-0.33PO carrier, and NK cell infiltration also increased, which is consistent with the more pronounced effect of the PAP-based vaccine.

5.3. Polyamidoamines

Long *et al.*[323] carried out screening of a library of thiourea-modified poly(*L*-lysine) derivatives (PLL-T) for the efficiency of fLuc–mRNA delivery into HEK293T cells; selected candidate materials were then assessed in relation to macrophage-like RAW264.7 cells.

The PLL-1A1B(T) polymer was among the most effective candidates: it produced an approximately 10^4-fold increase in the luciferase signal compared to the pristine non-modified PLL and surpassed the commercial Lipofectamine MessengerMAX reagent (LPMM) in both HEK293T and RAW264.7 cells. It was established that, under operating conditions, the selected polymer maintains an acceptable cell viability of more than 80% up to a concentration of 20 mg mL^{-1}. The authors concluded that owing to cooperative hydrogen bonds and electrostatic, and hydrophobic interactions, PLL-1A1B(T) ensures a more stable mRNA packing and finally surpasses LPMM, which is a commercial gold standard, in epithelial and immune cells.

Zhang *et al.*[324] compared polymeric carriers based on modified polyaspartamide (PDA) with two lipid systems, LPMM *in vitro* and SM102 LNPs *in vivo*. After the primary

Structure of PLL-1A1B(T)

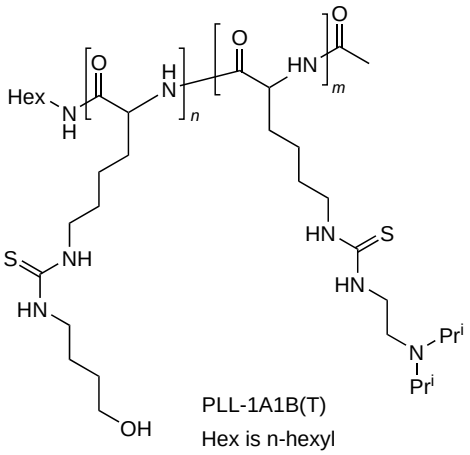

screening, three polymers, P-PDA, P-PDA-I, and P-PDA-BI, exhibited a noticeable luciferase activity in HEK293T cells.

An *in vitro* experiment using difficult-to-transfect DC2.4 cells (immortalized line of mouse dendritic cells) showed an approximately four times higher transfection of P-PDA compared to LPMM. In *in vivo* experiments involving the i.v. administration of Luc–mRNA in a dose of 0.25 mg kg^{-1}, the difference from the commercial lipid system became even more pronounced. All three polymer complexes provided predominant expression in the lungs, with no detectable expression in the

PDA structures

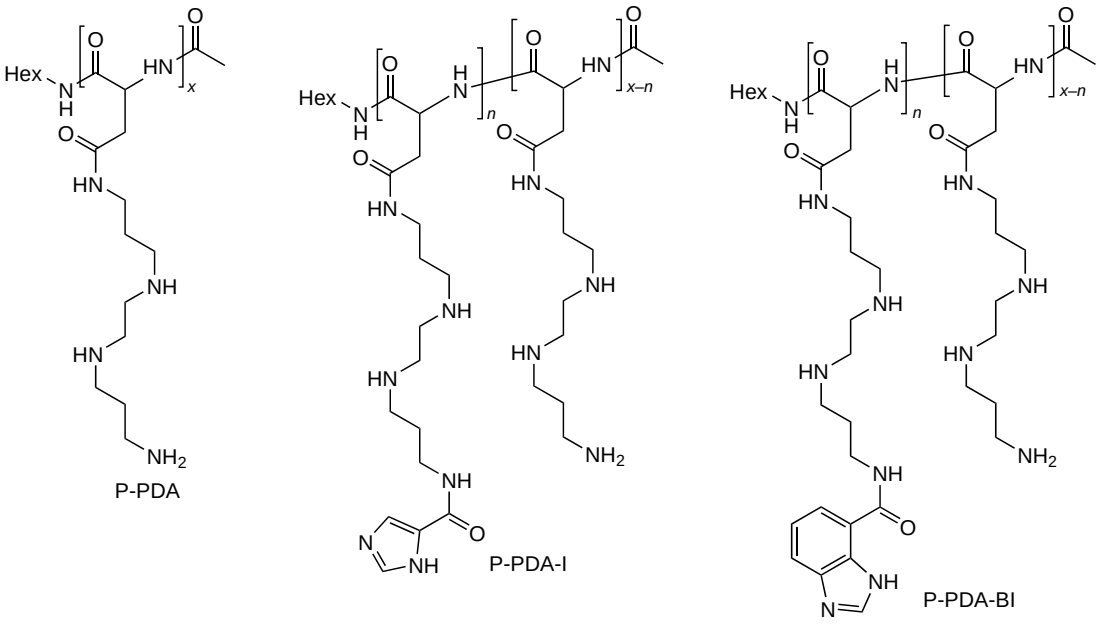

liver or spleen; the proportion of the total luciferase bioluminescence signal corresponding to the lungs was 85 to 95%. Conversely, the use of SM102 LNPs resulted in Luc expression mainly in the liver and in the spleen, with 75% of the whole luminescence signal being due to the liver. Thus, the new polymer not merely surpassed the commercial lipid carrier in DC2.4 transfection, but also crucially changed the organ selectivity of systemic mRNA administration, thus largely switching expression from the liver, which is characteristic of SM102 LNPs, to the lungs.

Like poly(β-amino esters), polyamidoamines are successfully employed in combination with lipid carriers. Norimatsu *et al*.[325] compared basic anionic LNPs (aLNPs) with LNPs additionally coated with the PAsp(EDA) polycation [PAsp(EDA)-LNP]. This modification barely changed the size and packing of mRNA, but sharply improved its intracellular integrity and thus provided long-term protein expression. The starting aLNPs had a size of 149 nm, PDI = 0.16, and ζ-potential of –12.6 mV. After the addition of PAsp(EDA) to N : P = 0.5, the size and PDI remained virtually the same, but the charge increased to +10 mV. This system preserved the invariable size, PDI, ζ-potential, and encapsulation for 7 days at 4°C. In experiments involving DC2.4 and HeLa cells, the PAsp(EDA)-LNP carrier was somewhat superior to the basic system: after 48 h, the signal increased approximately twofold for the former and approximately 1.5-fold for the latter. Mechanistically, this is not related to improved uptake or endosomal escape, but rather to the stabilization of mRNA within the cell: after removal of extracellular particles, the intracellular mRNA content in the aLNP group decreased to ~40% as early as within 1 h, while in the PAsp(EDA)-LNP group, it remained at about 60% after 3 h. Thus, according to this study, the main advantage of the new polymer over the lipid control is that PAsp(EDA), being associated with mRNA after endosomal escape, considerably inhibits its degradation and thus ensures longer and higher levels of protein expression for the lipid system.

5.4. Comparison of the polymeric delivery systems

To conclude this Section, Table 3 summarizes data on the application of modern NA delivery systems, demonstrating their comparative efficiency.

A review by Friesen and Blakney[79] devoted to the recent trends in the development of polymeric RNA delivery agents postulates the possible combination of all necessary functions within a single molecule to be the major advantage of polymers over conventional multicomponent reagents for lipofection. The fruitful idea of a rational approach to the development of polymeric NA delivery systems, considered in the review by Porello *et al*.,[78] is based on the design of the non-cationic segment of block copolymers, in particular with incorporation of receptors,[328] in a way similar to the selection of components and their ratios in conventional formulations for lipofection. Another promising direction is the use of non-cationic polymers capable of reversible NA binding.[74,329] A traditional and, perhaps, the only fundamental advantage of multicomponent reagents for lipofection lies in the reproducibility of composition and the relative ease of the control over composition during production using standard analytical methods.

Achieving high reproducibility of the polymer composition, microstructure, and topology is a practical challenge of a higher order, requiring the highest experimental level and non-trivial solutions in the design of monomers, polymers, and polymerization catalysts.

6. Conclusion

In the beginning, we would like to draw attention to the gap between the enormous amount of data on polymeric NA delivery systems accumulated to date[u] and partially covered in this review and actually a zero level of adaptation of polymeric NA delivery systems approved by regulatory authorities for clinical use. This is the case, but this is not indicative of some flaw of polyplexes: an equally large gap between the development of the scientific basis for lipid-based transfection agents and clinical approval of these agents was bridged only recently and only under pressure of circumstances, namely, the COVID-19 pandemic. In our opinion, this gap points to an impending shift toward personalized medicine based on gene therapy and mRNA vaccination. The relevant scientific basis has already been formed as a result of investigations of both lipid and macromolecular gene delivery systems. A comparison of the most important performance characteristics of LNPs and polyplexes is given in Table 4.

Polymeric NA delivery systems can be described as a flexible platform for gene therapy offering a wide range of degrees of freedom, ranging from a variety of chemical architectures and post-modifications to fine-tuning of the response to pH, temperature, and redox conditions. If polyplexes and lipid nanoparticles are viewed as two pathways to the same goal, that is, safe, reproducible, and targeted delivery of NAs *in vivo* (Fig. 28), it is necessary to state that LNP production processes and characterization methods have been developed much more thoroughly, largely owing to the design and mass use of lipid mRNA vaccines. The relative retardation of polymers is not an indication of their imperfection. On the contrary, it rather illustrates the untapped potential of polymeric NA carriers. The progress of LNPs provides researchers that work on polymeric transfection agents with a roadmap and a set of best practices that may and should be adapted for polymer-based delivery to accelerate switching from a variety of concepts to reproducible clinical solutions.

The coming years are expected to be a period of rapid convergence of approaches. The following trends will become the new standard for polymeric carriers:

(1) high-throughput design based on machine learning and systematic structure–property–function relationships;

(2) in-depth study of the biointerface, first of all, protein corona and cellular trajectories of particles;

(3) scalable particle assembly and quality control at a level comparable to that of LNPs, including the development of microfluidic mixing and standardization of formulation protocols;

(4) early attention to the CMC logic (CMC is chemistry, manufacturing and controls) in the development of pharmaceuticals needed to maintain the reproducibility and translational applicability of the results on going from laboratory protocols to preclinical models. Against this backdrop, especially promising are hybrid polymer–lipid systems in which the polymer core may provide enhanced stability and engineering controllability, while the lipid component may offer delivery efficiency and biocompatible mechanisms of interaction with the body, thus potentially

[u] We mean data on the efficiency of NA binding, the efficiency of polyplex internalization by various cells, and influence of the size, charge, and rigidity of the carrier on this process, as well as data on the mechanisms of degradation of various polymers and NA release under various conditions.

Table 3. Comparative efficiency of current polymeric nucleic acid delivery systems.

Type of NA	Carrier	Model	Experimental conditions	Outcome	Refs
mRNA	PEG-PβAE	FUS-treated brain parenchyma	*In vivo*, C57BL/6 mice, i.v. + FUS-opening of BBB; 0.5 mg kg^{-1} of Luc – mRNA; PEG-PβAE : mRNA = 60 : 1 (w/w); assessed after 24 h from Luc in the FUS-treated brain region	6 – 8 times superior to four-component LNPs	319
	FNP	ICR laboratory mice	*In vivo*, i.v. to mice, 0.3 mg kg^{-1} of mRNA; (DOTAP + PβAE) : mRNA = 20 : 1 (w/w); analysis after 6 h based on BLI/IVIS† in the lungs	300 times superior to four-component LNPs	320
	CD-PEI	Cell lines: HEK293T, L929, LLC, 4T1, MC38, RM1, B16F10, U87, DC2.4, RAW264.7, and Jurkat	*In vitro*, 0.5 μg of mRNA per cell, N : P = 10 or ~6 : 1 (w/w); transfection for 4 h + expression for 16 h; assessment of the proportion (%) of GFP + cells by flow cytometry	Surpasses Lipofectamine in efficiency by ⩽ 4 times	321
	PAP	IGROV1 cells,‡ C57Bl/6 and Ai9 laboratory mice	*In vitro*: fLuc – mRNA, 25 ng per well, PAP : mRNA = 20 : 1 (w/w), 24 h, luminescence measurement in relative units. *In vivo*: OVA – mRNA, 0.5 mg kg^{-1} (i.v.) on days 11, 14, and 17, PAP : mRNA = 20 : 1 (w/w)	Surpasses SM-102 LNPs *in vitro* by an order of magnitude; suppress the growth of melanoma *in vivo*, while SM-102 LNPs only retard the growth	322
	PLL-1A1B(T)	Cell lines: HEK293T and RAW264.7	*IIn vitro*, 0.2 μg of mRNA per well, PLL : mRNA = 10 : 1 (w/w); 24 h, luminescence measurement in relative units	Surpasses LPMM for RAW264.7 by an order of magnitude and is comparable for HEK293T	323
	P-PDA	Cell lines: HEK293T and DC2.4, C57BL/6 laboratory mice	*In vitro*: 200 ng of mRNA per well, P-PDA-M : mRNA = 20 : 1 (w/w), 24 h, luminescence measurement in relative units *In vivo*: i.v., Luc – mRNA 0.25 mg kg^{-1}, P-PDA-M : mRNA = 20 : 1 (w/w), 24 h	Comparable in efficiency with oLPMM for HEK293T and is 4 times superior for DC2.4; ~90% of the total BLI luciferase signal was in the lungs in *in vivo* experiment *vs.* 75% in the liver for SM-102 LNPs	324
miRNA	PONI-Guan	Cell line: RAW264.7	*IIn vitro*, 50 nM of miRNA, guanidinium : phosphate = 30 : 1, 48 h, the suppression of eGFP expression was assessed by the decrease in normalized fluorescence intensity	Surpasses commercial RNAiMAX by 25%	110
pDNA	SPAE	Cell lines: HeLa, HepG2, HCC-LM3, A2780, HaCaT, NHF	*In vitro*, 0.5 μg of DNA per well; SPAE-4 : DNA = 40 : 1 (w/w); evaluation of the fraction (%) of GFP + cells by flow cytometry after 48 h	2 – 9 times superior to Lipofectamine 3000	318
pDNA	PβAE	Cell line: Jurkat	*In vitro*, 1 μg of pDNA per well, PβAE : DNA = 20:1 (w/w) (~20 μg of the polymer per well; 100 μL of Opti-MEM,§ transfection for 3 h + expression for 48 h; evaluation of the proportion (%) of GFP + cells by flow cytometry	4 times superior to Lipofectamine 2000 (without preliminary treatment with polybrene)	326
pDNA	HPAE (hyper-branched PAE)	Cell lines: A375, A2058, and SK-MEL-2¶	*In vitro*, 0.5 μg of pDNA per well, HPAE-2 : DNA = 10:1 (w/w) (~5 μg of the polymer per well; 100 μg of serum-free DMEM), transfection for 4 h + expression for 48 h; assessment of the proportion of GFP + cells and the median intensity of GFP fluorescence by flow cytometry or gLuc luminescent activity	Approximately two times superior to jetPRIME	327

† BLI (bioluminescence imaging) is a method for recording the light produced in the luciferase reaction: if the delivered Luc – mRNA has been successfully translated to the luciferase protein, then the introduction of the luciferin substrate is followed by light emission by the tissue; IVIS (*in vivo* imaging system) is an instrument platform for recording this bioluminescence or fluorescence signals in living animals or in isolated organs. ‡ IGROV1 is a human ovarian carcinoma cell line. § DMEM is a standard culture medium for mammalian cells typically used with the addition of serum; Opti-MEM is a low-protein culture medium, often used in transfection experiments to prepare complexes of nucleic acids with carriers and for short-term incubation of cells under conditions of reduced influence of serum components. ¶ A375, A2058, and SK-MEL-2 are widely used human melanoma cells; A375 and A2058 are usually regarded as models of BRAF mutant melanoma, while SK-MEL-2 serves as a model of NRAS-mutant/BRAF-wild type melanoma.

Table 4. Performance characteristics of polyplexes and lipid nanoparticles.

Characteristics	Polymeric NA carriers	Lipid nanoparticles
Reproducibility of the synthesis	Highly dependent on the polymer type: PEI and simple PβAE are accessible and easy to handle, but *M*, *Đ*, and degree of substitution, as well as terminal groups and residual monomers can considerably affect the activity. The most reproducible results were obtained with copolymers produced *via* ROP and RAFT radical polymerization	The components are usually low-molecular-weight and analytically controllable; however, ionizable lipids often require a multistep synthesis and strict control of impurities
Formulation reproducibility	Polyplexes are sensitive to weight ratios and N : P, pH, ionic strength, order of reactant mixing, concentration, and incubation time; without controlled mixing, batch-to-batch variability in size and PDI is possible	The formulation technique is more standardized: fast mixing of an aqueous phase of NAs with an ethanolic phase of lipids, including microfluidic mixing, gives well controllable particles upon optimization of TFR, FRR, pH, and composition [330]
Scalability	Dependent on the complexity of synthesis: PEI, PLL, and other homopolymers are easily scalable, but the scalability of complex architectures may be compromised by difficulties in purification, polydispersity, and composition control. The clinical base is still limited	The most commercially mature nonviral platform for NA: experience in the industrial production of COVID-19 mRNA vaccines and the Onpattro drug confirms the process scalability under GMP conditions, although the process remains sensitive to mixing and sterile filtration parameters
Storage stability	Dry polymers are often stable; polyplexes can be stable, but for each system it is necessary to separately confirm the retention of size and PDI, NA binding, and transfection activity after storage or freeze-drying	Storage remains a bottleneck for mRNA-loaded LNPs: for example, Spikevax requires freezing at temperatures from –50 to –15°C and cannot be refrozen after thawing. For siRNA-loaded LNPs, milder conditions are possible: Onpattro is stored at 2 – 8°C; it does not freeze and allows short-term (up to 14 days) storage at room temperature.[331]
Toxicity	The main risks are charge-mediated cytotoxicity, membrane damage, aggregation with proteins, and the accumulation of chemically inert polycations; toxicity decreases with introduction of hydrolyzable bonds or shielding blocks and with a decrease in the excess of free polymer	Dependent on the ionizable lipid, dose, administration route, and organ distribution; for clinical LNPs, the therapeutic window has been established, but infusion reactions are possible, and premedication may be necessary, as for Onpattro.[332]
Immunogenicity and inflammatory activation	The polymer itself is not an antigen in the classical sense, but its cationic surface, residual impurities, CpG-containing DNA, and aggregation with serum proteins can enhance the innate immune response	The innate immunity can be activated through the lipid composition, PEG lipids, complement, and NA itself; this is desirable to some extent for vaccines; for protein replacement therapy or genome editing, it is a potential limiting factor

Note. TFR (total flow rate) is the sum of the aqueous and organic phase flow rates; FRR (flow-rate ratio) is the ratio of these flow rates; these parameters affect the local ethanol concentration, LNP self-assembly, particle size, PDI, and NA encapsulation efficiency; GMP is good manufacturing practice, that is, a regulated system for the industrial production of pharmaceuticals that ensures process reproducibility, quality control, sterility, and traceability for each product batch.

expanding both the routes of administration and the storage conditions of the pharmaceuticals.

Thus, the key current trend in polyfection is not only the emergence of new classes of delivery agents (such as PβAE, CART, and others, which tend to consist of a single component, although they are also undoubtedly important and interesting), but also the use of tools that have already been refined for LNPs. Even well-known platforms (such as PEI) are experiencing a resurgence in this context: for an appropriate formulation, biointerface control, and standardization of the assembly, they can occupy their own niche along with new materials. For example, in July 2025, phase 3 clinical trials were started for a DNA vaccine based on a pDNA polyplex and PEG-PEI copolymer modified with cholesterol for epithelial ovarian cancer.[333] In the very near future, as best practices of lipid delivery are transferred to polymer systems, the role of polymer carriers in biomedical technologies will steadily increase.

This review was prepared with financial support of the Russian Science Foundation (Project No. 21-73-30010P).

The authors declare no competing interest.

7. List of abbreviations and symbols

The following abbreviations and symbols are used in the review:

d — particle diameter,
$Đ_M$ — dispersity,
f_{tri} — molar ratio of the number of positive charges in an ABA-type polymer to the total number of positive charges,
f_{miRNA} — molar ratio of the number of negative charges in siRNA to the total number of negative charges,
l_p — persistence length,
M — molecular weight,
M_n — number-average molecular weight,
n_{Hill} — Hill coefficient,
R_g — radius of gyration (of a colloidal particle),
Ψ — pseudouridine,
$m^1Ψ$ — N^1-methylpseudouridine,
AIBN — azobis(isobutyronitrile),
AMA — alkyl methacrylate,
ASO — antisense oligonucleotide,
ATRP — atom transfer radical polymerization,
AUC — analytical ultracentrifugation,

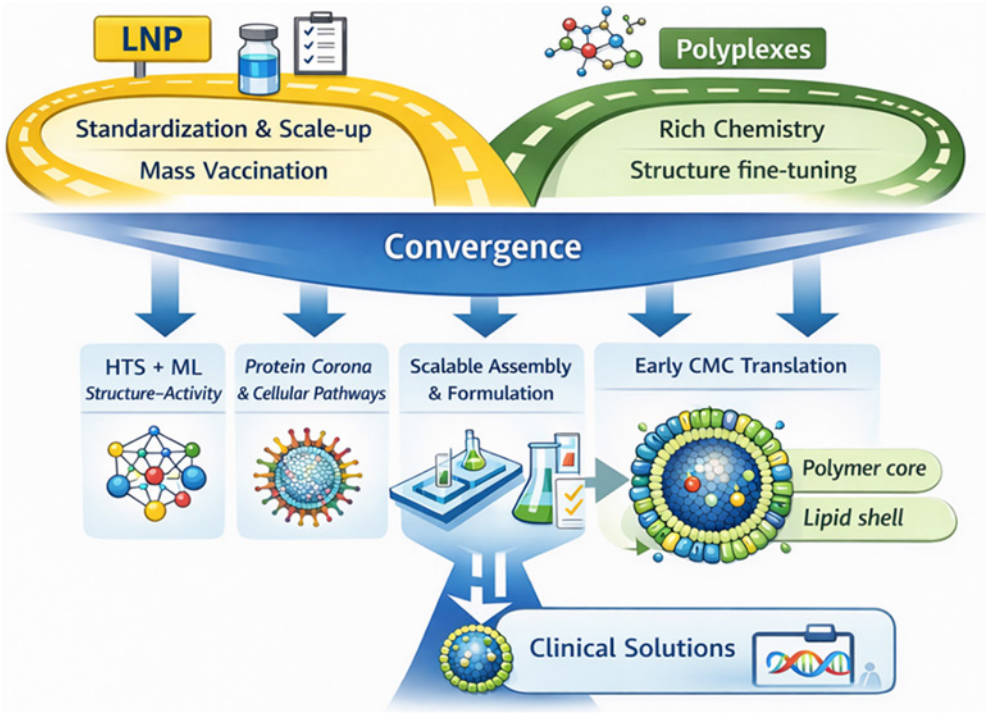

Figure 28. Schematic picture of LNP and polyplex benefits and pathways of clinical development.

BBB — blood–brain barrier,
Boc — *tert*-butoxycarbonyl,
bPEI — branched polyethylenimine,
BSA — bovine serum albumin,
CART — charge-altering releasable transporters,
CAR-T — chimeric antigen receptor T-cells,
Cat — catalyst,
Cbz — benzyloxycarbonyl,
CD — cyclic disulfides,
CL — caprolactone,
CME — clathrin-mediated endocytosis,
CMT — critical micellization temperature,
CNS — central nervous system,
CPP — cell-penetrating peptides,
CRISPR — clustered regularly interspaced short palindromic repeats,
CvME — caveolae-mediated endocytosis,
Daba — diaminobutanoic acid,
Dapa — diaminopropanoic acid,
DBU — 1,8-diazabicyclo[5.4.0]undec-7-ene,
DC-Chol — 3-[*N*-(*N*′,*N*′-dimethylaminoethyl)carbamoyl]-cholesterol,
DCM — dichloromethane,
DEAE-dextran — diethylaminoethyl dextran,
DEAEMA — 2-(diethylamino)ethyl methacrylate,
DIPAEMA — 2-(diisopropylamino)ethyl methacrylate,
DKP — diketopiperazines,
DLS — dynamic light scattering,
DMAEMA — 2-(dimethylamino)ethyl methacrylate,
DMAP — 4-dimethylaminopyridine,
DOPC — 1,2-dioleoyl-*sn*-glycero-3-phosphocholine,
DOPE — 1,2-dioleoyl-*sn*-glycero-3-phosphoethanolamine,
DOPG — 1,2-dioleoyl-*sn*-glycero-3-phosphoglycerol,
DOTAP — 1,2-dioleoyl-3-trimethylammonium-propane,
DOTMA — *N*-[1-(2,3-dioleyloxy)propyl]-*N*,*N*,*N*-trimethyl-ammonium,
FBS — fetal bovine serum,
FDA — US Food and Drug Administration,
FUS — focused ultrasound,
GalNAc — *N*-acetylgalactosamine,
GFP — green fluorescent protein,
HAp — hydroxyapatite,
Hex — n-hexyl,
i.v. — intravenous administration,
LCST — lower critical solution temperature,
LNP — lipid nanoparticle,
LPS — lipopolysaccharide,
Luc — luciferase,
mPEG — methoxypolyethylene glycol,
mRNA — messenger RNA,
NA — nucleic acid,
NLS — nuclear localization signals,
NP — nanoparticle,
bp — base pair,
nt — nucleotide,
OVA — ovalbumin,
pABOL — poly(cystamine bisacrylamide-*co*-1,4-amino-butanol),
PAGA — poly[α-(4-aminobutyl)-*L*-glycolic acid],
PAMAM — polyamidoamine,
PAP — phospholipidated and alkylated polymers,
PβAE — poly(β-amino esters),
PBA — poly(n-butyl acrylate),
PBE — polybenzyl ethers,
PDA — polyaspartamide,
PDI — polydispersity index,
pDNA — plasmid DNA,
PDEGEA — poly[ethoxy di(ethylene glycol) acrylate],
PDGFR — platelet-derived growth factor receptor,
PEG — polyethylene glycol,
PEI — polyethylenimine,
PGA — poly(α-glutamic acid),

PGBA — poly(glycidyl butylamine),
PIC micelles — polyion complex micelles,
PLL — poly(*L*-lysine),
PNIPAAm — poly(*N*-isopropylacrylamide),
PONI-Guan — poly(oxanorbornene)imides bearing guanidino groups in the side chains
PPI — poly(propylene imine),
RAFT — reversible addition — fragmentation chain-transfer,
RGD peptide — arginine–glycine–aspartic acid peptide (integrin-recognition motif of cell membranes),
RISC — RNA-induced silencing complex,
RLU — relative luminescence units,
ROMP — ring-opening metathesis polymerization,
ROP — ring-opening polymerization,
ROTEP — ring-opening transesterification polymerization,
rt — room temperature,
SANS — small-angle neutron scattering,
SAXS — small-angle X-ray scattering,
saRNA — self-amplifying RNA,
siRNA — small interfering RNA,
ssRNA — single-stranded RNA,
TBD — 1,5,7-triazabicyclo[4.4.0]dec-5-ene,
TBS — *tert*-butyldimethylsilyl,
TEA — triethylamine,
TEM — transmission electron microscopy,
TFA — trifluoroacetic acid,
TNF-α — tumour necrosis factor alpha,
Trt — trityl,
T(U) — (thio)urea,
uPIC — unit polyion complexes,
VEGF — vascular endothelial growth factor,
Cell lines:
A2780 — human ovarian endometrioid adenocarcinoma cells,
B16 (B16F10) — mouse melanoma cells,
DC2.4 — mouse dendritic cells,
HCC-LM3 — human hepatocellular carcinoma cells,
HEK293 — human embryonic kidney cells,
HEK293T — HEK293-derived cells stably expressing the SV40 large T antigen,
HepG2 — human hepatocellular carcinoma cells,
Jurkat — human leukemic T lymphocytes,
L929 — mouse fibroblasts,
LLC (LL/2) — Lewis lung carcinoma cells,
MC38 — mouse colon adenocarcinoma cells,
MCF-7 — human breast adenocarcinoma cells
RAW264.7 — mouse macrophage cells transformed by Abelson murine leukemia virus,
RM1 — mouse prostate cancer cells,
4T1 — mouse breast carcinoma cells,
U-87 (U-87MG) — human glioblastoma cells.

8. References

1. J.M.Sasso, B.J.B.Ambrose, R.Tenchov, R.S.Datta, M.T.Basel, R.K.DeLong, Q.A.Zhou. *J. Med. Chem.*, **65** (10), 6975 (2022); https://doi.org/10.1021/acs.jmedchem.2c00024
2. G.B.Mulamba, A.Hu, R.F.Azad, K.P.Anderson, D.M.Coen. *Antimicrob. Agents Chemother.*, **42** (4), 971 (1998); https://doi.org/10.1128/AAC.42.4.971
3. H.Zhang, H.Wang, Y.An, Z.Chen. *Mol. Ther. Nucleic Acids*, **34**, 102027 (2023); https://doi.org/10.1016/j.omtn.2023.09.004
4. B.B.Mendes, J.Conniot, A.Avital, D.Yao, X.Jiang, X.Zhou, N.Sharf-Pauker, Y.Xiao, O.Adir, H.Liang, J.Shi, A.Schroeder, J.Conde. *Nat. Rev. Methods Primers*, **2** (1), 24 (2022); https://doi.org/10.1038/s43586-022-00104-y
5. A.V.Ilina, N.V.Krylova, H.Al-Hilal, R.G.Sakhabeev, D.O.Vinokhodov. *Biotekhnologiya*, **41** (1), 50 (2025); https://doi.org/10.56304/s0234275825010065
6. M.P.Stewart, R.Langer, K.F.Jensen. *Chem. Rev.*, **118** (16), 7409 (2018); https://doi.org/10.1021/acs.chemrev.7b00678
7. D.Chancellor, D.Barrett, L.Nguyen-Jatkoe, S.Millington, F.Eckhardt. *Mol. Ther.*, **31** (12), 3376 (2023); https://doi.org/10.1016/j.ymthe.2023.11.001
8. G.Geng, Y.Xu, Z.Hu, H.Wang, X.Chen, W.Yuan, Y.Shu. *eBioMedicine*, **118**, 105834 (2025); https://doi.org/10.1016/j.ebiom.2025.105834
9. E.Shchukina, I.Eremin, I.Mazunin, A.Moskalev. *Biochem. Biophys. Res. Commun.*, **785**, 152708 (2025); https://doi.org/10.1016/j.bbrc.2025.152708
10. S.Han. *Clin. Exp. Vaccine Res.*, **4** (1), 46 (2015); https://doi.org/10.7774/cevr.2015.4.1.46
11. M.A.Kotterman, T.W.Chalberg, D.V.Schaffer. *Annu. Rev. Biomed. Eng.*, **17** (1), 63 (2015); https://doi.org/10.1146/annurev-bioeng-071813-104938
12. J.L.Shirley, Y.P.De Jong, C.Terhorst, R.W.Herzog. *Mol. Ther.*, **28** (3), 709 (2020); https://doi.org/10.1016/j.ymthe.2020.01.001
13. D.Y.Logunov, I.V.Dolzhikova, O.V.Zubkova, A.I.Tukhvatullin, D.V.Shcheblyakov, A.S.Dzharullaeva, D.M.Grousova, A.S.Erokhova, A.V.Kovyrshina, A.G.Botikov, F.M.Izhaeva, O.Popova, T.A.Ozharovskaya, I.B.Esmagambetov, I.A.Favorskaya, D.I.Zrelkin, D.V.Voronina, D.N.Shcherbinin, A.S.Semikhin, Y.V.Simakova, E.A.Tokarskaya, N.L.Lubenets, D.A.Egorova, M.M.Shmarov, N.A.Nikitenko, L.F.Morozova, E.A.Smolyarchuk, E.V.Kryukov, V.F.Babira, S.V.Borisevich, B.S.Naroditsky, A.L.Gintsburg. *Lancet*, **396** (10255), 887 (2020); https://doi.org/10.1016/s0140-6736(20)31866-3
14. D.Y.Logunov, I.V.Dolzhikova, D.V.Shcheblyakov, A.I.Tukhvatullin, O.V.Zubkova, A.S.Dzharullaeva, A.V.Kovyrshina, N.L.Lubenets, D.M.Grousova, A.S.Erokhova, A.G.Botikov, F.M.Izhaeva, O.Popova, T.A.Ozharovskaya, I.B.Esmagambetov, I.A.Favorskaya, D.I.Zrelkin, D.V.Voronina, D.N.Shcherbinin, A.S.Semikhin, Y.V.Simakova, E.A.Tokarskaya, D.A.Egorova, M.M.Shmarov, N.A.Nikitenko, V.A.Gushchin, E.A.Smolyarchuk, S.K.Zyryanov, S.V.Borisevich, B.S.Naroditsky, A.L.Gintsburg; Gam-COVID-Vac Vaccine Trial Group. *Lancet*, **397** (10275), 671 (2021); https://doi.org/10.1016/s0140-6736(21)00234-8
15. R.Bos, L.Rutten, J.E.M.van der Lubbe, M.J.G.Bakkers, G.Hardenberg, F.Wegmann, D.Zuijdgeest, A.H.de Wilde, A.Koornneef, A.Verwilligen, D.van Manen, T.Kwaks, R.Vogels, T.J.Dalebout, S.K.Myeni, M.Kikkert, E.J.Snijder, Z.Li, D.H.Barouch, J.Vellinga, J.P.M.Langedijk, R.C.Zahn, J.Custers, H.Schuitemaker. *npj Vaccines*, **5** (1), 91 (2020); https://doi.org/10.1038/s41541-020-00243-x
16. S.A.Mendonça, R.Lorincz, P.Boucher, D.T.Curiel. *npj Vaccines*, **6** (1), 97 (2021); https://doi.org/10.1038/s41541-021-00356-x
17. S.M.Hoy. *Drugs*, **79** (11), 1255 (2019); https://doi.org/10.1007/s40265-019-01162-5
18. M.Alsaggar, D.Liu. *Adv. Genet.*, **89**, 1 (2015); https://doi.org/10.1016/bs.adgen.2014.10.001
19. A.A.Mikheev, E.V.Shmendel, E.S.Zhestovskaya, G.V.Nazarov, M.A.Maslov. *Fine Chem. Technol.*, **15** (1), 7 (2020); https://doi.org/10.32362/2410-6593-2020-15-1-7-27
20. W.Ho, M.Gao, F.Li, Z.Li, X.-Q.Zhang, X.Xu. *Adv. Healthcare Mater.*, **10** (8), 2001812 (2021); https://doi.org/10.1002/adhm.202001812
21. O.V.Fedorova, I.G.Ovchinnikova, G.L.Rusinov, V.V.Avdeeva, A.P.Zhdanov, K.Yu.Zhizhin, N.T.Kuznetsov, L.Ya.Zakharova, D.A.Kuznetsova, Yu.S.Razuvaeva, E.P.Zhiltsova, O.G.Sinyashin, A.S.Alekseeva, E.L.Vodovozova,

I.I.Abdrakhmanova, A.Ibrahim, V.V.Solovyeva, A.V.Maltsev, V.P.Fisenko, S.O.Bachurin, Yu.M.Mikhailov, Yu.I.Aleksandrova, D.N.Shurpiki, I.I.Stoikov, A.Y.Ziganshina, S.E.Solovieva, I.S.Antipin, M.A.Agafonov, I.V.Terekhova, P.M.Ilicheva, P.S.Pidenko, N.A.Burmistrova, R.I.Moustafine, V.R.Timergalieva, Y.N.Zabolotnaya, V.V.Khutoryanskiy, A.M.Demin, G.L.Levit, V.N.Charushin, V.P.Krasnov, O.A.Goryacheva, O.A.Mayorova, S.M.Mesheryakova, I.Yu.Goryacheva, A.I.Ayupova, A.A.Fattakhova, A.A.Rizvanov, O.A.Inozemtseva, O.I.Gusliakova, D.A.Gorin, A.V.Gerasimov, L.S.Zubaidullina, M.A.Ziganshin, S.V.Valiulin, A.A.Onischuk, A.N.Bezrukov, Yu.G.Galyametdinov, P.L.Padnya, A.A.Nazarova, E.D.Sultanova, V.A.Burilov. *Russ. J. Gen. Chem.*, **95** (s1), S1 (2025); https://doi.org/10.1134/s1070363225606726

22. O.Volodina, S.Smirnikhina. *Mol. Biotechnol.*, **67** (2), 425 (2025); https://doi.org/10.1007/s12033-024-01070-4
23. J.S.Pagano, A.Vaheri. *Arch. Virusforsch.*, **17** (3), 456 (1965); https://doi.org/10.1007/bf01241201
24. J.H.McCutchan, J.S.Pagano. *J. Natl. Cancer Inst.*, **41** (2), 351 (1968); https://doi.org/10.1093/jnci/41.2.351
25. D.Warden, H.V.Thorne. *J. Gen. Virol.*, **3** (3), 371 (1968); https://doi.org/10.1099/0022-1317-3-3-371
26. F.L.Graham, A.J.van der Eb. *Virology*, **52** (2), 456 (1973); https://doi.org/10.1016/0042-6822(73)90341-3
27. Y.-W.Chao, Y.-L.Lee, C.-S.Tseng, L.U.-H.Wang, K.-C.Hsia, H.Chen, J.-M.Fustin, S.Azeem, T.-T.Chang, C.-Y.Chen, F.-C.Kung, Y.-P.Hsueh, Y.-S.Huang, H.-W.Chao. *ACS Nano*, **18** (6), 4822 (2024); https://doi.org/10.1021/acsnano.3c09608
28. Q.Ren, L.Wang, W.Qian, B.Chen, Q.Shuai, Y.Yan. *Macromol. Biosci.*, **23** (7), 2300085 (2023); https://doi.org/10.1002/mabi.202300085
29. N.Rabiee, M.Bagherzadeh, A.M.Ghadiri, M.Kiani, S.Ahmadi, V.Jajarmi, Y.Fatahi, A.Aldhaher, M.Tahriri, T.J.Webster, E.Mostafavi. *J. Nanostruct. Chem.*, **12** (5), 919 (2022); https://doi.org/10.1007/s40097-021-00446-1
30. N.Valatabar, F.Oroojalian, M.Kazemzadeh, A.A.Mokhtarzadeh, R.Safaralizadeh, A.Sahebkar. *J. Nanobiotechnol.*, **22** (1), 386 (2024); https://doi.org/10.1186/s12951-024-02648-5
31. C.A.Mirkin, S.H.Petrosko. *ACS Nano*, **17** (17), 16291 (2023); https://doi.org/10.1021/acsnano.3c06564
32. G.Lin, R.A.Revia, M.Zhang. *Adv. Funct. Mater.*, **31** (5), 2007096 (2021); https://doi.org/10.1002/adfm.202007096
33. D.C.Luther, R.Huang, T.Jeon, X.Zhang, Y.-W.Lee, H.Nagaraj, V.M.Rotello. *Adv. Drug Deliv. Rev.*, **156**, 188 (2020); https://doi.org/10.1016/j.addr.2020.06.020
34. F.Yanar, D.Carugo, X.Zhang. *Molecules*, **28** (15), 5694 (2023); https://doi.org/10.3390/molecules28155694
35. F.C.MacLaughlin, R.J.Mumper, J.Wang, J.M.Tagliaferri, I.Gill, M.Hinchcliffe, A.P.Rolland. *J. Control. Release*, **56** (1–3), 259 (1998); https://doi.org/10.1016/s0168-3659(98)00097-2
36. R.Joshi, T.Paliwal, S.Sharma, D.U.Kapoor, B.G.Prajapati. *Carbohydr. Polym.*, **368** (1), 124080 (2026); https://doi.org/10.1016/j.carbpol.2025.124080
37. P.L.Felgner, T.R.Gadek, M.Holm, R.Roman, H.W.Chan, M.Wenz, J.P.Northrop, G.M.Ringold, M.Danielsen. *Proc. Natl. Acad. Sci. USA*, **84** (21), 7413 (1987); https://doi.org/10.1073/pnas.84.21.7413
38. A.G.Fedorovskiy, D.N.Antropov, A.S.Dome, P.A.Puchkov, D.M.Makarova, M.V.Konopleva, A.M.Matveeva, E.A.Panova, E.V.Shmendel, M.A.Maslov, S.E.Dmitriev, G.A.Stepanov, O.V.Markov. *Pharmaceutics*, **16** (5), 684 (2024); https://doi.org/10.3390/pharmaceutics16050684
39. S.V.Milagina, P.A.Puchkov. *Fine Chem. Technol.*, **21** (1), 51 (2026); https://doi.org/10.32362/2410-6593-2026-21-1-51-72
40. G.S.Naidu, S.-B.Yong, S.Ramishetti, R.Rampado, P.Sharma, A.Ezra, M.Goldsmith, I.Hazan-Halevy, S.Chatterjee, A.Aitha, D.Peer. *Adv. Sci*., **10** (19), 2301929 (2023); https://doi.org/10.1002/advs.202301929
41. E.V.Shmendel, A.O.Buyanova, O.V.Markov, N.G.Morozova, M.A.Zenkova, M.A.Maslov. *Russ. J. Bioorg. Chem.*, **50** (6), 826 (2024); https://doi.org/10.31857/s0132342324060098
42. E.V.Shmendel, O.V.Markov, M.A.Zenkova, M.A.Maslov *Biological Products. Prevention, Diagnosis, Treatment*, **24** (2), 188 (2024); https://doi.org/10.30895/2221-996x-2024-24-2-188-199
43. G.Y.Wu, C.H.Wu. *J. Biol. Chem.*, **263** (29), 14621 (1988); https://doi.org/10.1016/s0021-9258(18)68081-0
44. J.Haensler, F.C.Szoka. *Bioconjug. Chem.*, **4** (5), 372 (1993); https://doi.org/10.1021/bc00023a012
45. O.Boussif, F.Lezoualch, M.A.Zanta, M.D.Mergny, D.Scherman, B.Demeneix, J.P.Behr. *Proc. Natl. Acad. Sci. USA*, **92** (16), 7297 (1995); https://doi.org/10.1073/pnas.92.16.7297
46. J.-Y.Cherng, P.van de Wetering, H.Talsma, D.J.A.Crommelin, W.E.Hennink. *Pharm. Res.*, **13** (7), 1038 (1996); https://doi.org/10.1023/A:1016054623543
47. J.Buck, P.Grossen, P.R.Cullis, J.Huwyler, D.Witzigmann. *ACS Nano*, **13** (4), 3754 (2019); https://doi.org/10.1021/acsnano.8b07858
48. E.V.Shmendel, P.A.Puchkov, M.A.Maslov. *Pharmaceutics*, **15** (5), 1400 (2023); https://doi.org/10.3390/pharmaceutics15051400
49. F.Ponti, M.Campolungo, C.Melchiori, N.Bono, G.Candiani. *Chem. Phys. Lipids*, **235**, 105032 (2021); https://doi.org/10.1016/j.chemphyslip.2020.105032
50. K.K.Ewert, P.Scodeller, L.Simón-Gracia, V.M.Steffes, E.A.Wonder, T.Teesalu, C.R.Safinya. *Pharmaceutics*, **13** (9), 1365 (2021); https://doi.org/10.3390/pharmaceutics13091365
51. N.L.Klyachko, M.J.Haney, A.V.Lopukhov, I.M.Le-Deygen. *Sci. Rep.*, **14** (1), 25818 (2024); https://doi.org/10.1038/s41598-024-75985-y
52. O.V.Markov, D.N.Antropov, E.V.Shmendel, P.A.Puchkov, O.A.Yakovlev, M.D.Kerbitskaya, E.S.Zhuravlev, A.S.Dome, E.P.Goncharova, D.N.Shcherbakov, M.A.Zenkova, M.A.Maslov, G.A.Stepanov. *Eur. J. Pharm. Biopharm.*, **220**, 114981 (2026); https://doi.org/10.1016/j.ejpb.2026.114981
53. D.A.Kuznetsova, D.M.Kuznetsov, L.A.Vasileva, S.K.Amerhanova, D.N.Valeeva, D.V.Salakhieva, V.A.Nikolaeva, I.R.Nizameev, D.R.Islamov, K.S.Usachev, A.D.Voloshina, L.Ya.Zakharova. *Pharmaceutics*, **14** (12), 2685 (2022); https://doi.org/10.3390/pharmaceutics14122685
54. I.Cocchiararo, M.Cornut, H.Soldati, A.Bonavoglia, P.Castets. *Exp. Cell Res.*, **421** (2), 113392 (2022); https://doi.org/10.1016/j.yexcr.2022.113392
55. I.Urits, D.Swanson, M.C.Swett, A.Patel, K.Berardino, A.Amgalan, A.A.Berger, H.Kassem, A.D.Kaye, O.Viswanath. *Neurol. Ther.*, **9** (2), 301 (2020); https://doi.org/10.1007/s40120-020-00208-1
56. E.Fang, X.Liu, M.Li, Z.Zhang, L.Song, B.Zhu, X.Wu, J.Liu, D.Zhao, Y.Li. *Signal Transduct. Target. Ther.*, **7** (1), 94 (2022); https://doi.org/10.1038/s41392-022-00950-y
57. *Quarterly Industry Landscape Report*. ASGCT; https://www.asgct.org/news-publications/landscape-report (Last access 10.07.2026)
58. A.Y.Shchaslyvyi, S.V.Antonenko, M.G.Tesliuk, G.D.Telegeev. *Pharmaceuticals*, **16** (10), 1416 (2023); https://doi.org/10.3390/ph16101416
59. B.Ghanem, E.Seoane-Vazquez, L.Brown, R.Rodriguez-Monguio. *Med. Care*, **61** (7), 438 (2023); https://doi.org/10.1097/MLR.0000000000001840
60. J.Olaghere, D.A.Williams, J.Farrar, H.Büning, C.Calhoun, T.Ho, M.S.Inamdar, D.Liu, J.Makani, K.Nyarko, S.Ruiz, J.Tisdale, J.M.McCune, E.Boadi, Reagan-Udall Foundation for the FDA. *Biomedicines*, **13** (3), 758 (2025); https://doi.org/10.3390/biomedicines13030758
61. F.Wang, L.Liang, C.Wang, C.Zhang, Y.Ye, L.Dou, L.Shi, D.Zhou, X.Sun. *Chem. – Asian J.*, **20** (20), e00684 (2025); https://doi.org/10.1002/asia.202500684

62. S.Awasthi. *Mater. Adv.*, **6** (17), 5831 (2025); https://doi.org/10.1039/d5ma00490j
63. E.Xu, W.M.Saltzman, A.S.Piotrowski-Daspit. *J. Control. Release*, **335**, 465 (2021); https://doi.org/10.1016/j.jconrel.2021.05.038
64. V.C.Vetter, E.Wagner. *J. Control. Release*, **346**, 110 (2022); https://doi.org/10.1016/j.jconrel.2022.04.013
65. S.Shah, M.B.Chougule, A.K.Kotha, R.Kashikar, C.Godugu, R.S.Raghuvanshi, S.B.Singh, S.Srivastava. *J. Control. Release*, **338**, 80 (2021); https://doi.org/10.1016/j.jconrel.2021.08.011
66. Y.Yan, X.-Y.Liu, A.Lu, X.-Y.Wang, L.-X.Jiang, J.-C.Wang. *J. Control. Release*, **342**, 241 (2022); https://doi.org/10.1016/j.jconrel.2022.01.008
67. A.Wahane, A.Waghmode, A.Kapphahn, K.Dhuri, A.Gupta, R.Bahal. *Molecules*, **25** (12), 2866 (2020); https://doi.org/10.3390/molecules25122866
68. K.Ma, C.-L.Mi, X.-X.Cao, T.-Y.Wang. *Appl. Microbiol. Biotechnol.*, **105**, 525 (2021); https://doi.org/10.1007/s00253-020-11028-6
69. C.Wang, C.Pan, H.Yong, F.Wang, T.Bo, Y.Zhao, B.Ma, W.He, M.Li. *J. Nanobiotechnol.*, **21** (1), 272 (2023); https://doi.org/10.1186/s12951-023-02044-5
70. K.A.Hajj, K.A.Whitehead. *Nat. Rev. Mater.*, **2**, 17056 (2017); https://doi.org/10.1038/natrevmats.2017.56
71. P.S.Kowalski, A.Rudra, L.Miao, D.G.Anderson. *Mol. Ther.*, **27** (4), 710 (2019); https://doi.org/10.1016/j.ymthe.2019.02.012
72. I.Gómez-Aguado, J.Rodríguez-Castejón, M.Vicente-Pascual, A.Rodríguez-Gascón, M.Á.Solinís, A.del Pozo-Rodríguez. *Nanomaterials*, **10** (2), 364 (2020); https://doi.org/10.3390/nano10020364
73. M.D.Buschmann, M.J.Carrasco, S.Alishetty, M.Paige, M.G.Alameh, D.Weissman. *Vaccines*, **9** (1), 65 (2021); https://doi.org/10.3390/vaccines9010065
74. W.Chen, D.Zhu, M.Chen, J.Liu, X.Liu. *WIREs Nanomed. Nanobiotechnol.*, **17** (6), e70039 (2025); https://doi.org/10.1002/wnan.70039
75. D.Su, M.Coste, A.Diaconu, M.Barboiu, S.Ulrich. *J. Mater. Chem. B*, **8** (41), 9385 (2020); https://doi.org/10.1039/d0tb01836h
76. X.Cai, R.Dou, C.Guo, J.Tang, X.Li, J.Chen, J.Zhang. *Pharmaceutics*, **15** (5), 1502 (2023); https://doi.org/10.3390/pharmaceutics15051502
77. M.Khan. *Polymers*, **16** (18), 2629 (2024); https://doi.org/10.3390/polym16182629
78. I.Porello, N.Bono, G.Candiani, F.Cellesi. *Polym. Chem.*, **15** (28), 2800 (2024); https://doi.org/10.1039/d4py00234b
79. J.J.Friesen, A.K.Blakney. *J. Gene Med.*, **26** (2), e3672 (2024); https://doi.org/10.1002/jgm.3672
80. Y.Li, R.Tian, J.Xu, Y.Zou, T.Wang, J.Liu. *Polym. Chem.*, **15** (19), 1908 (2024); https://doi.org/10.1039/d4py00124a
81. Q.Wan, Y.Sun, X.Sun, Z.Zhou. *Polym. Chem.*, **15** (24), 2437 (2024); https://doi.org/10.1039/d4py00206g
82. C.M.Jogdeo, K.Siddhanta, A.Das, L.Ding, S.Panja, N.Kumari, D.Oupický. *Adv. Mater.*, **36** (31), 2404608 (2024); https://doi.org/10.1002/adma.202404608
83. H.Liu, R.Su, W.Qi, Y.Wang. *ChemBioChem*, **26** (10), e202500029 (2025); https://doi.org/10.1002/cbic.202500029
84. J.Hyun, J.Eom, J.Song, I.Seo, S.H.Um, K.M.Park, S.H.Bhang. *Macromol. Biosci.*, **21** (8), 2100106 (2021); https://doi.org/10.1002/mabi.202100106
85. X.Wang, Z.Zhang, N.Hadjichristidis. *Prog. Polym. Sci.*, **136**, 101634 (2023); https://doi.org/10.1016/j.progpolymsci.2022.101634
86. J.Karlsson, K.R.Rhodes, J.J.Green, S.Y.Tzeng. *Expert Opin. Drug Deliv.*, **17** (10), 1395 (2020); https://doi.org/10.1080/17425247.2020.1796628
87. M.Navalón-López, A.Dols-Perez, S.Grijalvo, C.Fornaguera, S.Borrós. *Nanoscale Adv.*, **5** (6), 1611 (2023); https://doi.org/10.1039/d2na00800a
88. J.Wei, L.Zhu, Q.Lu, G.Li, Y.Zhou, Y.Yang, L.Zhang. *J. Control. Release*, **354**, 337 (2023); https://doi.org/10.1016/j.jconrel.2023.01.002
89. J.Zhang, X.Cai, R.Dou, C.Guo, J.Tang, Y.Hu, H.Chen, J.Chen. *Mol. Ther. Nucleic Acids*, **32**, 568 (2023); https://doi.org/10.1016/j.omtn.2023.04.019
90. J.R.M.Rodriguez, M.Guerra-Rebollo, S.Borrós, C.Fornaguera. *Drug Deliv. Transl. Res.*, **14**, 3477 (2024); https://doi.org/10.1007/s13346-024-01585-y
91. J.Casper, S.H.Schenk, E.Parhizkar, P.Detampel, A.Dehshahri, J.Huwyler. *J. Control. Release*, **362**, 667 (2023); https://doi.org/10.1016/j.jconrel.2023.09.001
92. A.Ismail, S.-F.Chou. *Polymers*, **17** (15), 2150 (2025); https://doi.org/10.3390/polym17152150
93. S.Alamos-Musre, D.Beltrán-Chacana, J.Moyano, V.Márquez-Miranda, Y.Duarte, S.Miranda-Rojas, Y.Olguín, J.A.Fuentes, D.González-Nilo, M.C.Otero. *Pharmaceutics*, **17** (7), 927 (2025); https://doi.org/10.3390/pharmaceutics17070927
94. L.Dong, Y.Li, H.Cong, B.Yu, Y.Shen. *Carbohydr. Polym.*, **324**, 121562 (2024); https://doi.org/10.1016/j.carbpol.2023.121562
95. A.D.Gholap, H.S.Kapare, S.Pagar, P.Kamandar, D.Bhowmik, N.Vishwakarma, S.Raikwar, A.Garkal, T.A.Mehta, S.Rojekar, N.Hatvate, S.Mohanto. *Int. J. Biol. Macromol.*, **260** (2), 129581 (2024); https://doi.org/10.1016/j.ijbiomac.2024.129581
96. V.Antoniou, E.A.Mourelato, E.Galatou, K.Avgoustakis, S.Hatziantoniou. *Pharmaceutics*, **16** (7), 868 (2024); https://doi.org/10.3390/pharmaceutics16070868
97. D.G.Knorre, V.V.Vlasov. *Russ. Chem. Rev.*, **54** (9), 836 (1985); https://doi.org/10.1070/rc1985v054n09abeh003115
98. I.G.Shishkina, A.S.Levina, V.F.Zarytova. *Russ. Chem. Rev.*, **70** (6), 491 (2001); https://doi.org/10.1070/rc2001v070n06abeh000640
99. S.I.Antsypovitch. *Russ. Chem. Rev.*, **71** (1), 71 (2002); https://doi.org/10.1070/rc2002v071n01abeh000691
100. T.V.Abramova, V.N.Silnikov. *Russ. Chem. Rev.*, **80** (5), 429 (2011); https://doi.org/10.1070/rc2011v080n05abeh004188
101. M.Paurević, M.Šrajer Gajdošik, R.Ribić. *Int. J. Mol. Sci.*, **25** (3), 1370 (2024); https://doi.org/10.3390/ijms25031370
102. J.K.Vasir, V.Labhasetwar. *Biomaterials*, **29** (31), 4244 (2008); https://doi.org/10.1016/j.biomaterials.2008.07.020
103. X.Shao, X.Wei, X.Song, L.Hao, X.Cai, Z.Zhang, Q.Peng, Y.Lin. *Cell Prolif.*, **48** (4), 465 (2015); https://doi.org/10.1111/cpr.12192
104. A.Lesniak, A.Salvati, M.J.Santos-Martinez, M.W.Radomski, K.A.Dawson, C.Åberg. *J. Am. Chem. Soc.*, **135** (4), 1438 (2013); https://doi.org/10.1021/ja309812z
105. M.Weiss, J.Fan, M.Claudel, T.Sonntag, P.Didier, C.Ronzani, L.Lebeau, F.Pons. *J. Nanobiotechnol*., **19** (1), 5 (2021); https://doi.org/10.1186/s12951-020-00747-7
106. H.Derakhshankhah, S.Jafari. *Biomed. Pharmacother.*, **108**, 1090 (2018); https://doi.org/10.1016/j.biopha.2018.09.097
107. B.M.de Ronde, J.A.Torres, L.M.Minter, G.N.Tew. *Biomacromolecules*, **16** (10), 3172 (2015); https://doi.org/10.1021/acs.biomac.5b00795
108. E.I.Geihe, C.B.Cooley, J.R.Simon, M.K.Kiesewetter, J.A.Edward, R.P.Hickerson, R.L.Kaspar, J.L.Hedrick, R.M.Waymouth, P.A.Wender. *Proc. Natl. Acad. Sci. USA*, **109** (33), 13171 (2012); https://doi.org/10.1073/pnas.1211361109
109. J.M.Sarapas, C.M.Backlund, B.M.de Ronde, L.M.Minter, G.N.Tew. *Chem. – Eur. J.*, **23** (28), 6858 (2017); https://doi.org/10.1002/chem.201700423
110. T.Jeon, D.C.Luther, R.Goswami, C.Bell, H.Nagaraj, Y.A.Cicek, R.Huang, J.A.Mas-Rosario, J.L.Elia, J.Im, Y.-W.Lee, Y.Liu, F.Scaletti, M.E.Farkas, J.Mager, V.M.Rotello. *ACS Nano*, **17** (5), 4315 (2023); https://doi.org/10.1021/acsnano.2c08690
111. T.Jeon, R.Goswami, H.Nagaraj, Y.A.Cicek, V.Lehot, J.Welton, C.J.Bell, J.Park, D.C.Luther, J.Im, C.M.Rotello, J.Mager, V.M.Rotello. *Adv. Funct. Mater.*, **34** (42), 2406763 (2024); https://doi.org/10.1002/adfm.202406763
112. K.Ita. *Eur. J. Pharm. Sci.*, **150**, 105358 (2020); https://doi.org/10.1016/j.ejps.2020.105358

113. A.Albanese, P.S.Tang, W.C.W.Chan. *Annu. Rev. Biomed. Eng.*, **14** (1), 1 (2012); https://doi.org/10.1146/annurev-bioeng-071811-150124
114. K.Von Gersdorff, N.N.Sanders, R.Vandenbroucke, S.C.De Smedt, E.Wagner, M.Ogris. *Mol. Ther.*, **14** (5), 745 (2006); https://doi.org/10.1016/j.ymthe.2006.07.006
115. M.Sousa De Almeida, E.Susnik, B.Drasler, P.Taladriz-Blanco, A.Petri-Fink, B.Rothen-Rutishauser. *Chem. Soc. Rev.*, **50** (9), 5397 (2021); https://doi.org/10.1039/d0cs01127d
116. F.Zhao, D.Nayyar, Y.S.Hwang, R.Bartucci, A.Salvati. *Int. J. Pharm.*, **681**, 125881 (2025); https://doi.org/10.1016/j.ijpharm.2025.125881
117. L.Mott, C.Akers, D.W.Pack. *J. Drug Deliv. Sci. Technol.*, **84**, 104465 (2023); https://doi.org/10.1016/j.jddst.2023.104465
118. J.Wang, R.Chen, Y.Xie, X.Qin, Y.Zhou, C.Xu. *Pharmaceutics*, **17** (7), 803 (2025); https://doi.org/10.3390/pharmaceutics17070803
119. S.S.Meerasa, A.Ahmad, A.A.Khan, S.Haque, I.Saleem. *Int. J. Pharm.*, **685**, 126263 (2025); https://doi.org/10.1016/j.ijpharm.2025.126263
120. Z.-R.Lu, D.Sun. *Pharm. Res.*, **42** (7), 1065 (2025); https://doi.org/10.1007/s11095-025-03890-8
121. M.Grau, E.Wagner. *Curr. Opin. Chem. Biol.*, **81**, 102506 (2024); https://doi.org/10.1016/j.cbpa.2024.102506
122. M.J.Mehta, H.J.Kim, S.B.Lim, M.Naito, K.Miyata. *Macromol. Biosci.*, **24** (4), 2300366 (2024); https://doi.org/10.1002/mabi.202300366
123. J.Huotari, A.Helenius. *EMBO J.*, **30** (17), 3481 (2011); https://doi.org/10.1038/emboj.2011.286
124. J.Gilleron, W.Querbes, A.Zeigerer, A.Borodovsky, G.Marsico, U.Schubert, K.Manygoats, S.Seifert, C.Andree, M.Stöter, H.Epstein-Barash, L.Zhang, V.Koteliansky, K.Fitzgerald, E.Fava, M.Bickle, Y.Kalaidzidis, A.Akinc, M.Maier, M.Zerial. *Nat. Biotechnol.*, **31** (7), 638 (2013); https://doi.org/10.1038/nbt.2612
125. H.Liu, M.Z.Chen, T.Payne, C.J.H.Porter, C.W.Pouton, A.P.R.Johnston. *Adv. Funct. Mater.*, **34** (39), 2404510 (2024); https://doi.org/10.1002/adfm.202404510
126. L.Jin, X.Zeng, M.Liu, Y.Deng, N.He. *Theranostics*, **4** (3), 240 (2014); https://doi.org/10.7150/thno.6914
127. Y.Wang, V.Ukwattage, Y.Xiong, G.K.Such. *Mater. Horiz.*, **12** (11), 3622 (2025); https://doi.org/10.1039/d4mh01781a
128. J.-P.Behr. *Chimia*, **51** (1–2), 34 (1997); https://doi.org/10.2533/chimia.1997.34
129. S.Roy, D.Zhu, W.J.Parak, N.Feliu. *ACS Nano*, **14** (7), 8012 (2020); https://doi.org/10.1021/acsnano.9b10219
130. A.Akinc, M.Thomas, A.M.Klibanov, R.Langer. *J. Gene Med.*, **7** (5), 657 (2005); https://doi.org/10.1002/jgm.696
131. L.M.P.Vermeulen, S.C.De Smedt, K.Remaut, K.Braeckmans. *Eur. J. Pharm. Biopharm.*, **129**, 184 (2018); https://doi.org/10.1016/j.ejpb.2018.05.034
132. A.G.Berger, C.De Lorenzo, C.Vo, J.A.Kaskow, N.Nabar, P.T.Hammond. *Biomacromolecules*, **25** (5), 2934 (2024); https://doi.org/10.1021/acs.biomac.4c00062
133. A.M.Funhoff, C.F.Van Nostrum, G.A.Koning, N.M.E.Schuurmans-Nieuwenbroek, D.J.A.Crommelin, W.E.Hennink. *Biomacromolecules*, **5** (1), 32 (2004); https://doi.org/10.1021/bm034041+
134. M.Wojnilowicz, A.Glab, A.Bertucci, F.Caruso, F.Cavalieri. *ACS Nano*, **13** (1), 187 (2019); https://doi.org/10.1021/acsnano.8b05151
135. Z.U.Rehman, D.Hoekstra, I.S.Zuhorn. *ACS Nano*, **7** (5), 3767 (2013); https://doi.org/10.1021/nn3049494
136. D.Ulkoski, M.J.Munson, M.E.Jacobson, C.R.Palmer, C.S.Carson, A.Sabirsh, J.T.Wilson, V.R.Krishnamurthy. *ACS Appl. Bio Mater.*, **4** (2), 1640 (2021); https://doi.org/10.1021/acsabm.0c01463
137. T.Haraguchi, T.Koujin, T.Shindo, Ş.Bilir, H.Osakada, K.Nishimura, Y.Hirano, H.Asakawa, C.Mori, S.Kobayashi, Y.Okada, Y.Chikashige, T. Fukagawa, S.Shibata, Y.Hiraoka. *Commun. Biol.*, **5** (1), 78 (2022); https://doi.org/10.1038/s42003-022-03021-8
138. Y.Nie, G.Fu, Y.Leng. *Cells*, **12** (12), 1637 (2023); https://doi.org/10.3390/cells12121637
139. H.Kamiya, Y.Fujimura, I.Matsuoka, H.Harashima. *Biochem. Biophys. Res. Commun.*, **298** (4), 591 (2002); https://doi.org/10.1016/s0006-291x(02)02485-3
140. G.Grandinetti, A.E.Smith, T.M.Reineke. *Mol. Pharm.*, **9** (3), 523 (2012); https://doi.org/10.1021/mp200368p
141. C.Wu, H.Liu, D.Zhong, X.Yang, Z.Liao, Y.Chen, S.Zhang, D.Su, B.Zhang, C.Li, L.Tian, C.Xu, P.Su. *Genes Dis.*, **11** (2), 964 (2024); https://doi.org/10.1016/j.gendis.2023.02.012
142. G.Feng, Z.Zhang, M.Dang, X.Zhang, Y.Doleyres, Y.Song, D.Chen, P.X.Ma. *Biomaterials*, **131**, 86 (2017); https://doi.org/10.1016/j.biomaterials.2017.03.029
143. K.J.Kauffman, J.R.Dorkin, J.H.Yang, M.W.Heartlein, F.De Rosa, F.F.Mir, O.S.Fenton, D.G.Anderson. *Nano Lett.*, **15** (11), 7300 (2015); https://doi.org/10.1021/acs.nanolett.5b02497
144. J.A.Kulkarni, J.L.Myhre, S.Chen, Y.Y.C.Tam, A.Danescu, J.M.Richman, P.R.Cullis. *Nanomed. Nanotechnol. Biol. Med.*, **13** (4), 1377 (2017); https://doi.org/10.1016/j.nano.2016.12.014
145. R.Ni, R.Feng, Y.Chau. *Life*, **9** (3), 59 (2019); https://doi.org/10.3390/life9030059
146. P.Kreiss. *Nucleic Acids Res.*, **27** (19), 3792 (1999); https://doi.org/10.1093/nar/27.19.3792
147. A.A.Goryaev, M.V.Savkina, Yu.I.Obukhov, V.A.Merkulov, Yu.V.Olefir. *BIOpreparations. Prevention, Diagnosis, Treatment*, **19** (2), 72 (2019); https://doi.org/10.30895/2221-996X-2019-19-2-72-80
148. J.A.Kretzmann, C.W.Evans, C.Moses, A.Sorolla, A.L.Kretzmann, E.Wang, D.Ho, M.J.Hackett, B.F.Dessauvagie, N.M.Smith, A.D.Redfern, C.Waryah, M.Norret, K.S.Iyer, P.Blancafort. *Chem. Sci.*, **10** (33), 7718 (2019); https://doi.org/10.1039/c9sc01432b
149. C.Janich, D.Ivanusic, J.Giselbrecht, E.Janich, S.R.Pinnapireddy, G.Hause, U.Bakowsky, A.Langner, C.Wölk. *Pharmaceutics*, **12** (9), 805 (2020); https://doi.org/10.3390/pharmaceutics12090805
150. M.Maeki, S.Uno, K.Sugiura, Y.Sato, Y.Fujioka, A.Ishida, Y.Ohba, H.Harashima, M.Tokeshi. *ACS Appl. Mater. Interfaces*, **16** (2), 2110 (2024); https://doi.org/10.1021/acsami.3c14714
151. G.Liu, D.Li, M.K.Pasumarthy, T.H.Kowalczyk, C.R.Gedeon, S.L.Hyatt, J.M.Payne, T.J.Miller, P.Brunovskis, T.L.Fink, O.Muhammad, R.C.Moen, R.W.Hanson, M.J.Cooper. *J. Biol. Chem.*, **278** (35), 32578 (2003); https://doi.org/10.1074/jbc.m305776200
152. T.L.Fink, P.J.Klepcyk, S.M.Oette, C.R.Gedeon, S.L.Hyatt, T.H.Kowalczyk, R.C.Moen, M.J.Cooper. *Gene Ther.*, **13** (13), 1048 (2006); https://doi.org/10.1038/sj.gt.3302761
153. W.S.Boyle, K.Twaroski, E.C.Woska, J.Tolar, T.M.Reineke. *Bioconjug. Chem.*, **30** (2), 418 (2019); https://doi.org/10.1021/acs.bioconjchem.8b00760
154. J.Kurreck. *Eur. J. Biochem.*, **270** (8), 1628 (2003); https://doi.org/10.1046/j.1432-1033.2003.03555.x
155. K.Kawabata, Y.Takakura, M.Hashida. *Pharm. Res.*, **12** (6), 825 (1995); https://doi.org/10.1023/A:1016248701505
156. J.Soutschek, A.Akinc, B.Bramlage, K.Charisse, R.Constien, M.Donoghue, S.Elbashir, A.Geick, P.Hadwiger, J.Harborth, M.John, V.Kesavan, G.Lavine, R.K.Pandey, T.Racie, K.G.Rajeev, I.Röhl, I.Toudjarska, G.Wang, S.Wuschko, D.Bumcrot, V.Koteliansky, S.Limmer, M.Manoharan, H.-P.Vornlocher. *Nature*, **432** (7014), 173 (2004); https://doi.org/10.1038/nature03121
157. R.S.Geary, D.Norris, R.Yu, C.F.Bennett. *Adv. Drug Deliv. Rev.*, **87**, 46 (2015); https://doi.org/10.1016/j.addr.2015.01.008
158. P.Morais, H.Adachi, Y.-T.Yu. *Front. Cell Dev. Biol.*, **9**, 789427 (2021); https://doi.org/10.3389/fcell.2021.789427
159. A.Liu, X.Wang. *Front. Cell Dev. Biol.*, **10**, 901510 (2022); https://doi.org/10.3389/fcell.2022.901510

160. C.A.Teko-Agbo, E.Josse, K.Konate, S.Deshayes, P.De Santa Barbara, S.Faure, P.Boisguérin, E.Vivès. *Mol. Ther. Nucleic Acids*, **36** (3), 102650 (2025); https://doi.org/10.1016/j.omtn.2025.102650
161. A.K.Blakney, G.Yilmaz, P.F.McKay, C.R.Becer, R.J.Shattock. *Biomacromolecules*, **19** (7), 2870 (2018); https://doi.org/10.1021/acs.biomac.8b00429
162. L.Opsomer, S.Jana, I.Mertens, X.Cui, R.Hoogenboom, N.N.Sanders. *J. Mater. Chem. B*, **12** (16), 3927 (2024); https://doi.org/10.1039/d3tb03003b
163. A.K.Blakney, Y.Zhu, P.F.McKay, C.R.Bouton, J.Yeow, J.Tang, K.Hu, K.Samnuan, C.L.Grigsby, R.J.Shattock, M.M.Stevens. *ACS Nano*, **14** (5), 5711 (2020); https://doi.org/10.1021/acsnano.0c00326
164. P.Gurnani, A.K.Blakney, J.Yeow, C.R.Bouton, R.J.Shattock, M.M.Stevens, C.Alexander. *Polym. Chem.*, **11** (36), 5861 (2020); https://doi.org/10.1039/d0py00912a
165. A.Monaco, B.D.Barbieri, G.Yilmaz, R.J.Shattock, C.R.Becer. *Polym. Chem.*, **14** (22), 2750 (2023); https://doi.org/10.1039/D3PY00260H
166. B.D.Barbieri, D.J.Peeler, K.Samnuan, S.Day, K.Hu, H.J.Sallah, J.S.Tregoning, P.F.McKay, R.J.Shattock. *J. Control. Release*, **374**, 280 (2024); https://doi.org/10.1016/j.jconrel.2024.08.016
167. E.De Lombaerde, X.Cui, Y.Chen, Z.Zhong, J.Deckers, G.Mencarelli, L.Opsomer, H.Wang, J.De Baere, S.Lienenklaus, B.N.Lambrecht, N.N.Sanders, B.G.De Geest. *ACS Nano*, **18** (41), 28311 (2024); https://doi.org/10.1021/acsnano.4c09677
168. H.H.Ly, S.Daniel, S.K.V.Soriano, Z.Kis, A.K.Blakney. *Mol. Pharm.*, **19** (6), 1892 (2022); https://doi.org/10.1021/acs.molpharmaceut.2c00032
169. J.Moreno Herrero, T.B.Stahl, S.Erbar, K.Maxeiner, A.Schlegel, T.Bacic, J.Schumacher, L.P.Cavalcanti, M.A.Schroer, D.I.Svergun, U.Sahin, H.Haas. *Nat. Nanotechnol.*, **20** (9), 1323 (2025); https://doi.org/10.1038/s41565-025-01961-w
170. H.Bayraktutan, R.J.Kopiasz, A.Elsherbeny, M.Martinez Espuga, N.Gumus, U.C.Oz, K.Polra, P.F.McKay, R.J.Shattock, P.Ordóñez-Morán, A.Mata, C.Alexander, P.Gurnani. *Polym. Chem.*, **15** (18), 1862 (2024); https://doi.org/10.1039/d4py00064a
171. P.Gurnani, A.K.Blakney, R.Terracciano, J.E.Petch, A.J.Blok, C.R.Bouton, P.F.McKay, R.J.Shattock, C.Alexander. *Biomacromolecules*, **21** (8), 3242 (2020); https://doi.org/10.1021/acs.biomac.0c00698
172. N.K.Dastgerdi, N.Gumus, H.Bayraktutan, D.Jackson, K.Polra, P.F.McKay, F.Atyabi, R.Dinarvand, R.J.Shattock, L.Martinez-Pomares, P.Gurnani, C.Alexander. *Nanoscale Adv.*, **6** (5), 1409 (2024); https://doi.org/10.1039/d3na00794d
173. J.Li, C.Foged. *Expert Opin. Drug Deliv.*, **21** (10), 1441 (2024); https://doi.org/10.1080/17425247.2024.2409142
174. I.A.Bauer, E.V.Dmitrienko. *Pharmaceutics*, **16** (11), 1447 (2024); https://doi.org/10.3390/pharmaceutics16111447
175. C.Chen, Z.Yang, X.Tang. *Med. Res. Rev.*, **38** (3), 829 (2018); https://doi.org/10.1002/med.21479
176. S.M.Sarett, T.A.Werfel, L.Lee, M.A.Jackson, K.V.Kilchrist, D.Brantley-Sieders, C.L.Duvall. *Proc. Natl. Acad. Sci. USA*, **114** (32), E6490 (2017); https://doi.org/10.1073/pnas.1621240114
177. Z.Yao, T.Liu, J.Wang, Y.Fu, J.Zhao, X.Wang, Y.Li, X.Yang, Z.He. *Biotechnol. Adv.*, **81**, 108546 (2025); https://doi.org/10.1016/j.biotechadv.2025.108546
178. M.Moazzam, M.Zhang, A.Hussain, X.Yu, J.Huang, Y.Huang. *Mol. Ther.*, **32** (2), 284 (2024); https://doi.org/10.1016/j.ymthe.2024.01.005
179. S.Uchida, C.Y.J.Lau, M.Oba, K.Miyata. *Adv. Drug Deliv. Rev.*, **199**, 114972 (2023); https://doi.org/10.1016/j.addr.2023.114972
180. Z.Ma, H.Kamizawa, R.Ota, B.J.Li, F.Aulia, T.Nii, T.Mori, Y.Katayama, A.Kishimura. *Polym. J.*, **58**, 439 (2025); https://doi.org/10.1038/s41428-025-01124-7
181. T.R.Blake, O.A.W.Haabeth, A.Sallets, R.L.McClellan, T.J.Del Castillo, J.G.Vilches-Moure, W.C.Ho, P.A.Wender, R.Levy, R.M.Waymouth. *Bioconjug. Chem.*, **34** (4), 673 (2023); https://doi.org/10.1021/acs.bioconjchem.3c00019
182. K.Hayashi, H.Chaya, S.Fukushima, S.Watanabe, H.Takemoto, K.Osada, N.Nishiyama, K.Miyata, K.Kataoka. *Macromol. Rapid Commun.*, **37** (6), 486 (2016); https://doi.org/10.1002/marc.201500661
183. I.V.Chernikov, V.V.Vlassov, E.L.Chernolovskaya. *Front. Pharmacol.*, **10**, 444 (2019); https://doi.org/10.3389/fphar.2019.00444
184. H.Wang, S.Zhang, J.Lv, Y.Cheng. *View*, **2** (3), 20200026 (2021); https://doi.org/10.1002/VIW.20200026
185. D.Kim, S.Han, Y.Ji, S.Moon, H.Nam, J.B.Lee. *J. Control. Release*, **345**, 770 (2022); https://doi.org/10.1016/j.jconrel.2022.03.052
186. S.-Y.Lee, M.S.Huh, S.Lee, S.J.Lee, H.Chung, J.H.Park, Y.-K.Oh, K.Choi, K.Kim, I.C.Kwon. *J. Control. Release*, **141** (3), 339 (2010); https://doi.org/10.1016/j.jconrel.2009.10.007
187. C.A.Hong, S.H.Lee, J.S.Kim, J.W.Park, K.H.Bae, H.Mok, T.G.Park, H.Lee. *J. Am. Chem. Soc.*, **133** (35), 13914 (2011); https://doi.org/10.1021/ja2056984
188. A.Sang, S.Zhuo, A.Bochanis, J.E.Manautou, R.Bahal, X.Zhong, T.P.Rasmussen. *BioDrugs*, **38** (4), 511 (2024); https://doi.org/10.1007/s40259-024-00665-2
189. S.Wang, D.Weissman, Y.Dong. *Nat. Rev. Drug Discov.*, **24** (11), 828 (2025); https://doi.org/10.1038/s41573-025-01237-x
190. M.Liu, Y.Wang, Y.Zhang, D.Hu, L.Tang, B.Zhou, L.Yang. *Signal Transduct. Target. Ther.*, **10** (1), 73 (2025); https://doi.org/10.1038/s41392-024-02112-8
191. J.Guan, H.Guo, T.Tang, Y.Wang, Y.Wei, P.Seth, Y.Li, S.M.Dehm, E.Ruoslahti, H.Pang. *Adv. Funct. Mater.*, **31** (24), 2100478 (2021); https://doi.org/10.1002/adfm.202100478
192. C.Y.J.Lau, H.Kinoh, X.Liu, J.Feng, F.Aulia, K.Taniwaki, N.Qiao, S.Ogura, M.Naito, K.Miyata. *J. Am. Chem. Soc.*, **147** (30), 26286 (2025); https://doi.org/10.1021/jacs.5c04234
193. Y.N.Lim, I.S.Ryu, Y.-J.Jung, G.Helmlinger, I.Kim, H.W.Park, H.Kang, J.Lee, H.J.Lee, K.S.Lee, H.-N.Jang, D.-I.Ha, J.Park, J.Won, K.S.Lim, C.-Y.Jeon, H.-J.Cho, H.S.Min, J.-H.Ryu. *Mol. Ther. Nucleic Acids*, **35** (4), 102340 (2024); https://doi.org/10.1016/j.omtn.2024.102340
194. A.Kuzmich, O.Rakitina, D.Didych, V.Potapov, M.Zinovyeva, I.Alekseenko, E.Sverdlov. *Polymers*, **12** (8), 1695 (2020); https://doi.org/10.3390/polym12081695
195. N.T.Jarzebska, M.Mellett, J.Frei, T.M.Kündig, S.Pascolo. *Pharmaceutics*, **13** (6), 877 (2021); https://doi.org/10.3390/pharmaceutics13060877
196. M.Alberer, U.Gnad-Vogt, H.S.Hong, K.T.Mehr, L.Backert, G.Finak, R.Gottardo, M.A.Bica, A.Garofano, S.D.Koch, M.Fotin-Mleczek, I.Hoerr, R.Clemens, F.von Sonnenburg. *Lancet*, **390** (10101), 1511 (2017); https://doi.org/10.1016/s0140-6736(17)31665-3
197. M.Sebastian, A.Schröder, B.Scheel, H.S.Hong, A.Muth, L.von Boehmer, A.Zippelius, F.Mayer, M.Reck, D.Atanackovic, M.Thomas, F.Schneller, J.Stöhlmacher, H.Bernhard, A.Gröschel, T.Lander, J.Probst, T.Strack, V.Wiegand, U.Gnad-Vogt, K.-J.Kallen, I.Hoerr, F.von der Muelbe, M.Fotin-Mleczek, A.Knuth, S.D.Koch. *Cancer Immunol. Immunother.*, **68** (5), 799 (2019); https://doi.org/10.1007/s00262-019-02315-x
198. X.Xu, L.Li, X.Li, D.Tao, P.Zhang, J.Gong. *Int. J. Pharm.*, **590**, 119963 (2020); https://doi.org/10.1016/j.ijpharm.2020.119963
199. Z.Zeng, C.H.Tung, Y.Zu. *Cancers*, **12** (4), 780 (2020); https://doi.org/10.3390/cancers12040780
200. Y.Mai, J.Guo, Y.Zhao, S.Ma, Y.Hou, J.Yang. *Cell. Immunol.*, **354**, 104143 (2020); https://doi.org/10.1016/j.cellimm.2020.104143
201. D.Fischer, Y.Li, B.Ahlemeyer, J.Krieglstein, T.Kissel. *Biomaterials*, **24** (7), 1121 (2003); https://doi.org/10.1016/s0142-9612(02)00445-3

202. C.Siewert, H.Haas, T.Nawroth, A.Ziller, S.S.Nogueira, M.A.Schroer, C.E.Blanchet, D.I.Svergun, A.Radulescu, F.Bates, Y.Huesemann, M.P.Radsak, U.Sahin, P.Langguth. *Biomaterials*, **192**, 612 (2019); https://doi.org/10.1016/j.biomaterials.2018.10.020
203. X.Liu, Z.Li, X.J.Loh, K.Chen, Z.Li, Y.-L.Wu. *Macromol. Rapid Commun.*, **40** (5), 1800117 (2019); https://doi.org/10.1002/marc.201800117
204. M.P.Ryndyk, I.E.Nifant'ev, A.N.Tavtorkin, P.V.Ivchenko. *Polym. Chem., Ser. C*, **67** (1), 1 (2025); https://doi.org/10.1134/s1811238225600326
205. https://www.yeasenbio.com/ru/blogs/news/exciting-news-yeasen-s-gmp-grade-ultraaav-transfection-reagent-successfully-registered-in-fda-dmf-system (Last access 12.04.2026)
206. H.-L.Jiang, M.A.Islam, L.Xing, J.Firdous, W.Cao, Y.-J.He, Y.Zhu, K.-H.Cho, H.-S.Li, C.-S.Cho. *Top. Curr. Chem.*, **375**, 113 (2017); https://doi.org/10.1007/s41061-017-0124-9
207. Z.Kadlecova, Y.Rajendra, M.Matasci, L.Baldi, D.L.Hacker, F.M.Wurm, H.A.Klok. *J. Control. Release*, **169** (3), 276 (2013); https://doi.org/10.1016/j.jconrel.2013.01.019
208. A.Alazzo, N.Gumus, P.Gurnani, S.Stolnik, R.Rahman, K.Spriggs, C.Alexander. *J. Mater. Chem. B*, **10** (2), 236 (2022); https://doi.org/10.1039/d1tb01793d
209. V.Korzhikov-Vlakh, P.Teterina, N.Gubina, A.Dzhuzha, T.Tennikova, E.Korzhikova-Vlakh. *Polysaccharides*, **6** (3), 60 (2025); https://doi.org/10.3390/polysaccharides6030060
210. D.Putnam, R.Langer. *Macromolecules*, **32** (11), 3658 (1999); https://doi.org/10.1021/ma982004i
211. Y.B.Lim, S.O.Han, H.U.Kong, Y.Lee, J.-S.Park, B.Jeong, S.W.Kim. *Pharm. Res.*, **17** (7), 811 (2000); https://doi.org/10.1023/A:1007552007765
212. S.V.Gladnev, M.L.Levit, T.B.Tennikova, E.G.Korzhikova-Vlakh. *Mendeleev Commun.*, **35** (3), 295 (2025); https://doi.org/10.71267/mencom.7606
213. J.Wang, H.-Q.Mao, K.W.Leong. *J. Am. Chem. Soc.*, **123** (38), 9480 (2001); https://doi.org/10.1021/ja016062m
214. J.M.Priegue, D.N.Crisan, J.Martínez-Costas, J.R.Granja, F.Fernandez-Trillo, J.Montenegro. *Angew. Chem., Int. Ed.*, **55** (26), 7492 (2016); https://doi.org/10.1002/anie.201601441
215. V.L.Rose, F.Mastrotto, G.Mantovani. *Polym. Chem.*, **8** (2), 353 (2017); https://doi.org/10.1039/c6py01855f
216. J.Li, Y.Zhang, Y.Lu, L.Zhang, G.Shen, C.Jin. *Lett. Drug Des. Discov.*, **21** (2), 339 (2025); https://doi.org/10.2174/1570180819666220926140957
217. D.S.H.Chu, J.G.Schellinger, J.Shi, A.J.Convertine, P.S.Stayton, S.H.Pun. *Acc. Chem. Res.*, **45** (7), 1089 (2012); https://doi.org/10.1021/ar200242z
218. M.V.Edeleva, S.R.A.Marque, E.G.Bagryanskaya. *Russ. Chem. Rev.*, **87** (4), 328 (2018); https://doi.org/10.1070/RCR4765
219. S.Agarwal, Y.Zhang, S.Maji, A.Greiner. *Mater. Today*, **15** (9), 388 (2012); https://doi.org/10.1016/s1369-7021(12)70165-7
220. X.Pan, F.Zhang, B.Choi, Y.Luo, X.Guo, A.Feng, S.H.Thang. *Eur. Polym. J.*, **115**, 166 (2019); https://doi.org/10.1016/j.eurpolymj.2019.03.016
221. D.Kaur, K.Jain, N.K.Mehra, P.Kesharwani, N.K.Jain. *J. Nanopart. Res.*, **18** (6), 146 (2016); https://doi.org/10.1007/s11051-016-3423-0
222. J.Wu, W.Huang, Z.He. *Sci. World J.*, **2013** (1), 630654 (2013); https://doi.org/10.1155/2013/630654
223. Z.Lyu, L.Ding, A.-Y.T.Huang, C.-L.Kao, L.Peng. *Mater. Today Chem.*, **13**, 34 (2019); https://doi.org/10.1016/j.mtchem.2019.04.004
224. F.Zhang, N.N.Parayath, C.I.Ene, S.B.Stephan, A.L.Koehne, M.E.Coon, E.C.Holland, M.T.Stephan. *Nat. Commun.*, **10**, 3974 (2019); https://doi.org/10.1038/s41467-019-11911-5
225. A.A.Al-Absi, A.E.Ogungbenro, A.M.Benneker, N.Mahinpey. *J. Environ. Chem. Eng.*, **12** (3), 112739 (2024); https://doi.org/10.1016/j.jece.2024.112739
226. R.Kumar, C.F.Santa Chalarca, M.R.Bockman, C.V.Bruggen, C.J.Grimme, R.J.Dalal, M.G.Hanson, J.K.Hexum, T.M.Reineke. *Chem. Rev.*, **121** (18), 11527 (2021); https://doi.org/10.1021/acs.chemrev.0c00997
227. B.Chen, Q.Ren, P.Jiang, Q.Wu, Q.Shuai, Y.Yan. *Macromol. Biosci.*, **24** (10), 2400168 (2024); https://doi.org/10.1002/mabi.202400168
228. S.Ros, J.S.Freitag, D.M.Smith, H.D.H.Stöver. *ACS Omega*, **5** (16), 9114 (2020); https://doi.org/10.1021/acsomega.9b03734
229. A.Dirisala, S.Uchida, J.Li, J.F.R.Van Guyse, K.Hayashi, S.V.C.Vummaleti, S.Kaur, Y.Mochida, S.Fukushima, K.Kataoka. *Macromol. Rapid Commun.*, **43** (12), 2100754 (2022); https://doi.org/10.1002/marc.202100754
230. C.J.McKinlay, J.R.Vargas, T.R.Blake, J.W.Hardy, M.Kanada, C.H.Contag, P.A.Wender, R.M.Waymouth. *Proc. Natl. Acad. Sci. USA*, **114** (4), E448 (2017); https://doi.org/10.1073/pnas.1614193114
231. T.R.Blake, W.C.Ho, C.R.Turlington, X.Zang, M.A.Huttner, P.A.Wender, R.M.Waymouth. *Chem. Sci.*, **11** (11), 2951 (2020); https://doi.org/10.1039/c9sc05267d
232. N.L.Benner, K.E.Near, M.H.Bachmann, C.H.Contag, R.M.Waymouth, P.A.Wender. *Biomacromolecules*, **19** (7), 2812 (2018); https://doi.org/10.1021/acs.biomac.8b00401
233. O.A.W.Haabeth, T.R.Blake, C.J.McKinlay, A.A.Tveita, A.Sallets, R.M.Waymouth, P.A.Wender, R.Levy. *Cancer Res.*, **79** (7), 1624 (2019); https://doi.org/10.1158/0008-5472.can-18-2867
234. C.J.McKinlay, N.L.Benner, O.A.Haabeth, R.M.Waymouth, P.A.Wender. *Proc. Natl. Acad. Sci. USA*, **115** (26), E5859 (2018); https://doi.org/10.1073/pnas.1805358115
235. H.P.Rahn, J.Sun, Z.Li, R.M.Waymouth, R.Levy, P.A.Wender. *Biomacromolecules*, **25** (7), 4305 (2024); https://doi.org/10.1021/acs.biomac.4c00373
236. Z.Li, L.Amaya, R.Pi, S.K.Wang, A.Ranjan, R.M.Waymouth, C.A.Blish, H.Y.Chang, P.A.Wender. *Nat. Commun.*, **14** (1), 6983 (2023); https://doi.org/10.1038/s41467-023-42672-x
237. N.L.Benner, R.L.McClellan, C.R.Turlington, O.A.W.Haabeth, R.M.Waymouth, P.A.Wender. *J. Am. Chem. Soc.*, **141** (21), 8416 (2019); https://doi.org/10.1021/jacs.9b03154
238. Z.Li, L.Amaya, A.Ee, S.K.Wang, A.Ranjan, R.M.Waymouth, H.Y.Chang, P.A.Wender. *J. Am. Chem. Soc.*, **146** (21), 14785 (2024); https://doi.org/10.1021/jacs.4c02704
239. M.M.Abd Elwakil, J.Ni, S.Ramsay-Burrough, P.J.Hurst, R.L.McClellan, S.R.Khasnavis, Y.Jia, S.R.Masud, T.R.Blake, A.Sallets, O.A.W.Haabeth, I.Sagiv-Barfi, D.K.Czerwinski, M.Herrera-Barrera, R.Levy, P.A.Wender, M.E.Kumar, R.M.Waymouth. *J. Am. Chem. Soc.*, **147** (44), 40146 (2025); https://doi.org/10.1021/jacs.5c06654
240. Y.Lim, Y.H.Choi, J.Park. *J. Am. Chem. Soc.*, **121** (24), 5633 (1999); https://doi.org/10.1021/ja984012k8
241. Z.Li, L.Huang. *J. Control. Release*, **98** (3), 437 (2004); https://doi.org/10.1016/j.jconrel.2004.05.013
242. Z.Tian, Y.Dai, C.Zhan, Y.Chen, Z.Ding, J.Wu, R.Hou, Y.Sun, Y.Li, W.He, N.Zhu, X.Hu, Y.Liu, K.Guo. *React. Funct. Polym.*, **216**, 106411 (2025); https://doi.org/10.1016/j.reactfunctpolym.2025.106411
243. E.D.Shaputkin, I.E.Nifant'ev, V.V.Bagrov, A.V.Shlyakhtin, D.A.Abashkin, A.A.Galiakberova, P.V.Ivchenko. *Eur. Polym. J.*, **181**, 111644 (2022); https://doi.org/10.1016/j.eurpolymj.2022.111644
244. E.D.Shaputkin, I.E.Nifant'ev, P.V.Ivchenko. *Mendeleev Commun.*, **34** (1), 28 (2024); https://doi.org/10.1016/j.mencom.2024.01.009
245. J.Shi, Y.Zhang, B.Ma, H.Yong, D.Che, C.Pan, W.He, D.Zhou, M.Li. *ACS Appl. Mater. Interfaces*, **15** (36), 42130 (2023); https://doi.org/10.1021/acsami.3c03802
246. L.Xue, Y.Yan, P.Kos, X.Chen, D.J.Siegwart. *Drug Deliv. Transl. Res.*, **11** (1), 255 (2021); https://doi.org/10.1007/s13346-020-00790-9
247. H.Liu, Y.Wang, M.Wang, J.Xiao, Y.Cheng. *Biomaterials*, **35** (20), 5407 (2014); https://doi.org/10.1016/j.biomaterials.2014.03.040

248. X.Bai, J.Nie, S.Cheng, D.Sheng, J.Xiao, W.Dong. *Colloids Surf. A: Physicochem. Eng. Asp.*, **705**, 135575 (2025); https://doi.org/10.1016/j.colsurfa.2024.135575
249. X.Wang, G.Rong, J.Yan, D.Pan, L.Wang, Y.Xu, M.Yang, Y.Cheng. *ACS Appl. Mater. Interfaces*, **12** (41), 45763 (2020); https://doi.org/10.1021/acsami.0c11967
250. C.Romani, P.Gagni, M.Sponchioni, A.Volonterio. *Bioconjug. Chem.*, **34** (6), 1084 (2023); https://doi.org/10.1021/acs.bioconjchem.3c00139
251. C.Romani, P.Gagni, M.E.Di Pietro, M.Sani, M.Sponchioni, A.Volonterio. *Bioconjug. Chem.*, **36** (1), 66 (2025); https://doi.org/10.1021/acs.bioconjchem.4c00434
252. Y.Deng, J.Zhang, X.Sun, L.Li, M.Zhou, S.Liu, F.Chen, C.Pan, Z.Yu, M.Li, W.Zhong, M.Zeng. *J. Control. Release*, **363**, 597 (2023); https://doi.org/10.1016/j.jconrel.2023.10.001
253. Y.Jin, W.Yu, W.Zhang, C.Wang, Y.Liu, W.-E.Yuan, Y.Feng. *J. Colloid Interface Sci.*, **648**, 287 (2023); https://doi.org/10.1016/j.jcis.2023.05.153
254. P.Gurnani, C.Sanchez-Cano, H.Xandri-Monje, J.Zhang, S.H.Ellacott, E.D.H.Mansfield, M.Hartlieb, R.Dallmann, S.Perrier. *Small*, **18** (38), 2203070 (2022); https://doi.org/10.1002/smll.202203070
255. Y.Liu, L.Zhou, X.Xu, Z.Cheng, Y.Chen, X.-A.Mei, N.Zheng, C.Zhang, Y.Bai. *Biomacromolecules*, **24** (12), 5698 (2023); https://doi.org/10.1021/acs.biomac.3c00682
256. T.Miyazaki, S.Uchida, S.Nagatoishi, K.Koji, T.Hong, S.Fukushima, K.Tsumoto, K.Ishihara, K.Kataoka, H.Cabral. *Adv. Healthcare Mater.*, **9** (16), 2000538 (2020); https://doi.org/10.1002/adhm.202000538
257. Y.Jiang, D.Sprouse, J.E.Laaser, Y.Dhande, T.M.Reineke, T.P.Lodge. *J. Phys. Chem. B*, **121** (27), 6708 (2017); https://doi.org/10.1021/acs.jpcb.7b03732
258. K.Osada. *Polymers*, **12** (7), 1603 (2020); https://doi.org/10.3390/polym12071603
259. B.J.Rackstraw, A.L.Martin, S.Stolnik, C.J.Roberts, M.C.Garnett, M.C.Davies, S.J.B.Tendler. *Langmuir*, **17** (11), 3185 (2001); https://doi.org/10.1021/la001456x
260. S.Bae, I.Oh, J.Yoo, J.S.Kim. *ACS Omega*, **6** (29), 18728 (2021); https://doi.org/10.1021/acsomega.1c01709
261. L.Wightman, R.Kircheis, V.Rössler, S.Carotta, R.Ruzicka, M.Kursa, E.Wagner. *J. Gene Med.*, **3** (4), 362 (2001); https://doi.org/10.1002/jgm.187
262. P.Neuberg, A.Kichler. *Adv. Genet.*, **88**, 263 (2014); https://doi.org/10.1016/b978-0-12-800148-6.00009-2
263. H.-H.Ahn, C.Carrington, Y.Hu, H.Liu, C.Ng, H.Nam, A.Park, C.Stace, W.West, H.-Q.Mao, M.G.Pomper, C.G.Ullman, I.Minn. *Sci. Rep.*, **11** (1), 9733 (2021); https://doi.org/10.1038/s41598-021-89124-4
264. Y.Li, Z.He, X.Wang, Z.Li, M.Johnson, R.Foley, A.Sigen, J.Lyu, W.Wang. *ACS Macro Lett.*, **12** (6), 780 (2023); https://doi.org/10.1021/acsmacrolett.3c00152
265. Y.Li, B.Qiu, L.Yao, J.Wei, T.Mao, M.Yu, X.Wang, A.Benedetto, Z.Zhang, J.Lyu, W.Wang. *Chem. Eng. J.*, **526**, 170828 (2025); https://doi.org/10.1016/j.cej.2025.170828
266. M.A.Cortez, W.T.Godbey, Y.Fang, M.E.Payne, B.J.Cafferty, K.A.Kosakowska, S.M.Grayson. *J. Am. Chem. Soc.*, **137** (20), 6541 (2015); https://doi.org/10.1021/jacs.5b00980
267. H.Wei, D.S.H.Chu, J.Zhao, J.A.Pahang, S.H.Pun. *ACS Macro Lett.*, **2** (12), 1047 (2013); https://doi.org/10.1021/mz400560y
268. Y.Cheng, H.Wei, J.-K.Y.Tan, D.J.Peeler, D.O.Maris, D.L.Sellers, P.J.Horner, S.H.Pun. *Small*, **12** (20), 2750 (2016); https://doi.org/10.1002/smll.201502930
269. C.Wang, X.Huang, L.Sun, Q.Li, Z.Li, H.Yong, D.Che, C.Yan, S.Geng, W.Wang, D.Zhou. *Chem. Commun.*, **58** (13), 2136 (2022); https://doi.org/10.1039/D1CC06480K
270. R.J.Dalal, R.Kumar, M.Ohnsorg, M.Brown, T.M.Reineke. *ACS Macro Lett.*, **10** (7), 886 (2021); https://doi.org/10.1021/acsmacrolett.1c00335
271. T.G.Floyd, J.-I.Song, A.Hapeshi, S.Laroque, M.Hartlieb, S.Perrier. *J. Mater. Chem. B*, **10** (19), 3696 (2022); https://doi.org/10.1039/d2tb00490a
272. S.S.Parelkar, D.Chan-Seng, T.Emrick. *Biomaterials*, **32** (9), 2432 (2011); https://doi.org/10.1016/j.biomaterials.2010.12.004
273. C.J.Grimme, M.G.Hanson, L.G.Corcoran, T.M.Reineke. *Biomacromolecules*, **23** (8), 3257 (2022); https://doi.org/10.1021/acs.biomac.2c00338
274. T.P.Loginova, I.A.Khotina, Y.A.Kabachii, S.Yu.Kochev, V.M.Abramov, V.S.Khlebnikov, N.L.Kulikova, Y.O.Mezhuev. *Polymers*, **15** (14), 3036 (2023); https://doi.org/10.3390/polym15143036
275. J.Grundler, C.Whang, K.Shin, N.A.Savan, M.Zhong, W.M.Saltzman. *Adv. Healthcare Mater.*, **13** (22), 2304040 (2024); https://doi.org/10.1002/adhm.202304040
276. Z.-J.He, B.Huang, L.-H.Cai. *ACS Nano*, **18** (27), 17586 (2024); https://doi.org/10.1021/acsnano.4c01983
277. S.Bauhuber, R.Liebl, L.Tomasetti, R.Rachel, A.Goepferich, M.Breunig. *J. Control. Release*, **162** (2), 446 (2012); https://doi.org/10.1016/j.jconrel.2012.07.017
278. S.Watanabe, K.Hayashi, K.Toh, H.J.Kim, X.Liu, H.Chaya, S.Fukushima, K.Katsushima, Y.Kondo, S.Uchida, S.Ogura, T.Nomoto, H.Takemoto, H.Cabral, H.Kinoh, H.Y.Tanaka, M.R.Kano, Y.Matsumoto, H.Fukuhara, S.Uchida, M.Nangaku, K.Osada, N.Nishiyama, K.Miyata, K.Kataoka. *Nat. Commun.*, **10** (1), 1894 (2019); https://doi.org/10.1038/s41467-019-09856-w
279. H.Chaya, M.Naito, M.Cho, K.Toh, K.Hayashi, S.Fukushima, Y.Yamasaki, K.Kataoka, K.Miyata. *Biomacromolecules*., **23** (1), 388 (2022); https://doi.org/10.1021/acs.biomac.1c01344
280. M.Naito, H.Chaya, K.Toh, B.S.Kim, K.Hayashi, S.Fukushima, T.Nagata, T.Yokota, K.Kataoka, K.Miyata. *J. Control. Release*, **330**, 812 (2021); https://doi.org/10.1016/j.jconrel.2021.01.001
281. H.Taniguchi, Y.Natori, Y.Miyagi, K.Hayashi, F.Nagamura, K.Kataoka, K.Imai. *Int. J. Cancer*, **149** (3), 646 (2021); https://doi.org/10.1002/ijc.33579
282. H.Chaya, M.Naito, K.Toh, N.Yamada, K.Taniwaki, Y.Kinoshita, S.Fukushima, K.Minegishi, Y.Aoki, T.Nagata, T.Yokota, K.Kataoka, K.Miyata. *ACS Omega*, **10** (31), 34363 (2025); https://doi.org/10.1021/acsomega.5c02207
283. J.L.Lawson, R.P.Sekar, A.R.E.Wright, G.Wheeler, J.Yanes, J.Estridge, C.G.Johansen, N.L.Farnsworth, P.Kumar, J.W.Tay, R.Kumar. *Biomacromolecules*, **25** (10), 6855 (2024); https://doi.org/10.1021/acs.biomac.4c01101
284. S.Porte, V.V.D.Sengupta. *Small*, **21** (43), e05404 (2025); https://doi.org/10.1002/smll.202505404
285. A.Udepurkar, C.Devos, P.Sagmeister, F.Destro, P.Inguva, S.Ahmadi, E.Boulais, Y.Quan, R.D.Braatz, A.S.Myerson. *ACS Nano*, **19** (23), 21206 (2025); https://doi.org/10.1021/acsnano.4c18274
286. M.R.Elzes, I.Mertens, O.Sedlacek, B.Verbraeken, A.C.A.Doensen, M.A.Mees, M.Glassner, S.Jana, J.M.J.Paulusse, R.Hoogenboom. *Biomacromolecules*, **23** (6), 2459 (2022); https://doi.org/10.1021/acs.biomac.2c00210
287. Y.Kakizawa, K Kataoka. *Adv. Drug Deliv. Rev.*, **54** (2), 203 (2002); https://doi.org/10.1016/s0169-409x(02)00017-0
288. M.Lueckheide, J.R.Vieregg, A.J.Bologna, L.Leon, M.V.Tirrell. *Nano Lett.*, **18** (11), 7111 (2018); https://doi.org/10.1021/acs.nanolett.8b03132
289. Z.Tan, Y.Jiang, W.Zhang, L.Karls, T.P.Lodge, T.M.Reineke. *J. Am. Chem. Soc.*, **141** (40), 15804 (2019); https://doi.org/10.1021/jacs.9b06218
290. R.Sharma, J.-S.Lee, R.C.Bettencourt, C.Xiao, S.F.Konieczny, Y.-Y.Won. *Biomacromolecules*, **9** (11), 3294 (2008); https://doi.org/10.1021/bm800876v
291. D.J.Gary, H.Lee, R.Sharma, J.-S.Lee, Y.Kim, Z.Y.Cui, D.Jia, V.D.Bowman, P.R.Chipman, L.Wan, Y.Zou, G.Mao, K.Park, B.-S.Herbert, S.F.Konieczny, Y.-Y.Won. *ACS Nano*, **5** (5), 3493 (2011); https://doi.org/10.1021/nn102540y
292. P.J.Hurst, Y.Jia, S.Ramsay-Burrough, R.L.McClellan, J.T.Arens, S.R.Khasnavis, T.J.Del Castillo, M.M.Abd Elwakil, M.J.Lueckheide, V.M.Prabhu, R.M.Waymouth. *ACS Nano*, **19** (45), 38954 (2025); https://doi.org/10.1021/acsnano.5c07147

293. R.P.Sekar, J.L.Lawson, C.McGrath, G.Wheeler, G.Moreau, C.G.Johansen, N.L.Farnsworth, R.Kumar. *Langmuir*, **41** (27), 17426 (2025); https://doi.org/10.1021/acs.langmuir.5c00089
294. F.Coelho, C.Botelho, J.L.Paris, E.F.Marques, B.F.B.Silva. *J. Mol. Liq.*, **344**, 117930 (2021); https://doi.org/10.1016/j.molliq.2021.117930
295. V.Francia, R.M.Schiffelers, P.R.Cullis, D.Witzigmann. *Bioconjug. Chem.*, **31** (9), 2046 (2020); https://doi.org/10.1021/acs.bioconjchem.0c00366
296. F.Sebastiani, M.Yanez Arteta, M.Lerche, L.Porcar, C.Lang, R.A.Bragg, C.S.Elmore, V.R.Krishnamurthy, R.A.Russell, T.Darwish, H.Pichler, S.Waldie, M.Moulin, M.Haertlein, V.T.Forsyth, L.Lindfors, M.Cárdenas. *ACS Nano*, **15** (4), 6709 (2021); https://doi.org/10.1021/acsnano.0c10064
297. S.A.Dilliard, Q.Cheng, D.J.Siegwart. *Proc. Natl. Acad. Sci. USA*, **118** (52), e2109256118 (2021); https://doi.org/10.1073/pnas.2109256118
298. S.A.Dilliard, Y.Sun, M.O.Brown, Y.-C.Sung, S.Chatterjee, L.Farbiak, A.Vaidya, X.Lian, X.Wang, A.Lemoff, D.J.Siegwart. *J. Control. Release*, **361**, 361 (2023); https://doi.org/10.1016/j.jconrel.2023.07.058
299. V.Francia, Y.Zhang, M.H.Y.Cheng, R.M.Schiffelers, D.Witzigmann, P.R.Cullis. *Proc. Natl. Acad. Sci. USA*, **121** (11), e2307803120 (2024); https://doi.org/10.1073/pnas.2307803120
300. E.Voke, M.L.Arral, H.J.Squire, T.-J.Lin, L.Zheng, R.Coreas, A.Lui, A.T.Iavarone, R.L.Pinals, K.A.Whitehead, M.P.Landry. *Nat. Commun.*, **16** (1), 8699 (2025); https://doi.org/10.1038/s41467-025-63726-2
301. D.Zhu, H.Yan, Z.Zhou, J.Tang, X.Liu, R.Hartmann, W.J.Parak, N.Feliu, Y.Shen. *Biomater. Sci.*, **6** (7), 1800 (2018); https://doi.org/10.1039/c8bm00128f
302. D.Zhu, H.Yan, Z.Zhou, J.Tang, X.Liu, R.Hartmann, W.J.Parak, Y.Shen, N.Feliu. *Adv. Healthcare Mater.*, **10** (13), 2100125 (2021); https://doi.org/10.1002/adhm.202100125
303. M.I.Syga, E.Nicoli, E.Kohler, V.P.Shastri. *Biomacromolecules*, **17** (1), 200 (2016); https://doi.org/10.1021/acs.biomac.5b01308
304. S.Carrabino, S.Di Gioia, E.Copreni, M.Conese. *J. Gene Med.*, **7** (12), 1555 (2005); https://doi.org/10.1002/jgm.799
305. Z.Zhang, C.Wang, Y.Zha, W.Hu, Z.Gao, Y.Zang, J.Chen, J.Zhang, L.Dong. *ACS Nano*, **9** (3), 2405 (2015); https://doi.org/10.1021/nn505166x
306. N.Hartl, D.C.Jürgens, S.Carneiro, A.C.König, X.Xiao, R.Liu, S.M.Hauck, O.M.Merkel. *Int. J. Pharm.*, **643**, 123257 (2023); https://doi.org/10.1016/j.ijpharm.2023.123257
307. J.Lv, Q.Fan, Y.Zhang, X.Zhou, P.Yu, X.Yu, C.Xin, J.Hong, Y.Cheng. *Adv. Sci.*, **12** (13), 2413006 (2025); https://doi.org/10.1002/advs.202413006
308. G.Lin, J.Huang, X.Li, Y.Liu, T.Juenke, A.Finstad, M.Zhang. *Nanoscale Horiz.*, **10** (10), 2550 (2025); https://doi.org/10.1039/d5nh00299k
309. M.Kurisawa, M.Yokoyama, T.Okano. *J. Control. Release*, **69** (1), 127 (2000); https://doi.org/10.1016/s0168-3659(00)00297-2
310. M.Bikram, J.L.West. *Expert Opin. Drug Deliv.*, **5** (10), 1077 (2008); https://doi.org/10.1517/17425247.5.10.1077
311. M.Kotmakci, N.Toncheva-Moncheva, S.Tarkavannezhad, B.Debelec Butuner, I.Dimitrov, S.Rangelov. *Pharmaceutics*, **17** (8), 1012 (2025); https://doi.org/10.3390/pharmaceutics17081012
312. B.M.Matthews, A.M.Maley, K.M.Kartub, R.M.Corn. *J. Phys. Chem. C*, **123** (10), 6090 (2019); https://doi.org/10.1021/acs.jpcc.9b00444
313. N.Ozdemir, A.Tuncel, M.Duman, D.Engin, E.B.Denkbas. In *Functionalized Nanoscale Materials, Devices and Systems*. (Dordrecht: Springer Netherlands, 2008). P. 325; https://doi.org/10.1007/978-1-4020-8903-9_25
314. G.Sinani, M.E.Durgun, E.Cevher, Y.Özsoy. *Pharmaceutics*, **15** (8), 2021 (2023); https://doi.org/10.3390/pharmaceutics15082021
315. T.Egashira, H.Kamizawa, Y.Hamada, W.Fushimoto, H.Y.Yoshikawa, Y.Higaki, A.Takahara, T.Mori, Y.Katayama, A. Kishimura. *Small*, e05876 (2025); https://doi.org/10.1002/smll.202505876
316. S.Hossainy, S.Kang, J.G.Medellín, A.Alpar, K.Refvik, Y.Ma, I.Vuong, K.Chang, T.Wang, A.Solanki, S.Rowan, J.Hubbell. *Nat. Biomed. Eng.*, **10**, 427 (2025); https://doi.org/10.1038/s41551-025-01469-7
317. L.Luo, A.Eisenberg. *Angew. Chem., Int. Ed.*, **41** (6), 1001 (2002); https://doi.org/10.1002/1521-3773(20020315)41:6%3C1001::AID-ANIE1001%3E3.0.CO;2-Q
318. T.Bo, C.Wang, D.Yao, Q.Jiang, Y.Zhao, F.Wang, W.He, W.Xu, H.Zhou, M.Li, S.Zhang, R.Xue. *J. Control. Release*, **368**, 157 (2024); https://doi.org/10.1016/j.jconrel.2024.02.024
319. G.Kwak, A.Grewal, H.Slika, G.Mess, H.Li, M.Kwatra, A.Poulopoulos, G.F.Woodworth, C.G.Eberhart, H.S.Ko, A.Manbachi, J.Caplan, R.J.Price, B.Tyler, J.S.Suk. *ACS Nano*, **18** (35), 24139 (2024); https://doi.org/10.1021/acsnano.4c05270
320. Y.Cao, Z.He, Q.Chen, X.He, L.Su, W.Yu, M.Zhang, H.Yang, X.Huang, J.Li. *Nano Lett.*, **22** (16), 6580 (2022); https://doi.org/10.1021/acs.nanolett.2c01784
321. R.Ye, Q.Ren, L.Chang, S.Zhang, C.Deng, L.Cao, M.Shi, B.Lou, F.Meng, S.Du, K.Ren, X.Piao, C.Xu, Z.Zhong. *Nano Today*, **63**, 102741 (2025); https://doi.org/10.1016/j.nantod.2025.102741
322. L.Lin, K.Su, X.Zhang, L.Shi, X.Yan, Q.Fu, K.Yao, D.J.Siegwart, S.Liu. *Angew. Chem., Int. Ed.*, **64** (17), e202500306 (2025); https://doi.org/10.1002/anie.202500306
323. J.Long, S.Ma, R.Wan, A.Sun, Z.Zhu, R.Wang, Z.Guo, W.Song. *J. Control. Release*, **388**, 114371 (2025); https://doi.org/10.1016/j.jconrel.2025.114371
324. Y.Zhang, P.Sun, S.Ma, Z.Guo, H.Zhao, Y.Qi, M.Li, W.Song, Z.Tang. *Biomacromolecules*, **26** (11), 7343 (2025); https://doi.org/10.1021/acs.biomac.5c00802
325. J.Norimatsu, R.Hashim, T.A.Tockary, M.S.Nazir, Y.Mochida, S.Uchida. *ACS Appl. Nano Mater.*, **8** (21), 10898 (2025); https://doi.org/10.1021/acsanm.5c00633
326. A.Gharatape, A.Sayadmanesh, H.Sadeghi-Abandansari, H.Ghanbari, M.Basiri, R.Faridi-Majidi. *Nanoscale Adv.*, **7** (12), 3676 (2025); https://doi.org/10.1039/d5na00169b
327. Z.Chu, Z.Li, H.Yong, D.Che, B.Li, C.Yan, T.Zhou, X.Wang, Y.Feng, K.Guo, S.Geng. *J. Control. Release*, **367**, 197 (2024); https://doi.org/10.1016/j.jconrel.2024.01.026
328. A.V.Lopukhov, Z.Yang, M.J.Haney, T.K.Bronich, M.Sokolsky-Papkov, E.V.Batrakova, N.L.Klyachko, A.V.Kabanov. *Macromol. Biosci.*, **21**, 2000371 (2021); https://doi.org/10.1002/mabi.202000371
329. M.Nakanishi, Y.Endo-Takahashi, Y.Negishi, S.Asayama. *ACS Appl. Bio Mater.*, **9** (3), 1682 (2026); https://doi.org/10.1021/acsabm.5c02207
330. M.J.Javid-Naderi, S.A.M.Shaegh. *Int. J. Pharm.: X*, **10**, 100399 (2025); https://doi.org/10.1016/j.ijpx.2025.100399
331. https://www.fda.gov/vaccines-blood-biologics/spikevax (Last access 10.07.2026)
332. https://www.accessdata.fda.gov/drugsatfda_docs/label/2023/210922s012lbl.pdf (Last access 10.07.2026)
333. Imunon. *A Randomized Phase 3 Trial Evaluating the Safety & Efficacy of IMNN-001 Administered in Combination/Standard Neoadjuvant & Adjuvant Chemotherapy in Newly Diagnosed Patients/Advanced EOC, Fallopian Tube or Primary Peritoneal Cancer*; Clinical trial registration NCT06915025; clinicaltrials.gov, 2026; https://clinicaltrials.gov/study/NCT06915025 (Last access 10.07.2026)